Substratum Control of Hepatocyte Aggregate Morphology

by

Mark J. Powers

B.S., Chemical Engineering
Northwestern University, 1991

Submitted to the Department of Chemical Engineering
in partial fulfillment of the requirements for the degree of

Doctor of Philosophy

at the

Massachusetts Institute of Technology

February, 1997

Signature of Author .....
Department of Chemical Engineering
October 11, 1996

Certified by .....
Linda G. Griffith
Associate Professor of Chemical Engineering
Thesis Supervisor

Accepted by .....
Robert E. Cohen
Professor of Chemical Engineering
Chairman, Committee for Graduate Students

Substratum Control of Hepatocyte Aggregate Morphology

by

Mark J. Powers

Submitted to the Department of Chemical Engineering on October 11, 1996
in partial fulfillment of the requirements for the degree of
Doctor of Philosophy in Chemical Engineering

Abstract

The biological response of hepatocytes cultured on two-dimensional substrata *in vitro* correlates strongly with the morphology achieved by aggregates of these cells. Spheroidal aggregates typically exhibit liver-specific functions while monolayered aggregates exhibit characteristics of growth. In this thesis, the ability of a substratum to influence the aggregation of dispersed hepatocytes and the ultimate morphology achieved by these aggregates is examined.

Initial observations investigate the role of both biophysical and biochemical substratum properties on hepatocyte aggregation and aggregate morphology through systematic variation in both concentration and type of extracellular matrix. These results suggest that both aggregation and morphogenesis of hepatocytes are largely dependent on the biophysical features of the substratum. Subsequent investigations into the cellular mechanisms responsible for hepatocyte aggregation indicate that these cells typically aggregate after initiating contact with one another through cell membrane extension. In several instances this contact was followed by a cellular contraction event, which had the effect of pulling the cells towards one another.

This information leads to the formation of a hypothesis that hepatocyte aggregate morphogenesis is due to the relative magnitudes of cell-substratum adhesion strength and the force exerted during cellular contraction. When the contractile force is dominant, spheroids result; when cell-substratum adhesion is dominant, monolayers result. Quantification of cell substratum adhesion strengths on these different substrata confirm that spheroids form at low cell-substratum adhesion strengths, monolayers at high cell-substratum adhesion strengths. Comparison of these forces with literature values of cell traction force generation by other cell types provides strong support for the proposed hypothesis.

These results implicate the biophysical features of a substratum as important parameters in hepatocyte aggregation and aggregate morphogenesis, and provide a rational basis for the design of biomaterials and culture systems to be used in hepatic tissue engineering applications.

Thesis Supervisor: Linda G. Griffith
Title: Associate Professor of Chemical Engineering

Acknowledgments

I consider myself extremely fortunate to have been able to work under the direction of Linda Griffith during the course of this research. She has been a constant source of wisdom, guidance and support throughout my tenure at MIT. I am also greatly indebted to Doug Lauffenburger, whose insight and advice has proved invaluable to the completion of these studies. The other members of my thesis committee were Martin Yarmush and Elazer Edelman, both of whom were extremely generous with both their time and knowledge in helping me formulate a cohesive thesis.

I would also like to thank those with whom I have worked with during the past five years. Raul Rodriguez, Heather Lee, Shelly Sakiyama, Anna Pan and Nick Fidelman were undergraduates who worked with me on this project. Many of the studies described in this document were the result of their hard work and effort. Mitsuo Miyazawa provided a good deal of the hepatocytes used in these studies (and also introduced me to Japanese food -- although I think that he is now partial to Nick's Beef and Beer). Others who provided hepatocytes during this research were Kristin O'Neil, P.-Matthias Kauffman, and Magali Fontaine. Sue Allgor performed the XPS studies contained in this thesis.

I thank my lab mates from the Griffith-Cima lab, who made coming to work every day fun -- in particular, I thank Ann Park for hypothetical problem solving, Ed Perez for help in the machine shop (and for building that space-age nutcracker), Philip Kuhl for the sponge candy, Scott Borland for frequent supersizing, and Jeff Sperinde for still being the new guy. I was also glad to have worked with and gotten to know those in the Lauffenburger group, and I thank Cartikeya Reddy and Sean Palecek for allowing me to engage them in many helpful discussions.

There are several people from MIT whom I wish to thank for their friendship during the past five years. My roommates--Justin Hanes, Bobby Padera, and Troy Simpson--were just about the best I could have asked for and will always be among my closest friends. I am also grateful to Phil Cali, Tom Bratkovich, Mary Jane O'Rourke, Chris Dowd, Joanne Curley, Bill Stockton, Steffen Ernst, Glen Bolton, Kiko Aumond, Jason Haugh, Chase Orsello, Jeff Hrkach, Giovanni Caponetti, and everyone else who was willing to waste a little time with me during the past five years. I would especially like to acknowldege Karen Fu for being my buddy, for putting up with me, and for being much worse at crossword puzzles and swimming the sidestroke than I.

Finally, this thesis is dedicated to my family for their unending love, support, and encouragement.

Table of Contents

1 Introduction and Background

1.1 Introduction

1.1.1 Hepatic Tissue Engineering

The complex metabolic and secretory functions of the liver preclude artificial replacement of its functions, as is done with kidney and various connective tissues. Replacement of liver function requires the presence of viable liver cells. Organ transplant is currently the only widely-practiced clinical treatment for liver failure and inborn genetic defects. However, the profound lack of donor organs, the risk and expense involved in surgery, and post-surgical morbidity have recently motivated many approaches to hepatic tissue engineering to improve the clinical outcomes (130, 21, 144, 151, 72, 91, 38, 105, 107, 142, 44, 56).

A spectrum of clinical need exists -- from cirrhosis to hepatic failure induced by acute toxicity -- and these are being addressed with targeted approaches ranging from extracorporeal liver assist devices to cell transplantation. Primary cells cultured in extracorporeal reactors hold promise for treating acute toxicity by providing temporary liver assist while the patient's own liver recovers and are on the verge of clinical application (21, 151, 91, 44, 56, 58). A variety of cell transplantation methods for permanent replacement of liver function are in the development stage. Approaches include injection of a small complement of genetically-modified cells into the native liver for treatment of single-gene metabolic disorders (130, 38, 142) and ectopic transplantation of cells attached to erodible polymeric supports to generate completely functioning tissue for treatment of cirrhosis and other chronic disorders (21, 144). Almost all of these approaches to hepatic tissue engineering at some stage of the process use interactions of primary hepatocytes with solid surfaces to affect cellular behaviors such as growth, differentiation, and formation of three dimensional structures.

1.1.2 Substratum Control of Hepatocyte Behavior

Because the interactions between hepatocytes and biomaterials are principally mediated via endogenously added or cell-secreted extracellular matrix (ECM) proteins, it is essential to understand the ways in which a matrix can affect hepatocyte behavior in order to design surfaces and environments optimizing the desired response. The nature of extracellular matrix control over cellular behavior (e.g., morphogenesis, gene expression) is rather poorly understood, but a commonly held view is that a matrix exerts control over cellular function primarily through mechanisms involving biochemical signaling (for review, see ref. 57). While the biophysical properties of a matrix are given relatively little consideration in this role (e.g., ref. 115), they have been shown to be capable of effecting a variety of cell behavioral responses. Biophysical cell-matrix interactions have been shown to strongly influence cell migration (34, 117, 73) and, through control of cell shape, such functions as cell growth (31, 32, 35, 50, 85), differentiation (26, 12, 148, 77, 85), and tissue pattern formation(54, 95).

The ability of a matrix to control hepatocyte growth or differentiation has traditionally been attributed to the presence of specific molecules in the ECM. It was observed that cells seeded on collagen gel substrata form monolayered aggregates (see Fig. 1-1) and exhibited high levels of DNA synthesis but low levels of liver-specific protein secretion and gene expression (10, 115, 59, 102). In these same studies, hepatocytes cultured on Matrigel (a basement membrane extract from the Engelbreth-Holm-Swarm mouse tumor) were observed to form three-dimensional spherical aggregates ("spheroids" - see Fig. 1-1) and exhibited relatively low levels of DNA synthesis but high levels of liver-specific function. Based on these observations it was concluded that the differences in hepatocyte behavior were attributable to matrix-specific differences in biochemical signaling. Studies in which hepatocyte behavior was assessed on various rigid substrata illustrate that spheroids (and monolayers) are capable of forming both on "physiological" (e.g., proteoglycans, collagen) and "non-physiological" (e.g., uncoated polystyrene, poly

((hydroxyethyl) methacrylate) (poly-HEMA)) substrata (Table 1-1) (64, 97). Interestingly, the levels of albumin secretion and DNA synthesis in these aggregates were found to depend only on aggregate morphology (high albumin secretion, low DNA synthesis for spheroids; low albumin, high DNA for monolayers) and showed no significant dependence on the substrata to which the cells attached. These results suggest that aggregate morphology alone is capable of dictating the differentiated state of hepatocytes in a manner which is independent of biochemical signaling (25, 77, 152, 118, 150). Matrix control of hepatocyte behavior on these substrata is therefore tied at least in part to the ability of a matrix to stimulate (or permit) the formation of spheroids or monolayers.

It was observed during the course of these studies of hepatocyte culture on rigid substrata that monolayers tended to form on what were commonly thought to be "adhesive" surfaces (e.g., collagens, laminin), while spheroids seemed to form on the "abhesive" substrata (e.g., poly-HEMA, bovine serum albumin) (64, 97). These observations implicate the biophysical features of a substratum as potentially important contributors to hepatocyte aggregate morphogenesis. However, no quantitative studies were performed to verify this hypothesis. Furthermore, while it was found that conditions of low substratum adhesiveness (or high deformability) were optimal for spheroid formation, no attempts were made to determine the mechanistic bases for this behavior.

The studies performed during the course of this research serve to elucidate the manner in which the biophysical features of a substratum can control hepatocellular behavior via hepatocyte aggregation and subsequent aggregate morphogenesis. The results provide rational and quantitative design criteria for biomaterials to be used in hepatic tissue engineering applications.

1.2 Background

1.2.1 Cell-Matrix Interactions

The study of substratum influence over cellular behavior and the manipulation of substratum properties to control this behavior forms the basis of this research. The potential scope and magnitude of the resulting effects on hepatocellular behavior can be delineated from what is already known of the fundamental molecular components involved in cell-substratum interactions.

1.2.1.1 Cell-Surface Receptors

Cell-substratum interactions are mediated through trans-membrane receptors. Over the last 10 years, tremendous progress has been made in the identification and characterization of adhesion receptors. The primary receptors responsible for cell-substratum interactions are known as integrins.

Integrins are trans-membrane heterodimers composed of noncovalently attached α and β subunits (15, 48), each with a transmembrane domain and short cytoplasmic sequence (Figure 1-2). Thirteen α and eight β subunits have been identified to date, which combine to generate the 21 known integrins. These receptors are anchored to the cytoskeleton via a series of intermediates(87). Integrins are involved in both cell-cell and cell-substratum adhesion, but have primarily been known for binding to ligands in the extracellular matrix. The ligand specificity of an integrin is determined by the particular α and β subunit combination (2). Integrins have been shown to bind weakly to ECM ligands in soluble form, with dissociation constants (K_d's) ranging from 10^{-6}-10^{-7} M (74).

An obvious function of integrins and of cell-surface adhesion receptors in general is to provide physical points of attachment between a cell and its environment. Basic architectural principles dictate that mechanical loads are transmitted across physically interconnected structures (51), and so the ability of cells, cell aggregates, or tissues to remodel themselves and one another is largely dependent on the structural integrity of these

integrin linkages. Integrins provide additional biophysical signals to a cell by influencing cytoskeletal architecture and organization, which may result in the activation of intracellular signaling pathways (1, 51). However, it has been recognized that integrins can also play an important role in directly providing biochemical signals to cells. Although current knowledge of integrin-regulated signaling pathways is incomplete, it has been suggested that integrins regulate cell functions via a small number of common mechanisms. Several reports indicate that ligation of integrins can alter cellular patterns of tyrosine phosphorylation, most prominently through a 125 kDa polypeptide known as focal adhesion kinase (FAK) (60, 39, 68, 67, 112). Integrin binding can also increase intracellular pH through activation of the Na^+-H^+ antiporter (55, 116) and has been shown to alter intracellular free Ca^{2+} concentration (90). In addition, increases in intracellular phosphatidylinositol levels have been correlated with integrin binding (116). Each of these events is capable of having a dramatic impact on cellular gene expression and behavior, and so it is often concluded that ligation with specific ECM molecules in turn elicits certain cellular responses. (for review see ref. 57).

1.2.1.2 Extracellular Matrix

The initiation of integrin activity, whether biochemical or biophysical, is dependent on association with extracellular ligands. Since these studies are concerned with cell-substratum interactions, the ligands of interest are found in the extracellular matrix. The extracellular matrix is composed of macromolecules which are linked together via covalent and non-covalent bonds into an insoluble and organized complex. Its major constituents include collagenous molecules (types I-XII), glycoproteins (fibronectin, laminin, entactin, nidogen, vitronectin, thrombospondin, chondronectin, osteonectin, fibrin), elastin, proteoglycans (containing heparan sulfate, chondroitin sulfate, dermatan sulfate, or keratin sulfate) and glycosaminoglycans (42, 69).

A specialized ECM found at the basal domain of epithelial tissues is known as the basement membrane. The basement membrane is a flat "two-dimensional" molecular meshwork and provides mechanical support for resident cells, serves as a semipermeable barrier between tissue compartments, and acts as a regulator for cellular attachment and differentiation (114). In the liver, hepatocytes are found directly adjacent to the vascular, or sinusoidal, endothelium. Although a fully formed basement membrane is not found in the region between these cells (the space of Disse), a variety of ECM molecules have been identified there. In the healthy adult liver, these include collagen types IV, V, and VI, fibronectin, laminin, entactin, tenascin, and undulin (78). At least three proteoglycan species are also present in the space of Disse, including heparan sulfate proteoglycan (78). Martinez-Hernandez *et al.* (79) reported that during hepatic regeneration after partial hepatectomy laminin expression in the space of Disse is dramatically increased, while the amounts of collagen-IV and fibronectin stay relatively constant. This finding implicates laminin as a key factor in the liver regeneration process. In determining the matrices to be used in these studies, it is logical to choose ECM molecules which are associated with hepatocytes *in vivo*. Of these, the most prominent are collagen, laminin and fibronectin (18, 135, 123, 28, 79, 78).

Collagens are a family of fibrous proteins found in all animals. They are usually distinguishable by their stiff, triple-stranded helical structure. The polypeptide chains making up the helix are called α chains, about 120 of which have been identified to date (1a). These α chains have been shown to form at least 12 different collagen molecules (labeled types I-XII) (34a). Most of these types of collagen molecules (including type I collagen) associate to form fibrils and fibers with the exception of type IV collagen, which forms multi-layered two-dimensional lattices (1a).

Fibronectin (MW≈480 kDa) is a glycoprotein that is capable of attaching cells (via trans-membrane receptors) to various basement membrane components (e.g., collagen, heparan sulfate, fibrin) via a multitude of binding domains (47, 27). It is an asymmetric

molecule and consists of two similar or identical subunits of molecular weight on the order of 200 kDa held together by disulfide bonding near their carboxy termini (49). One well known domain of fibronectin responsible for cell binding has been identified as the tripeptide arginine-glycine-aspartic acid (RGD) (108, 109). Fibronectin is produced by both fibroblasts and epithelial cells, as well as many other cell types (62) and exists in three forms: (1) a soluble dimeric form, plasma fibronectin; (2) oligomers transiently attached to the surface of cells, known as cell-surface fibronectin; and (3) highly insoluble fibrils formed in the ECM, or matrix fibronectin (1a). It is the third of these forms, the matrix fibronectin, that is of interest in our investigations into cell-matrix interactions.

Laminin, like fibronectin, is a glycoprotein. Laminin is a large complex (MW≈850 kDa) consisting of three long polypeptide chains arranged in the shape of a cross held together by disulfide bonds. Like fibronectin, it contains a number of functional domains: one to bind collagen type IV, one for integrins, etc. (1a).

Matrigel is a fourth type of matrix used in these studies and is included due to its ability to support hepatocyte differentiation and its similarity to native hepatic basement membrane. Matrigel consists of a variety of components, many of which are unknown or present in unknown quantities. Matrigel is a solubilized basement membrane extract taken from the Engelbreth-Holm-Swarm (EHS) mouse sarcoma. Its major components are laminin and collagen IV (MW≈540 kDa), along with lesser amounts of heparan sulfate proteoglycans, entactin, and nidogen. Grant *et al.* (36) reported a molar ratio of laminin, collagen IV and heparan sulfate proteoglycan in the EHS sarcoma as 1:1:0.2. Matrigel also contains soluble factors in its native form, including transforming growth factor-beta, fibroblast growth factor, tissue plasminogen activator, and other growth factors that are present in the EHS tumor.

1.2.1.3 Hepatocyte-Substratum Interactions

Hepatocytes have been shown to utilize at least two different integrins in attaching to the ECM but can also associate with these ligands via non-integrin receptors. The known hepatocyte substratum receptors are summarized in Table 1-2. It is evident from inspection of this table that by changing the ligands present in the ECM presented to the cells, the receptors used by hepatocytes for substratum attachment can also be varied. This provides a systematic means by which variances in biochemical signaling can be taken into account.

1.2.2 Cell-Cell Interactions and Aggregation

While cell-ECM interactions are likely to be key determinants of hepatocyte behavior in these studies, it is also crucial to understand the role that cell-cell interactions may play in these studies. Hepatocytes, like a number of other cell types currently under investigation for tissue regeneration in organs such as skin, cornea, and intestine, are epithelial cells. Epithelial cell types exist naturally in sheets or aggregates and have been shown to reform such structures when dispersed *in vitro* (71, 9, 80, 97). The induction of cell-cell contact has been shown to be a critical event in the subsequent polarization and morphogenesis of these cells into functioning tissues (106). Hepatocytes in spheroidal aggregates appear to mimic the morphology, architecture and ultrastructure of an *in vivo* liver lobule(10, 5, 152, 150), which may contribute to the ability of these cells to differentiate and exhibit liver-specific function (84).

Epithelial tissue typically exists in a polarized state with two distinct domains -- apical and basolateral -- each specialized for particular functions. A primary purpose of the epithelial junctional complex is then to maintain a "barrier" between these domains as well as well as the integrity of the epithelial sheet. The components of the epithelial junctional complex normally include tight (occludens) junctions, adherens junctions (also known as belt desmosomes, zonula adherens, or intermediate junctions) and desmosomes(29)

(Figure 1-3). Tight junctions serve as a barrier between the apical and basolateral domains of epithelial cells *in vivo*. Desmosomes are button-like points of intercellular contact that also serve to anchor for the intermediate filaments of the cytoskeleton. Adherens junctions consist of cytoskeletal F-actin "adhesion belts" which are connected with adhesion belts from adjacent cells via cell-cell receptors. The primary receptors involved in adherens junctions are the cadherins (most notably E-cadherin, or uvomorulin), which are calcium dependent homophilic receptors (134). They appear to be vital for the induction and regulation of intercellular adhesions and the subsequent initiation of organizational events during development; adult tissues may also depend on cadherins to maintain epithelial polarity (88, 106, 147).

The architecture of the hepatic parenchyma is somewhat unique when compared with that of standard epithelia, as hepatocytes typically exhibit *three* distinct domains in their polarized state. The apical domain forms a bile canalicular network; bile is produced by hepatocytes and transported through this network to the bile ducts. Epithelial-type junctions form on the lateral domain. The basal, or sinusoidal, domain is adjacent to a layer of endothelial cells, Kupffer cells, and fat cells. These cells line the sinusoids, which provide blood flow from the portal vein and hepatic artery to the hepatocytes and then on to the central vein.

In order for hepatocytes to achieve an architecture reminiscent of these structures, it is clearly necessary for these cells to first aggregate and form stable cell-cell adhesions. *In vitro*, the degree of aggregation has been shown to have profound effects on hepatocellular behavior (9). Cultures in which hepatocytes aggregate were shown to maintain concentrations of functional parameters which were an average of 2-fold or more higher than those in single-cell hepatocyte cultures seeded onto identical substrata at the same inoculation densities (96, 97). Cadherins begin to cluster and connect as epithelial cells approach one another and touch, and discrete adherens junctions characterized by cytoplasmic plaques and associated cytoskeletal fibers are evident within 20 seconds of

cell-cell contact (63). These observations suggest that the rate-limiting step in the formation of stable cell-cell junctional complexes is the occurrence of cell-cell contact.

Cell aggregation is clearly an important event in the regeneration of epithelial tissue. However, it is evident from the studies described here that, on two-dimensional substrata, it is the subsequent morphology assumed by hepatocyte aggregates which ultimately dictates their ability to assume liver-specific activity.

1.2.3 Morphogenesis

The ability of dispersed cells to re-form native tissue structures, first observed during studies of normal development and regeneration (149), should also be appreciated as a crucial phenomenon in many current approaches to tissue engineering. Currently, the mechanisms which guide hepatocyte morphogenesis are quite poorly understood; delineation of these mechanisms is critical to understanding the nature of substratum control over this process.

Evolution of morphology in multi-cellular structures has long been of interest in the study of normal and pathological development. The demonstration by Townes and Holtfreter that the dissociated cells of vertebrate embryonic organs would not only re-aggregate but also reorganize in an appropriate manner (139) spawned enormous interest in the intrinsic cellular morphogenetic clues and the mechanisms by which this process is governed. It is generally agreed upon by developmental biologists that relatively few mechanisms are required to generate tissue organization, even if it is not known exactly how they lead to the formation of most structures. A variety of mechanisms have been studied in terms of their contribution to various aspects of morphogenesis including directed cell movement, cytoskeletal contraction, cell proliferation, differences in cell adhesion, and contact guidance (7). Townes and Holtfreter concluded from their initial studies that directed cell movements were responsible for cell sorting. It was later demonstrated by Steinberg that directed cell movements in fact played no role in the

observed phenomena and that differences in the intensity of cell adhesions alone could direct the sorting-out of intermixed embryonic cells, the spreading of one tissue over the surface of another, and the specific inside/outside tissue stratification that arises by either process (126, 127). An important implication of Steinberg's analysis is that different molecular arrangements could lead to identical outcomes, provided that they allowed comparable adhesion forces to be generated. A similar type of analysis was performed by Oster *et al.*, who developed a mathematical model capable of accurately predicting complex morphogenetic pattern formation based solely on biophysical parameters(95). It is certainly feasible for mechanical forces to coordinate shape changes in large cellular aggregates without the assistance of chemical signaling as it has been shown that forces generated by cell shape changes at one position in an epithelial sheet were equilibrated over the entire structure virtually instantly (92).

Thus, while epithelial morphogenesis is a complex process involving numerous signals and guidance clues which can be either chemical or physical in nature the fundamental mechanisms which are responsible for this process are very possibly biophysical in nature. Biophysical principles have been shown to govern a number of other cellular phenomena. For example, it has been shown that cell migration depends on cell-substratum adhesivity in a biphasic manner (23). This behavior was effectively modeled based on the relative magnitudes of cell-substratum adhesion strength and cell-generated contractile forces (22). Cellular contractile force has been hypothesized to play a key role in the morphogenesis of liver tissue (122), and its role in the morphogenesis of hepatocytes *in vitro* must also be considered in this analysis.

But regardless of what the specific mechanisms responsible for hepatocyte morphogenesis are determined to be (e.g., cellular contraction, cell-cell adhesion) it is clear that cell-substratum adhesion strength may play an important role in this process. The experimental design for this thesis, outlined in the following section, describes the analyses

to be performed and illustrates the key issues which must be addressed to delineate the role of these biophysical phenomena in hepatocyte aggregation and aggregate morphogenesis

1.3 Experimental Design

The studies performed in the course of this research were designed to consider both the biophysical and biochemical features of a substratum, allowing for an assessment of the relative abilities of each of these to control hepatocyte aggregation and aggregate morphogenesis. These investigations have been designed to allow for observations of these cellular parameters while (1) systematically varying the cell-substratum adhesion strength, and (2) doing so on different extracellular matrices which potentially deliver diverse biochemical signals to the cells.

Variation in cell-substratum adhesion strength can be accomplished by adsorbing different concentrations of an ECM to the substratumn (140, 23). Since the *type* of cell-surface receptors mediating attachment to these different ECM densities remains unchanged, the effects of variation in biophysical substratum properties can be examined under conditions which activate similar biochemical signaling pathways. By performing a similar analysis on different ECM types, the specific receptors recruited for substratum attachment can be varied (see Table 1-2). This allows for variation in the specific biochemical signal transduction properties of a substratum (132, 43, 133, 136, 57), which can then be studied while holding cell-substratum adhesion strength relatively constant.

The ECM molecules used in these studies are fibronectin, type I collagen, laminin, or Matrigel coated at concentrations between 0.01 $\mu g/cm^2$ - 10 $\mu g/cm^2$. The most comprehensive studies were conducted with Matrigel, which has traditionally been associated with the ability to impart biochemical signals to cells and to promote the formation of differentiated spheroidal hepatocyte aggregates *in vitro* (10, 115, 59, 102, 30). By demonstrating that Matrigel, through variation in its biophysical properties, can support not only spheroidal aggregation but also monolayered aggregation, the importance

of biophysical phenomena in hepatocyte aggregate morphogenesis can be effectively demonstrated.

A more detailed analysis follows in which it is shown that cell membrane extension is the primary cellular mechanism by which hepatocytes aggregate. Observations of cellular behavior indicate that a cell contraction event typically follows initial cell-cell contact. Arising from this analysis is a hypothesis that the relative magnitude of cell traction forces vs. cell substratum adhesion strengths controls the morphogenesis of hepatocyte aggregates: monolayers form when cell-substratum adhesion forces are larger than cell contraction forces, spheroids result when the reverse is true. The remainder of the thesis involves quantitative analysis and verification of this hypothesis.

Cell-substratum adhesion forces are quantified on the substrata on which morphogenesis was initially observed. Hepatocyte aggregate morphology essentialy shows a binary relationship with measured values of cell-substratum adhesion strength: spheroids form on relatively poorly adhesive substrata while monolayers form on highly adhesive substrata. When compared with standard literature values of cell traction force generation, these data provide strong support for the hypothesis and implicate the biophysical features of a substratum as primary determinants of hepatocyte aggregate morphology.

substratum coated with:	polystyrene dish: positive	hydrophobic	negative
U	S	M	M
HEMA	S	S	S
BSA	S	S	S
PG	M	M	M
GP	S	S	S
C	M	M	M

Table 1-1. The morphology of hepatocyte aggregates on various rigid substrata. Morphology was assessed on day 4. Spheroids (S) and monolayers (M) were observed to form on positively charged, hydrophobic and negatively charged polystyrene petri dishes which were either uncoated (U) or coated with one of the following: poly ((hydroxyethyl) methacrylate) (HEMA), bovine serum albumin (BSA), proteoglycans isolated from rat reticulin fibers (PG), glycoproteins (fibronectin or laminin) (GP), or collagens (type I or type IV) (C). Results are from references 64 and 97.

ECM	Receptor	Binding Site	References
FN	$\alpha_5\beta_1$	RGD	125, 101
	AGp110 (non-integrin glycoprotein)	??(not RGD)	124
	Dipeptidyl Peptidase IV (non-int. glycop.)	??	41
CI	$\alpha_1\beta_1$	??(not RGD)	40
CIV	$\alpha_1\beta_1$	??	120
LM	$\alpha_1\beta_1$	??(not RGD)	33
	38, 45, 80 kDa	RGD	20
	32, 45, 67, 80 kDa	IKVAV	20, 104
	36, 38, 80 kDa	YIGSR	20
HSP	**38 kDa**	??	19

Table 1-2. Hepatocyte cell-surface receptors. The known receptors utilized in hepatocyte binding to fibronectin (FN), type I collagen (CI), type IV collagen (CIV), laminin (LM), and heparan sulfate proteoglycan (HSP) along with the ligand amino acid sequences (if known) recognized by these receptors.

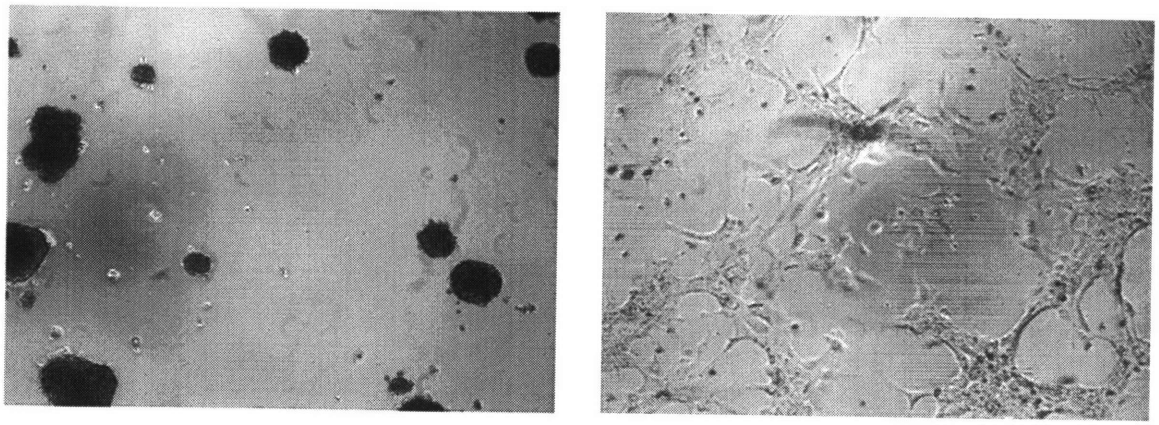

(a) (b)

Figure 1-1. Hepatocye aggregate morphology. *In vitro* images of (a) spheroidal aggregation; (b) monolayered aggregation.

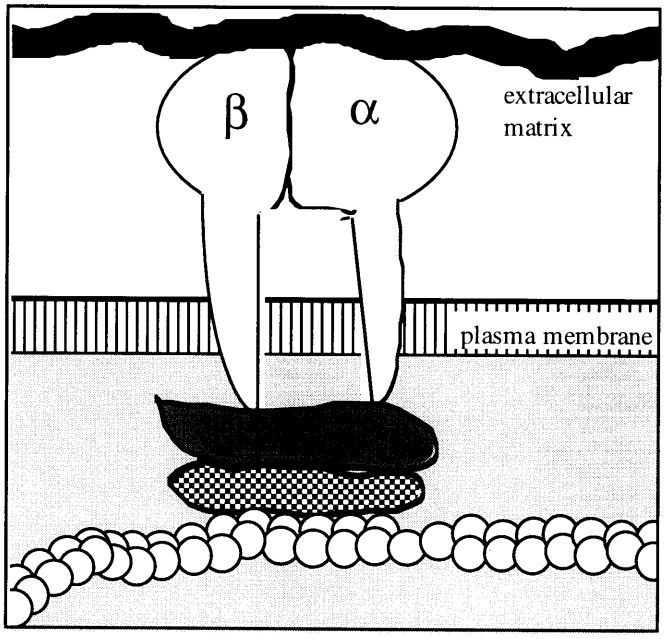

Figure 1-2. Schematic diagram of an integrin receptor.

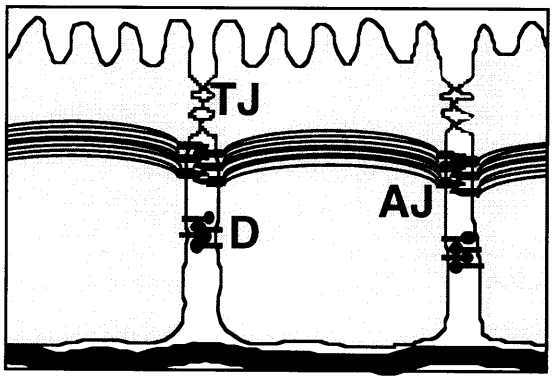

Figure 1-3. Schematic diagram of the typical epithelial junctional complex, illustrating tight junctions (TJ), adherens junctions (AJ) and desmosomes (D).

2 Materials and Methods

2.1 Cell Isolation and Culture

Hepatocytes were isolated from 180-250g male Fisher rats. The liver was perfused in the retrograde direction first with Ca^{2+}-free perfusion buffer (143 mM NaCl, 7 mM KCl, 10 mM HEPES, pH 7.4) for 6 minutes and subsequently with the same perfusion buffer containing 5 mM $CaCl_2$ and 0.5 mg/ml collagenase D (Boehringer-Mannheim Biochemicals; Indianapolis, IN) until the liver became soft. Cells were dispersed in chemically-defined serum-free Williams' E medium (GIBCO Laboratories; Grand Island, NY) with 10 ng/ml epidermal growth factor (Collaborative Biomedical Products; Bedford, MA), 20 mU/ml insulin (Gibco Laboratories), 5 nM dexamethasone (Sigma Chemicals; St. Louis, MO), 20 mM pyruvate (GIBCO Laboratories), and 100 U/ml penicillin-streptomycin (GIBCO Laboratories). This medium will be referred to as "complete medium". Dead cells and debris were removed by centrifugation in an isodensity Percoll solution and the resulting pellet was washed three times with the complete medium. Cell viability prior to cell seeding was 80-95% as determined by trypan blue exclusion.

Cells were seeded in complete medium at densities of 4,000, 6,000, 8,000, 15,000, 30,000 or 45,000 viable cells/cm^2 culture surface area. An even seeding density was obtained by seeding the cells over as much of the dish surface as possible followed by rocking the dish several times. Following an attachment period of 18 to 24 hours the medium was changed to remove unattached cells, after which the cells were maintained in complete medium with daily medium changes.

2.2 Preparation of ECM substrata

2.2.1 Standard Substratum Preparation

Most surfaces were prepared using 35mm bacteriological polystyrene petri dishes (Falcon no. 1008). The undersides of dishes used in aggregation and morphology assays were scored in 5 different areas using a diamond stylus. All ECM components, including Matrigel, were coated onto polystyrene via adsorption from buffered solution. (Matrigel was not used in the common gel form.) Matrigel (Collaborative Biomedical Products), laminin (Collaborative Biomedical Products), fibronectin (Sigma Chemicals), or collagen I (Celtrix; Santa Clara, CA) aliquots were thawed at 4°C overnight and diluted in sterile phosphate buffered saline (PBS) pH 7.4 to the highest desired concentrations of material. Lower concentrations were obtained via serial dilution. Solution concentrations used corresponded to surface densities of 0.001 $\mu g/cm^2$, 0.01 $\mu g/cm^2$, 0.1 $\mu g/cm^2$, 1 $\mu g/cm^2$, and (for Matrigel only) 10 $\mu g/cm^2$; these are calculated concentrations based on the assumption that essentially all ECM proteins present in solution adsorbed to the surface. Dishes were coated with 2 ml ECM solution and incubated for 70-80 minutes at room temperature. After the ECM solution was aspirated, the dishes were exposed to 1.5 ml of a 1 wt.% BSA in PBS solution for 45 minutes at room temperature to block non-specific cell adhesion. The dishes were then washed twice with PBS before medium was added and stored at 4°C. Cells were seeded onto surfaces within 24 hours of ECM coating.

2.2.2 Adhesion Assay Substratum Preparation

Surfaces to be used in the cell-substratum adhesion assays were prepared by cutting rectangular (approx. 75mm x 25mm) pieces ("slides") from the culture surfaces of sterile 100mm polystyrene petri dishes (VWR Scientific; Boston, MA). These slides were then transferred to intact 100mm dishes and coated with Matrigel in the same manner as described above. Solution concentrations were adjusted based on the surface area of the

petri dish to correspond with surface densities of 0.01 $\mu g/cm^2$, 0.1 $\mu g/cm^2$ and 1$\mu g/cm^2$ Matrigel.

Cells were seeded onto these petri dishes at densities of 3,000 - 6,000 cells/cm^2 for 1 $\mu g/cm^2$ dishes and 6,000 - 9,000 cells/cm^2 for 0.1 and 0.01 $\mu g/cm^2$ dishes. These seeding densities allowed for the analysis of a cell population that consisted primarily of single cells. In order to obtain an even seeding density, cells were seeded along the entire length of the slide, after which the dish was rocked back and forth several times.

2.3 Characterization of Substrata

Matrigel is a complex mixture of several proteins, and thus standard methods of measuring protein adsorption are technically challenging. Any method of labeling (e.g., ^{125}I) may selectively label individual components, which may then selectively adsorb. The same issues are encountered using fluorometric assays of protein left in solution after adsorption. One could potentially use antibody probes for the relevant binding sites, but at such low protein concentrations, obtaining unambiguous data requires enormous effort which is not really warranted for the particular points addressed in this study.

The total amount of protein adsorbed at each of the nominal concentrations used in these studies (1 $\mu g/cm^2$, 0.1 $\mu g/cm^2$, 0.01 $\mu g/cm^2$) was assessed by measuring the total nitrogen content as determined by X-ray photoelectron spectroscopy (XPS). This allows for analysis of the relative amounts of adsorbed protein on each substratum.

Matrigel was allowed to adsorb to polystyrene surfaces as described above, after which the surfaces were rinsed four times with PBS. Three samples from each substratum were examined, with ten nitrogen scans and twenty sulfur scans (spot 600μm, resolution 4, window 20 eV, floodgun 5 eV) performed on each sample. An SSX-100 X-ray photoelectron spectrometer (Surface Sciences, Inc.) with a monochromatized Al Kα X-ray source was used for XPS measurements (analyzing the top ca. 50 Å of the surface). Scans

were peak fitted using software provided with the instrument. The lower detection limit for the spectrometer is approximately 500. The intensities of the nitrogen scans (mean ± SD) for each nominal protein concentration were: 9150±923 (1 $\mu g/cm^2$), 1967±286 (0.1 $\mu g/cm^2$), <500 (0.01 $\mu g/cm^2$). The nitrogen level for 0.01 $\mu g/cm^2$ is below the sensitivity range. Independent calibration to relate scan intensities to adsorbed amount was not performed during these studies since the intent of this analysis is simply to assess differences in the amount of material on the surface. Allgor correlated XPS nitrogen intensities with adsorbed protein and found 0.1 $\mu g/cm^2 \approx$ 6000 counts, 0.05 $\mu g/cm^2 \approx$ 3500 counts, and 0.02 $\mu g/cm^2 \approx$ 1500 counts (3). Our surfaces thus have ≈ 0.2, 0.02, and < 0.007 $\mu g/cm^2$. This correlates to approximate molecular densities (assuming that Matrigel consists primarily of laminin) of ≈ 10^{11}, 10^{10}, and < $5x10^9$ molecules/cm^2. Sulfur scans gave readings which were below the machine sensitivity except at the highest nominal concentration. Thus, the concentration of protein on the surface indeed varies in approximately the expected fashion. Throughout the text, substrata are referred to according to their nominal protein concentrations. The possibility of using N:S ratios to try to assess the relative constancy of molecular composition was also examined, but the amount of adsorbed material is below the sensitivity of the sulfur detection at the two lowest adsorbed amounts.

Other protein assays were also utilized in attempting to measure the concentration of adsorbed protein. These are summarized in Appendix A.

2.4 Videomicroscopy and Computer-Based Image Processing

Long-term microscopic observation was accomplished with a Zeiss Axiovert 100 inverted microscope (Carl Zeiss; Germany) equipped with a 10X objective lens. An incubated petri dish holder (Ludl Electronic Products, Ltd.; Hawthorne, NY) on the stage allows long-term culture under microscopic observation. This incubated stage provides a

37°C environment by circulation of water from a constant temperature bath through the stage. Culture medium temperature was read at the conclusion of each experiment to verify that the 37°C temperature was maintained. Compressed air from laboratory fixtures was mixed with CO_2 and flowed continuously through the incubated chamber to maintain a culture medium pH of 7.4 as determined by pH paper. This air/CO2 mixture was heated and humidified immediately prior to introduction into the chamber by bubbling through warm (approx. 50°C) distilled water. This eliminated evaporation of culture medium for up to 12 hrs. (the maximum duration of exposure to the incubated stage environment) as determined by measurement of medium volume.

Cell motility behavior was assessed by recording cells incubated in the above chamber with a Panasonic AG6720A time lapse VCR (Research Precision Instruments; Wayland, MA) at 1/240 real time. The 10x objective lens was used in these analyses and a Hitachi KP-M1U CCD videocamera (Research Precision Instruments; Wayland, MA) provided an additional magnification of 25x, providing a field of view encompassing an area of 0.5 mm^2.

Digital image processing was used to acquire images for morphological analysis, for generating cell number and area data in the adhesion assays, and acquisition of data on cell aggregation and surface coverage. Images were acquired through a Hitachi KP-M1U CCD videocamera and a phase contrast inverted microscope. All images have 320 x 240 pixel areas. For assessment of multicellular aggregate morphology, a Nikon Diaphot microscope with a 4X objective (Research Precision Instruments) was used, allowing for a field of view (after magnification by the camera) of 3.1 mm^2. NIH Image (version 1.49) was also used to arrange digitized images in montage. Quantitative analysis (i.e., adhesion images and analysis of cell areas) were processed from a Zeiss Axiovert 100 microscope with a 10X objective, which gives a 0.5 mm^2 field of view. The limit of resolution provided by this objective is less than 1% of the calculated cell areas. The image

processing software is Macintosh-based and was developed by Engineering Technology Center (Mystic, CT) from a programming environment of LabVIEW (National Instruments; Austin, TX) and Concept Vi (Graftek Imaging; Mystic, CT). The software is set up to analyze and process images from the Zeiss Axiovert 100 microscope and was used with a 10X objective. The system is capable of identifying cells and cell boundaries by subjecting the image to a sequence of two-tailed thresholding, dilation, hole filling, erosion, and low pass filtering. The fundamental image unit recognized is termed a "track," and refers to any material within a single boundary, whether it is a single cell or a group of contiguous cells. For example, a field containing 2 single cells, an aggregate of two cells, and an aggregate of 5 cells would be scored as having 4 tracks (and subsequent steps allow this image to be further parsed into the number of cells). After the image processing steps, several parameters are measured in each observed field, including the number of tracks, location of each track centroid, and the area occupied by each track. Characteristic single-cell sizes can be chosen based on the spreading areas of analyzed cells for use in determining the number of cells in each track.

The image processing software is capable of microscope stage motion control, which was used in cell surface coverage and cell-substratum adhesion measurements.. The software allows for up to 24 separate fields to be selected and analyzed. A Ludl 99S008 motorized microscope stage (Ludl Electronic Products; Hawthorne, NY) was mounted on the Zeiss microscope and interfaced with the software via a nuDrive amplifier (nuLogic Inc.; Needham, MA).

2.5 Cell Aggregation

Aggregation of hepatocytes on the different surfaces was measured by capturing and analyzing digitized images of all pre-scored areas once per day from days 1 through 4. "Macroscopic" aggregation was considered to have occurred when *either* spheroidal

(spherical or hemispherical shaped multicellular units) *or* trabecular (well spread, interconnected monolayers) type aggregates (Figure 2-2) formed from the coupling of cells or groups of cells. Only aggregates that formed during the time frame of day 1-4 were counted as undergoing macroscopic aggregation, i.e., cells that were either seeded as aggregates or that aggregated due to cell spreading between day 0 and day 1 were not considered to have undergone macroscopic aggregation. Detached, floating cells were occasionally observed floating in the medium, but these were primarily non-viable, and so did not contribute to aggregation. Data are reported as the fraction of the total number of fields observed that exhibited this macroscopic aggregation. These measurements were made for surfaces coated with Matrigel, laminin, and fibronectin at solution concentrations corresponding to surface densities of 0.001 $\mu g/cm^2$, 0.01 $\mu g/cm^2$, 0.1 $\mu g/cm^2$, 1 $\mu g/cm^2$, and (for Matrigel only) 10 $\mu g/cm^2$. For each condition, samples from three or four separate cell isolations were examined, with six to ten fields examined in each sample.

2.6 Surface Coverage

The determination of fractional cell surface coverage areas was accomplished by summing the track areas (Σ track areas = Σ single cell areas + Σ cell aggregate areas) present in the observed fields and then dividing this value by the field of view area (0.5 mm^2). Each petri dish was analyzed in this manner at 5 randomly selected areas, and for each given set of conditions (inoculation density, ECM concentration) this procedure was duplicated, providing for 10 data points. These were subsequently averaged to obtain a representative fractional surface coverage. All fractional surface coverage data were obtained on day 1 after cell seeding. This time point was chosen because most cells have attached and spread, but in general have not yet undergone large scale aggregation and morphogenesis. In addition, since the aggregation analysis begins at this time point, it is the most relevant in determining a propensity of these cells to aggregate.

2.7 Morphological Analysis

Aggregates were defined as having spheroidal morphology (spherical or hemispherical shaped multicellular units) *or* monolayered morphology (spread, flattened interconnected cells, or clumps of cells that fail to retract) (Figure 2-2). In some cases spheroids had not formed by day 4, but there appeared to be a darkening and retraction of specific areas of an aggregate characteristic of early spheroid development (Figure 2-2). Since these aggregates exhibited three-dimensional spheroidal-type cellular morphologies in some areas but could not be scored as spheroidal aggregates, they were defined as pre-spheroids. Measurements were made for surfaces coated with Matrigel at nominal surface densities of 0.01 $\mu g/cm^2$, 0.1 $\mu g/cm^2$ and 1 $\mu g/cm^2$. For each condition, samples from approximately six separate cell isolations were examined. Ten separate fields per Matrigel surface density were inspected from each isolation, and morphologies were assigned only in those fields in which aggregates were observed to occur (i.e., fields exhibiting only single cells could not be scored). Assignment of a characteristic morphology was based on the morphology of aggregates on day 4. While monolayers and spheroids never appeared together in the same field, pre-spheroids were observed with both monolayers and spheroids. Since almost all nascent aggregates exist as monolayers (i.e., all cells initially attached to both surface and other cells), and since pre-spheroids are generally observed prior to spheroid formation, we score these "mixed" fields as having the morphologies of the more chronologically advanced type of aggregate. Therefore, fields with both spheroids and pre-spheroids were scored as spheroidal aggregation, while fields with pre-spheroids and monolayers were scored as pre-spheroids.

2.8 Cell Motility

Analysis of cell migration and membrane extension was accomplished using time-lapse videotape analysis. Dishes were observed consecutively during days 1-4 after cell

seeding at 12 hour intervals. This time interval was found to be sufficiently long enough to observe occurrences of hepatocyte migration. At the conclusion of each experiment, the entire videotape was reviewed and scored for the occurrence of classical single-cell locomotion and/or active membrane extension, for solitary cells as well as cell aggregates. All measurements were made for surfaces coated with Matrigel, laminin, and fibronectin at solution concentrations corresponding to surface densities of 0.001 $\mu g/cm^2$, 0.01 $\mu g/cm^2$, 0.1 $\mu g/cm^2$, 1 $\mu g/cm^2$, and (for Matrigel only) 10 $\mu g/cm^2$. Results for cells on Matrigel samples were obtained from 11 separate cell isolations. Although not all protein concentrations were used as substrata for each isolation, data from between 7 and 10 isolations were obtained on each of these concentrations. Results for cells on fibronectin and laminin represent a combination of 4 separate isolations each, with all protein concentrations used as substrata for each isolation. From a given isolation, 5 to 20 cells or cell groups were typically tracked at each concentration.

2.8.1 Cell Locomotion

Classical single-cell locomotion was defined to occur when a cell centroid translocated at least one body length in any direction without contacting another cell over the 12-hour time period observed. Importantly, cells were seeded at low enough surface concentrations so that most cells observed had sufficient free space surrounding them to allow them to meet this criterion if their migratory behavior was sufficiently substantial. Cells that moved at least one body length only after making contact with other cells (i.e., "coupling") were not considered to be exhibiting classical single-cell locomotion but rather an aggregation phenomenon.

2.8.2 Membrane Extension

Membrane extension was defined by the presence of either filopodial or lamellipodial extensions. Long, thin (usually <15 micron width), finger-like projections that extended at least one body length from the edge of the cell were scored as filopodia. Short (i.e., extending less than one body length), broad (usually at least 1/2 cell diameter) extensions were considered to be lamellipodia. Lamellipodia were further categorized as being circumferential (active around the entire cell periphery) or polarized (active at 1, 2 or 3 discrete areas of the membrane). Data generated from the 2-hour and 12-hour observation time periods were indistinguishable, and so were combined.

2.9 Cell-Substratum Adhesion Assay

2.9.1 Design

Cell-substratum adhesion strength was measured by shear flow detachment of cells. With this method a well-defined laminar flow is applied to a surface causing a fraction of adherent cells to detach. The surface shear stress present from such a flow acts as a distractive force to these cells, causing them to detach only when the cell-substratum attachment force is exceeded. By obtaining a relationship between shear stress and cell detachment, we can obtain measurements for relative and (with further analysis and assumptions) absolute values of cell-substratum adhesion strength.

The design of the shear flow detachment chamber used in these studies was based on that of Usami *et al.* (143), and is shown schematically in Figure 2-3. It induces Hele-Shaw flow patterns in the chamber, which provide for a surface shear stress that varies linearly along the centerline of the flow field according to the formula: $\tau_w = \frac{6\mu Q}{h^2 w_1}(1 - \frac{z}{L})$, where τ_w is surface shear stress, μ is fluid viscosity, Q is flowrate, h is channel height (spacing), w_1 is the width at the beginning (origin) of the flow field, z is the distance from the origin along the centerline, and L is the length of the flow field (origin to outlet) along

the centerline. The chamber was machined from 1/4" lexan and the gasket cut to the proper shape from a uniform 260 μm Teflon sheet. Two-sided Scotch tape (3M; Product # 665) was cut in this shape to attach the gasket to the chamber. Subtracting a 350 μm entrance length, the dimensions of the chamber are w_1=1.35 mm, L=5.65 cm, and h=365 μm. Flowrate, Q, is controlled by changing the height of a constant head tank. The tank outlet is equipped with a stopcock to turn flow on and off. PBS (pH 7.4) with Ca^{2+} and Mg^{2+} was the fluid used in these experiments and was maintained at 37°C by immersing the constant head tank in a water bath. In some cases increased fluid viscosity was desired (to increase the shear stress), and so 1.5 wt.% high molecular wt. dextran (SIGMA Chemical Co.; Product # D-1037) was added to the PBS which doubled the viscosity (from 0.6 cp to 1.3 cp) as measured at 37°C by a Brookfield model DV-II digital viscometer (Brookfield Engineering Laboratories, Inc.; Stoughton, MA).

2.9.2 Operation

Slide substrata are prepared as described in section 2.2.2. Immediately prior to the introduction of the cell-coated slide to the chamber, a positive meniscus of PBS is allowed to form in the flow area (i.e., the area outlined by the gasket). Cell medium is aspirated from the petri dish containing the slide to be assayed, after which the slide is removed with forceps. The slide is placed on the top of the chamber (cells facing the gasket), which causes the meniscus to flatten and spread. Introduction of the slide in the chamber in this manner minimizes the formation of bubbles in the device. The excess fluid is then wiped from the top and sides of the slide, after which the slide is sandwiched between the top of the chamber and a glass microscope slide to provides rigidity. Two parallel bar clamps are applied to the apparatus perpendicular to the direction of flow (one near the inlet to the flow field, one near the outlet) to ensure the formation of a tight seal and to prevent movement of the slides. The entire assembly process takes approximately 2 minutes. PBS is then

slowly (<1ml/min.) perfused through the chamber to remove dead cells and residual debris. Within 5 minutes of exposure to this slow flow, the number of tracks is counted in each of 20 fields. Cell areas and total number of cells are determined as described above. The fields are spaced at 2.5 mm intervals along the centerline and are counted using the image processing system and microscope stage motion control described above. Shear flow is then initiated by opening the stopcock. Flowrates are measured with a stopwatch and a graduated cylinder, which collects the PBS exiting the chamber. After the cells are exposed to the flow for 2 min., the stopcock is closed. A 2 min. exposure time was chosen based on previous observations of cell detachment during exposure to shear flow for up to 30 min. Nearly all those cells that detached did so within 2 min. of exposure to flow. Final track counts are then taken at each of the positions initially analyzed.

During the time to which cells are exposed to PBS in the course of an adhesion experiment (less than 10 minutes), no significant changes in cell morphology were observed to occur. Experiments in which cells are cultured in both PBS and complete medium indicate that the initial spreading behavior is also not altered by exposure to PBS (155). In addition, our previous attempts to detach hepatocytes from Matrigel substrata by incubating the cells overnight in calcium free PBS with EDTA resulted in neither cell detachment nor alteration of morphology. These results suggest that the adhesive behavior of hepatocytes after 10 minutes of exposure to PBS is indistinguishable from the behavior of these cells in complete medium.

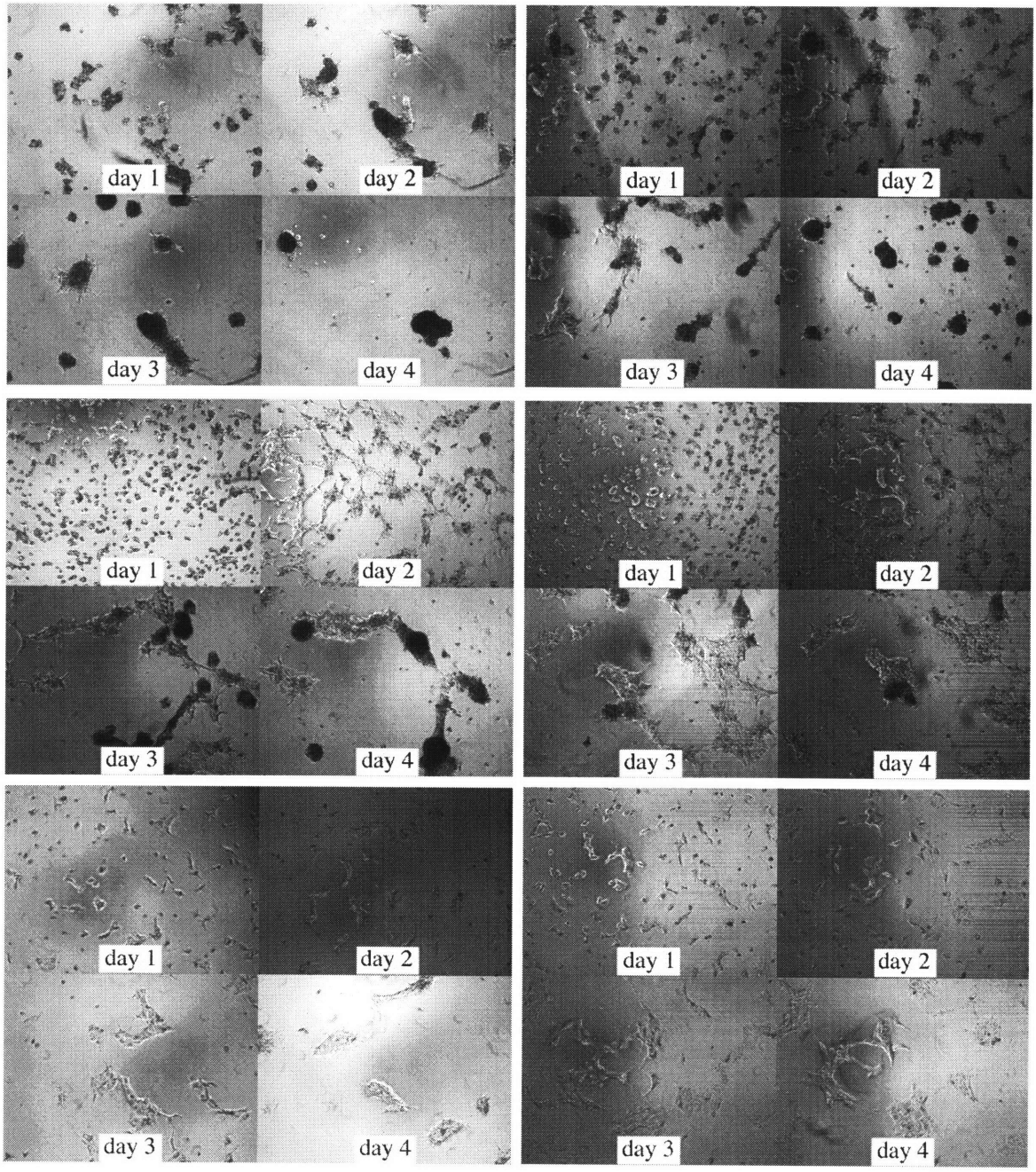

Figure 2-1. Morphological classification of hepatocyte aggregates *in vitro*. Photographs were taken of hepatocyte aggregation during a 4-day period on Matrigel substrata: top left -- spheroids (0.01 $\mu g/cm^2$); top right -- spheroids (0.1 $\mu g/cm^2$); middle left -- spheroids/pre-spheroids (0.1 $\mu g/cm^2$); middle right -- monolayers/pre-spheroids (0.1 $\mu g/cm^2$); bottom left -- cell clumps (1 $\mu g/cm^2$); bottom right -- monolayers (1 $\mu g/cm^2$).

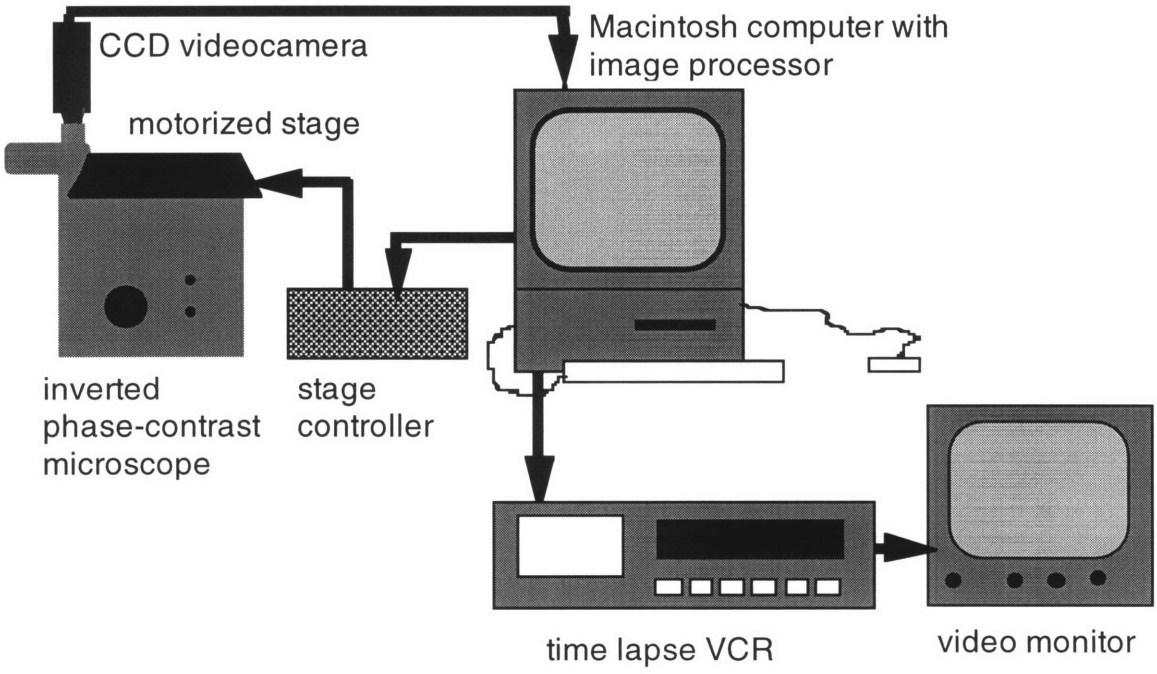

Figure 2-2. Schematic diagram of videomicroscopy apparatus.

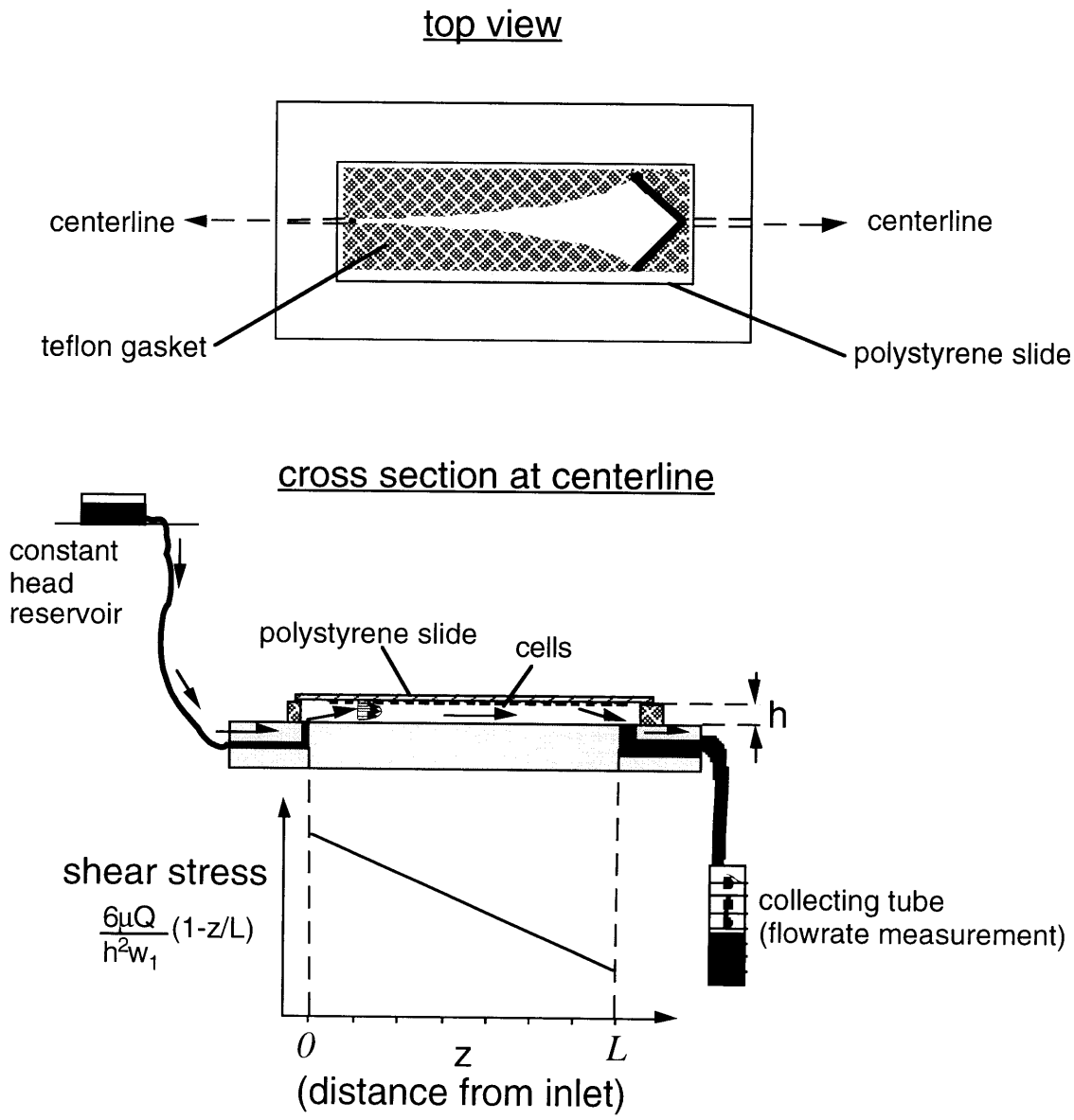

Figure 2-3. Schematic diagram of cell detachment assay.

3 Effects of Variation in Substratum Properties on Hepatocyte Aggregation and Aggregate Morphogenesis

3.1 Introduction

The aggregation of primary hepatocytes has been observed on a variety of surfaces comprised of different architectures and/or molecular compositions (71, 65, 64, 111, 96, 97). It has been demonstrated on these substrata that the extent of aggregation (96) as well as the resulting aggregate morphology (71, 65) play an important role in determining the ultimate behavior of these cells. Both of these parameters were observed to depend on the particular substratum onto which the hepatocytes were initially seeded. It is highly desirable, then, to achieve an understanding of *how* a surface can control these "macroscopic" parameters in order to predictably manipulate cell behavior.

The substratum presents both biophysical and biochemical signals to the cells through interactions with adhesion receptors. The objective of this work is to delineate the roles each of these play in cellular response. This can be accomplished through systematic variation of these signals. In terms of biochemical signals, it has been demonstrated that hepatocytes attach to different extracellular matrix components (e.g., laminin, fibronectin, collagens, heparan sulfate proteoglycan, etc.) through different sets of receptors (Table 1-2). Exposure of hepatocytes to each of these different matrices individually while biophysical substratum properties are held approximately constant can then facilitate the analysis of the effects of biochemical signaling on cellular behavior. From a biophysical perspective, changing the concentration of each of these same matrix molecules will in turn influence the number of receptor-ligand interactions. This presumably alters the strength of adhesion between cell and substratum, thereby altering the biophysical nature of cell-substratum interactions.

The results described in this chapter suggest that substratum effects are largely biophysical in nature. This finding provides a fundamental basis for the detailed mechanistic analyses performed in subsequent chapters.

3.2 Results

Hepatocyte aggregation and aggregate morphogenesis were observed on ECM-coated substrata. Photographs were taken of pre-scored fields using a 4X objective at various time intervals (typically every 24 hours) from days 1 to 4 after seeding. From these pictures, the extent of aggregation and resulting morphology were determined as described in chapter 2. In addition, the level of cell surface coverage for each set of conditions (i.e., matrix type, concentration, seeding density, perfusion date) was determined by averaging the cell coverage fractions of 10 separate fields as measured by image analysis.

3.2.1 Dependence of Hepatocyte Aggregation on Extracellular Matrix Type and Concentration

The macroscopic aggregation of hepatocytes on polystyrene petri dishes coated with Matrigel, laminin, or fibronectin was investigated. Aggregation was quantified by examining pre-scored areas on each petri dish for the occurrence of macroscopic aggregation from day 1 to day 4, as described in chapter 2. The fraction of fields examined that exhibited macroscopic aggregation was determined over the range of coating concentrations of Matrigel, laminin, and fibronectin for hepatocytes initially seeded at identical inoculation densities (4000 cells/cm^2). The resulting data are shown in Figure 3-1. On each of the substrata the extent of aggregation increased as ECM coating concentration was increased. In addition, at this low cell seeding density the extent of aggregation depended on the type of ECM substratum. Hepatocytes seeded onto Matrigel aggregated at all of the concentrations investigated, with a maximum of approximately 70%

of the observed fields exhibiting aggregation at 1 and 10 μg/cm^2. Cells seeded on laminin did not aggregate below 0.1 μg/cm2 and showed a maximum aggregation of roughly 40% of the observed fields at 1 μg/cm^2. Similarly, hepatocytes seeded on 1 μg/cm^2 fibronectin gave rise to the highest extent of aggregation observed on this ECM, about 40% of the observed fields.

3.2.2 Cell Attachment and Surface Coverage

An important trend observed during the previous studies is that the initial cell attachment numbers and cell spreading areas increased as each ECM concentration increased. The initial cell attachments for 4,000 cells/cm^2 seeding density ranged from about 1,500 cells/cm^2 at the lowest ECM concentrations to nearly 4,000 cells/cm^2 for surfaces coated with 10 μg/cm^2 Matrigel. The corresponding diameters of these cells were approximately 25 μm on low ECM concentrations to 65 μm on high ECM concentrations. This means that the corresponding total cell coverage ranged from about 0.7% to 13% of substratum surface area, making aggregation much more likely to occur at the higher ECM concentrations. Therefore, while these constant cell seeding density experiments show that hepatocyte aggregation depends on ECM surface concentration, it is unclear from this data whether the observed effects can be directly attributed to particular matrix types and concentrations or are instead simply due to an increased cell coverage area at higher ECM concentrations.

In order to address this issue the relationship between the number of cells initially seeded and the 24 hr. fractional surface coverage achieved by the cells on various concentrations of Matrigel (0.01 μg/cm^2 - 10 μg/cm^2) was determined. Fractional surface coverage, defined as the fraction of the petri dish surface covered by cells, incorporates effects due to differences in both attached cell numbers and cell spreading that occur at different ECM concentrations. Variation in surface coverage values was attained by seeding the cells at a range of inoculation densities (4,000 cells/cm^2 - 45,000 cells/cm^2) on

each Matrigel concentration. Analysis of variance (ANOVA) at a significance level of 0.05 indicates that these data can be grouped into two levels--a low initial seeding level (4,000 - 8,000 cells/cm^2) and a high initial seeding level (15,000 - 45,000 cells/cm^2). Figure 3-2 shows the dependence of fractional surface coverage on Matrigel concentration at these two levels of cell seeding. A companion graph of initial cell attachment vs. Matrigel concentration is shown in Figure 3-3.

In order to accurately represent the aggregation of hepatocytes on different substrata it is necessary to first incorporate the effects of cell surface coverage. Ideally, hepatocyte aggregation could then be compared for cells attached varying ECM concentrations with identical fractional surface coverages. In this way any "advantage" in aggregation gained by those cells seeded on the highest ECM concentrations due to increased cell attachment and spreading areas is effectively eliminated. Figure 3-4 represents the levels of aggregation observed in a number of experiments on Matrigel concentrations from 0.01-10 $\mu g/cm^2$. These data are plotted as functions of the fractional cell surface coverage, which was quantified during the course of each experiment. As expected, a positive correlation is observed between aggregation and fractional surface coverage for all Matrigel concentrations examined.

Preliminary aggregation data of hepatocytes on laminin and fibronectin substrata were also obtained to determine whether the effects of these matrix molecules on aggregation when normalized to cell surface coverage are as significantly different from those of Matrigel as in the cases when the cells are seeded at constant (low seeding) densities (i.e., Figure 3-1). These data are shown in Figure 3-5 combined with Matrigel aggregation data and show the same positive correlation observed with the Matrigel data. Chi-square contingency analysis (significance level of 0.05) indicates that laminin and fibronectin data are indistinguishable from Matrigel data, and so the differences between aggregation behavior on these different ECM proteins are not detectable when the data are sorted according to cell surface coverage alone.

Analysis of hepatocyte aggregation as in Figure 3-4 allows for aggregation data to be plotted as a function of extracellular matrix concentration by separating these data into low, medium, and high fractional surface coverage ranges, which is significant in that these results are presumably due only to the effects of cell-cell and cell-substratum interactions as cell attachment and spreading effects are no longer an issue. Such an analysis is shown in Figure 3-6 for hepatocytes attached to varying concentrations of Matrigel. Aggregation data for this plot are grouped into low (1% - 8%), intermediate (9% - 16%) and high (17% - 24%) surface coverage bins. Statistical analysis (chi-square contingency at a significance level of 0.05) of these data indicates that aggregation varies with Matrigel concentration at low and high surface coverage concentrations. Further comparisons among data within these two groups via two-sample t-tests (significance level =0.05) reveal no comprehensive relationship between aggregation and Matrigel concentration.

These results provide quantitative verification that the ability of hepatocytes to aggregate is dependent not only on the initial coverage of the substratum by cells, but also on the ECM concentration of this substratum.

3.2.3 Dependence of Aggregate Morphology on Extracellular Matrix Type and Concentration

Qualitative observations of hepatocyte aggregate morphology on ECM-coated polystyrene provide for a preliminary analysis of the effects of substratum properties on morphogenesis. Matrigel, fibronectin, laminin and collagen I substrata were prepared as described in chapter 2 and fields from each petri dish examined on days 1 and 4 after seeding. By day 4, aggregates generally form into either spheroids (spherical or hemispherical multicellular aggregates, cells adhere other cells but not necessarily to the substratum) or monolayers (single layered aggregates, all cells attach to both other cells and the substratum). As Figure 3-7 illustrates, both spheroids and monolayers form on each type of matrix examined. But while monolayers form preferentially at high ECM

concentrations, spheroids form exclusively at low matrix concentrations. Hepatocytes interact with these matrix components via different sets of receptors(78). Therefore, these results are not limited to the presence or absence of particular ECM molecules and/or growth factors and appear to depend only on ECM *concentration,* suggesting that the primary mechanism is biophysical.

In order to test the dependence of hepatocyte aggregate morphogenesis on ECM concentration, aggregate morphology was quantified on Matrigel-coated substrata. Quantification was accomplished by analyzing fields in which aggregation occurs and determining the morphology on day 4 in each of these. The data in Table 3-1 show the results from this analysis and indicate that aggregate morphology can be considered to have a binary relationship (i.e., spheroidal or monolayered) with Matrigel concentration. It is clear that spheroidal and hemispheroidal aggregates form predominantly at low nominal Matrigel concentrations (0.01, 0.1 $\mu g/cm^2$), while high Matrigel coating concentrations (1 $\mu g/cm^2$) support cell spreading and the formation of trabecular or monolayered aggregates. Chi-square analysis followed by paired t-tests at a significance level of 0.05 confirm this observation. These results are independent of cell seeding density and cell surface coverage. Monolayers were observed to form on 1 $\mu g/cm^2$ substrata at all observed seeding densities and at surface coverages (measured on day 1) that ranged from 4% coverage to nearly 73% coverage (Figure 3-2). Likewise, spheroids formed on 0.1 and 0.01 $\mu g/cm^2$ substrata at both low and high cell seeding densities and at surface coverages (measured on day 1) ranging from 2% to 23% coverage (Figure 3-2).

3.3 Discussion

The aggregation of epithelial cells and subsequent morphogenesis of aggregates is an important phenomenon in the functional reconstruction of three dimensional tissues both *in vitro* and *in vivo*. The studies described in this chapter deal with the effects that changes in substratum properties have on hepatocyte aggregation and aggregate morphogenesis.

Hepatocyte aggregation was measured by determining the fraction of fields exhibiting macroscopic aggregation as defined in chapter 2. It should be noted that this type of analysis does not attempt to account for the fate of each individual cell in a particular field but instead serves as an indication of the tendency of cells on each substratum to aggregate.

It was initially found that the extent of aggregation *in vitro* depends on the type *and* concentration of the extracellular matrix substratum. Figure 3-1 illustrates the fraction of observed fields in which aggregation is present as a function of both ECM type and concentration for cells seeded at identical inoculum densities. Hepatocytes were observed to aggregate to the greatest degree on Matrigel, with a minimum of about 25% of observed fields showing aggregation at low coating concentrations (0.001 and 0.01 $\mu g/cm^2$) and a maximum of approximately 70% at 1 and 10 $\mu g/cm^2$. Aggregation also occurred on laminin, but to a lesser extent at all concentrations; noticeable aggregation was not found below a laminin coating concentration of 0.1 $\mu g/cm^2$ and was roughly 40% at 1 $\mu g/cm^2$. Fibronectin was even less supportive, with no significant aggregation observed below a concentration of 1 $\mu g/cm^2$, where about 20% of the observed fields showed aggregates. However, it is important to point out that these results are potentially misleading due to the observed increase in initial cell attachment and spreading areas for cells seeded at higher ECM concentrations.

To address this issue, the aggregation behavior of hepatocytes on a range of Matrigel concentrations (0.01 to 10 $\mu g/cm^2$) was compared based on the total cell surface coverage present at each concentration. These results indicate a strong dependence of aggregation on cell surface coverage (Figure 3-4). This is a logical result, as hepatocyte cultures with high levels of cell coverage would obviously be expected to aggregate to a higher degree than those with low levels of cell coverage. Less intuitive is the result that ECM concentration plays a role in guiding hepatocyte aggregation (Figure 3-6) but that ECM type is not actively involved (Figure 3-5). While the nature of the hepatocyte-

substratum interactions influencing aggregation behavior is still unknown, the observation that the *concentration* of ligand present on the surface is important (and not the *type* of ligand) suggests that the biophysical properties of the substratum (e.g., adhesivity) may be the primary determinants of aggregation behavior with integrin signaling playing a lesser role. At any rate, further analysis of this process requires detailed mechanistic information regarding hepatocyte aggregation. This topic is studied in greater detail in chapters 4 and 5.

Once hepatocytes have aggregated, it has been shown that their resulting morphology is a key factor in determining the metabolic behavior of these cells in culture. Hepatocytes in spheroidal aggregates typically exist in a differentiated, non-proliferative state, whereas those cells that develop into monolayers or flattened "trabecular" aggregates are more likely to proliferate and less likely to differentiate (96, 152). It has been shown that the substratum to which hepatocytes are initially seeded is a key parameter in the determination of hepatocyte aggregate morphology (71, 64, 138). Studies described in this chapter provide observations of hepatocyte aggregate morphogenesis on various types and concentrations of ECM substrata, allowing for thorough analysis of this phenomenon.

In the initial studies of hepatocyte aggregation phenomena the maturation and morphogenesis of hepatocyte aggregates were observed through the first four days in culture on substrata ranging from 0.001 $\mu g/cm^2$ to 1 $\mu g/cm^2$ Matrigel, laminin, collagen I or fibronectin. Each ECM type was observed to support both spheroidal and monolayered aggregate morphology depending on the initial molecular coating concentration (Figure 3-7). Spheroids tended to form at low adsorption levels of each matrix component while monolayers formed at high levels. Hepatocytes interact with each these components via different receptors (78), which indicates that a specific receptor-ligand signaling event is apparently not necessary in the evolution of either morphological type. Rather, as with the extent of aggregation, final aggregate morphology appears to depend on matrix concentration, indicating that the primary mechanism responsible for hepatocyte aggregate morphology is biophysical in nature.

A more detailed analysis of the dependence of hepatocyte aggregate morphogenesis on ECM concentration was performed with hepatocytes seeded onto Matrigel-coated surfaces. Morphology on each Matrigel concentration is now quantified, as shown in Table 3-1. Typically, spheroidal-type aggregates formed on 0.01 $\mu g/cm^2$ and 0.1 $\mu g/cm^2$ and monolayered aggregates formed on 1 $\mu g/cm^2$. These results verify a binary relationship between aggregate morphology and matrix concentration: spheroids form on substrata with low matrix concentrations, monolayers form on substrata with high matrix concentration. This result is *independent* of matrix type (Figure 3-7).

Since initial cell attachment was observed to depend on initial matrix coating concentration, one concern that arises from the above analysis is that the results may be due to differences in cell number rather than substratum matrix concentrations. This possibility was investigated by examining the morphologies of all hepatocyte aggregates which formed on the range of seeding densities and Matrigel concentrations shown in Figures 3-2 and 3-3. These observations indicate that whenever aggregation occurs, regardless of the seeding density or surface coverage, monolayered morphology results at high matrix concentrations and spheroidal morphology results at low matrix concentrations.

It is therefore established that the extracellular matrix plays a role in the evolution of hepatocyte aggregates. Matrix concentration exhibits influence over hepatocyte aggregation, although the manner in which this occurs cannot be ascertained based only on the data reported in this chapter. Matrix type appears to affect the aggregation process in a passive manner and only insofar as it affects cell surface coverage. The effects of matrix on aggregate morphogenesis are more prominent and appear depend on matrix concentration in a binary relationship with spheroids forming at low matrix concentrations and monolayers forming at high matrix concentrations. These results are independent of the type of molecules present in the ECM. While these results suggest that biophysical phenomena play important roles in hepatocyte aggregation and morphogenesis, further analysis requires more detailed mechanistic information regarding the aggregation process.

It is clear then that the next step in these studies of hepatocyte aggregation must involve the elucidation and analysis of the cellular mechanisms underlying hepatocyte aggregation.

Matrigel conc.	Fraction of fields exhibiting: spheroids	pre-spheroids	monolayers
1 $\mu g/cm^2$	0/63	1/63	62/63
0.1 $\mu g/cm^2$	63/75	9/75	3/75
0.01 $\mu g/cm^2$	58/60	0/60	2/60

Table 3-1. The fractions of observed aggregate-containing fields exhibiting spheroids, pre-spheroids, and monolayers on 1 $\mu g/cm^2$, 0.1 $\mu g/cm^2$, and 0.01 $\mu g/cm^2$ Matrigel substrata.

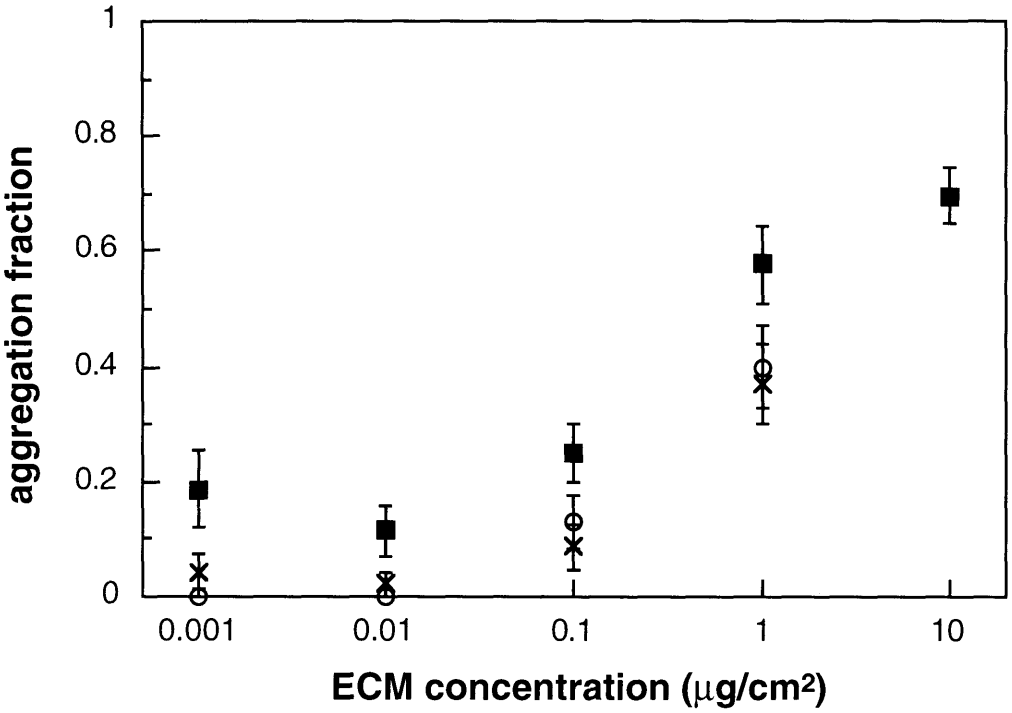

Figure 3-1. Dependence of hepatocyte aggregation on composition of the extracellular matrix substratum. The fraction of observed fields in which aggregates formed is plotted as a function of the calculated surface-coating concentration for Matrigel (■), laminin (O), and fibronectin (×) substrata. Cells were seeded at an inoculation density of 4,000 cells/cm^2.

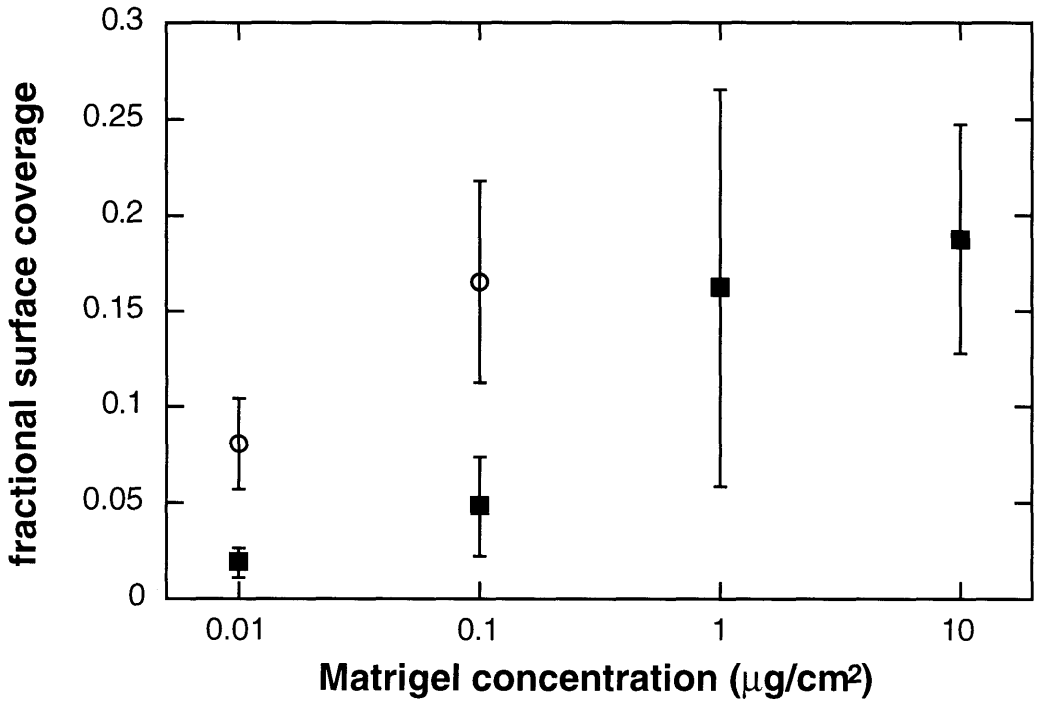

Figure 3-2. Fractional coverage of the surface by hepatocytes seeded at low (4,000 - 8,000 cells/cm^2) (■) and high (15,000 - 45,000 cells/cm^2) (○) inoculation densities on Matrigel substrata.

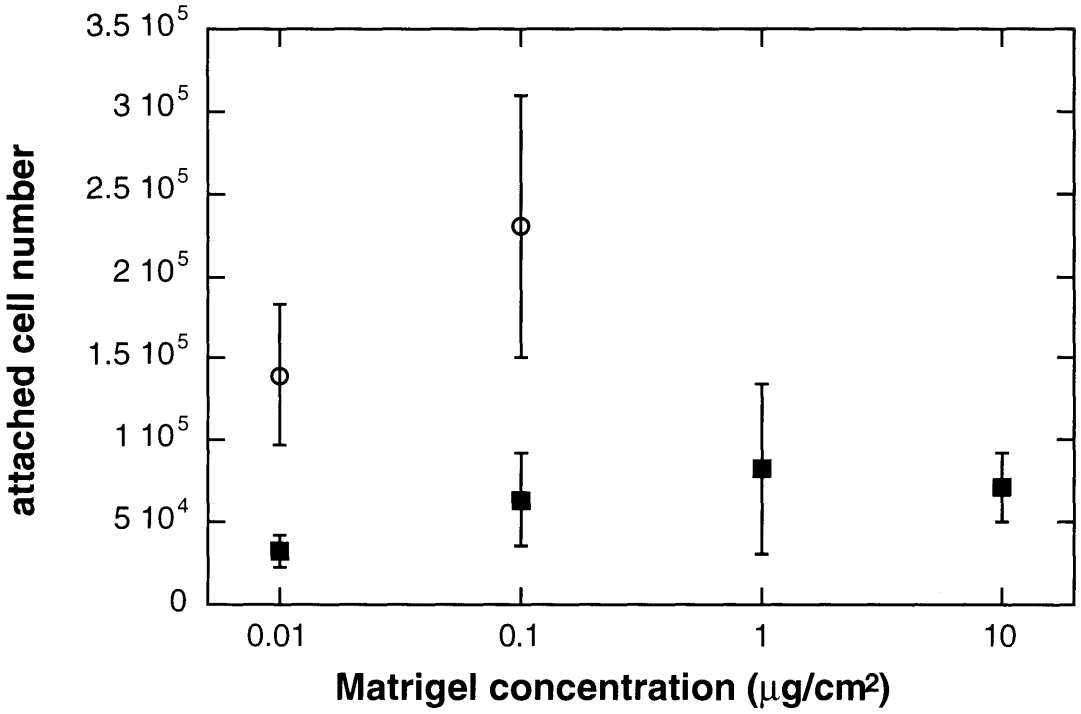

Figure 3-3. Cell attachment to Matrigel substrata for hepatocytes seeded at low (4,000 - 8,000 cells/cm^2) (■) and high (15,000 - 45,000 cells/cm^2) (○) inoculation densities.

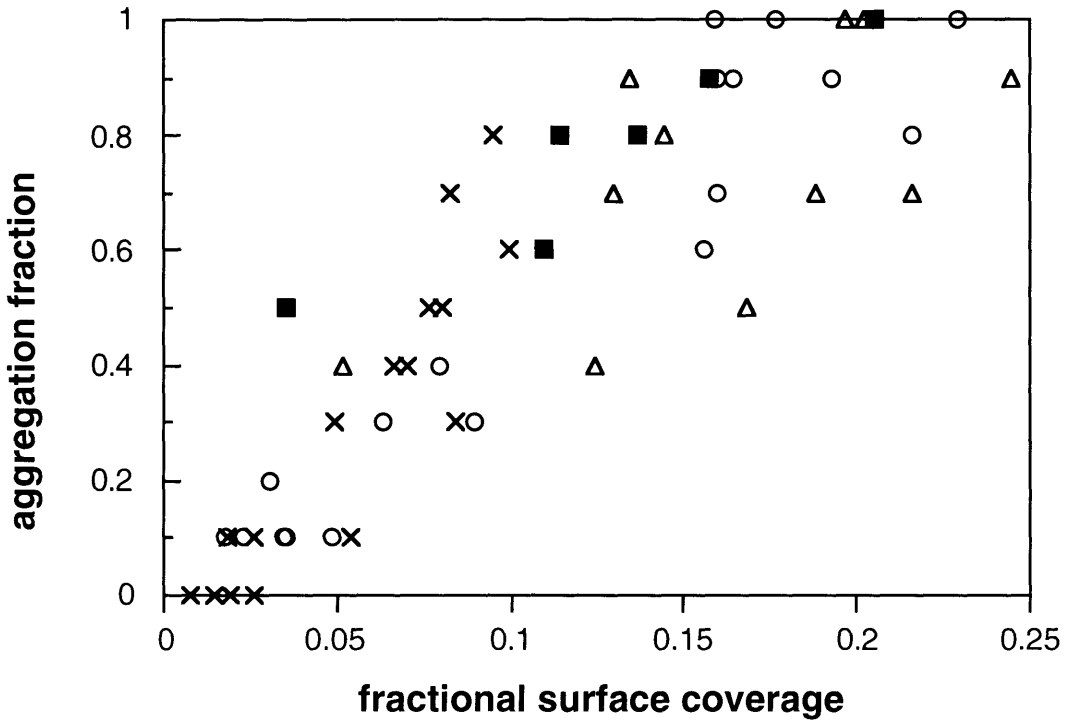

Figure 3-4. Dependence of hepatocyte aggregation on cell coverage area. The fraction of observed fields in which aggregates formed is plotted as a function of the average fractional surface area in each observed field occupied by cells for nominal Matrigel surface-coating concentrations of 10 μg/cm^2 (Δ), 1 μg/cm^2 (■), 0.1 μg/cm^2 (○), and 0.01 μg/cm^2 (×).

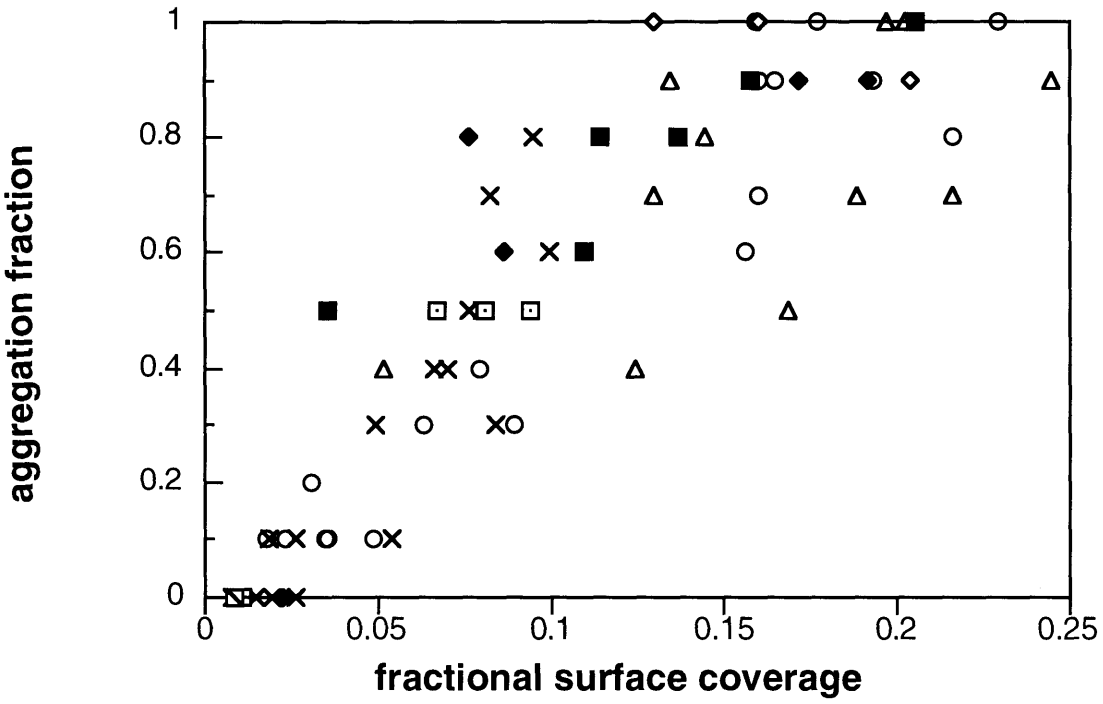

Figure 3-5. Dependence of hepatocyte aggregation on cell coverage area for different types of ECM. The fraction of observed fields in which aggregates formed is plotted as a function of the average fractional surface area in each observed field occupied by cells for nominal surface-coating concentrations of 10 μg/cm^2 Matrigel (Δ), 1 μg/cm^2 Matrigel (■), 0.1 μg/cm^2 Matrigel (○), 0.01 μg/cm^2 Matrigel (×), 1 μg/cm^2 laminin (◆), 0.1 μg/cm^2 laminin (◇), 1 μg/cm^2 fibronectin (□), 0.1 μg/cm^2 fibronectin (⊞), and 0.01 μg/cm^2 fibronectin (⧅).

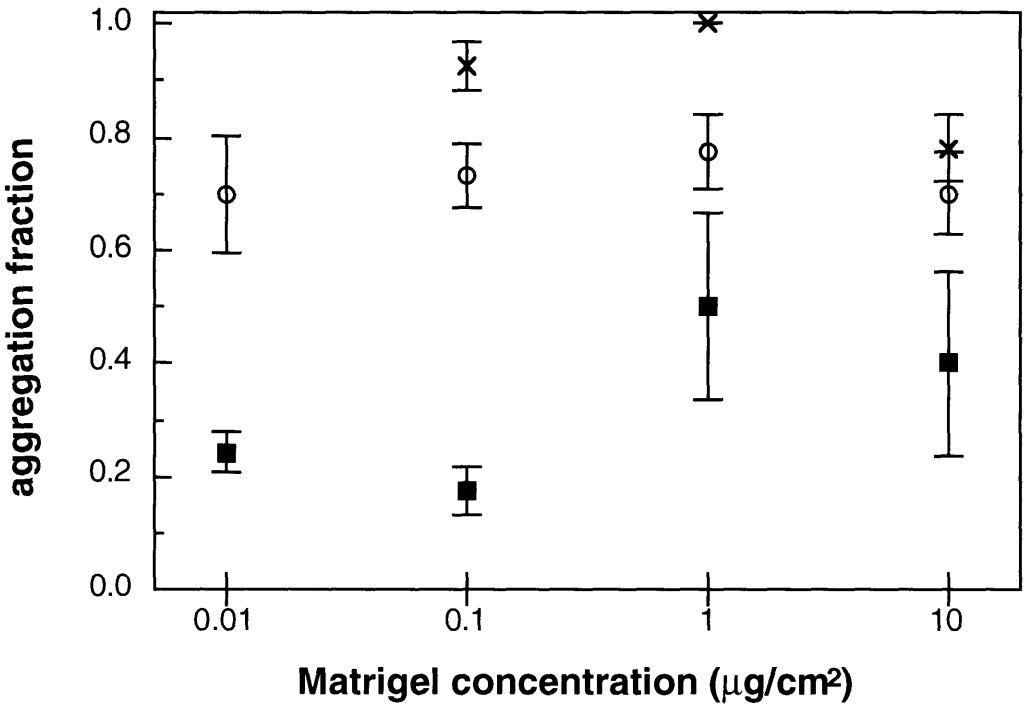

Figure 3-6. Dependence of hepatocyte aggregation on Matrigel concentration for culture systems of similar fractional surface coverages. The fraction of observed exhibiting macroscopic aggregation is plotted as a function of Matrigel concentration for low (0.01 - 0.08) (■), medium (0.09 - 0.16) (○), and high (0.17 - 0.24) (×) ranges of fractional surface coverage.

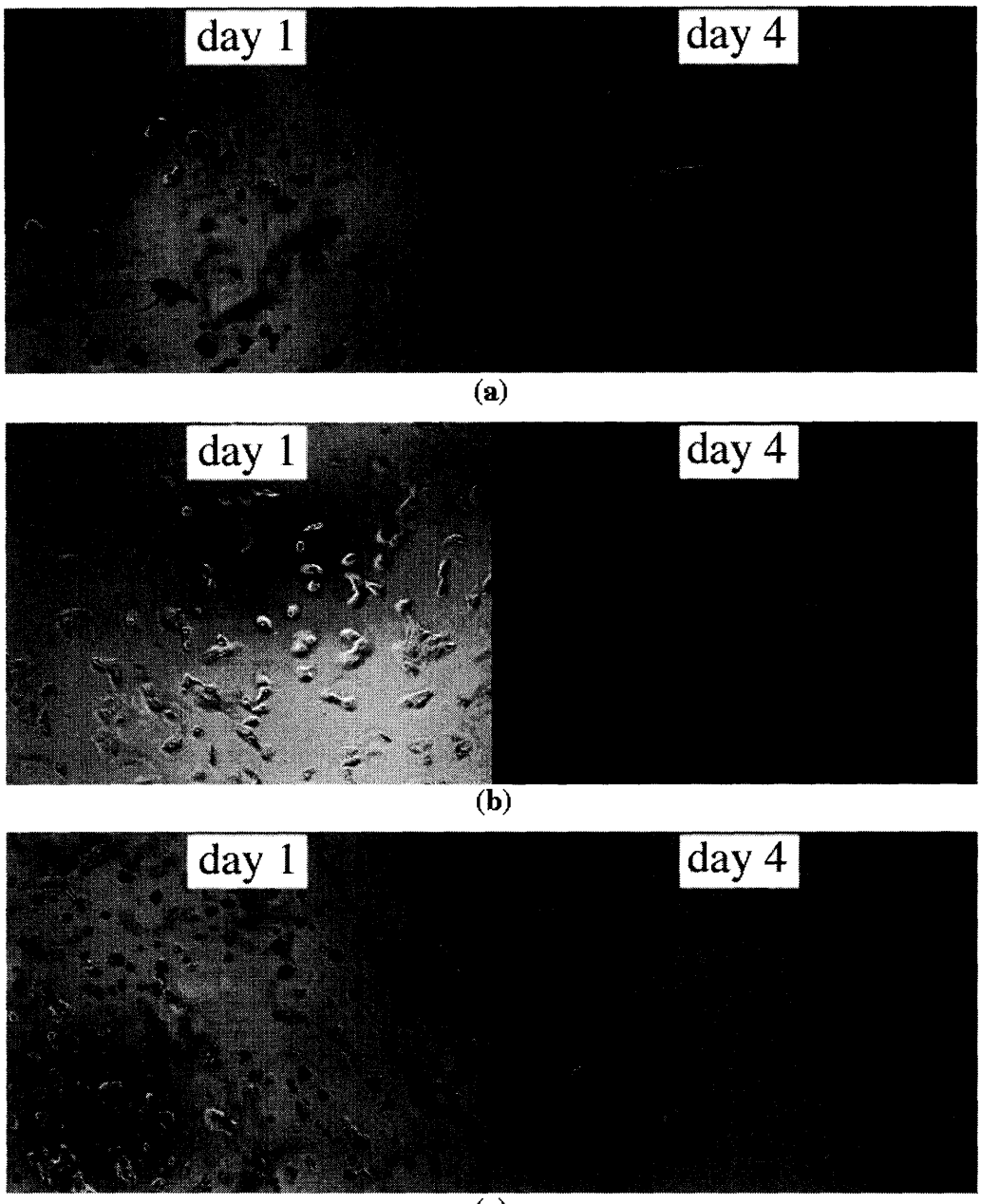

Figure 3-7. Morphology of hepatocyte aggregates on substrata of different ECM types and concentrations. Photographs are taken on day 1 and day 4; a) spheroids forming on 0.01 $\mu g/cm^2$ laminin; b) monolayers forming on 1 $\mu g/cm^2$ laminin; c) spheroids forming on 0.01 $\mu g/cm^2$ fibronectin; d) monolayers forming on 1 $\mu g/cm^2$ fibronectin; e) spheroids forming on 0.001 $\mu g/cm^2$ collagen I; f) monolayers forming on 1 $\mu g/cm^2$ collagen I

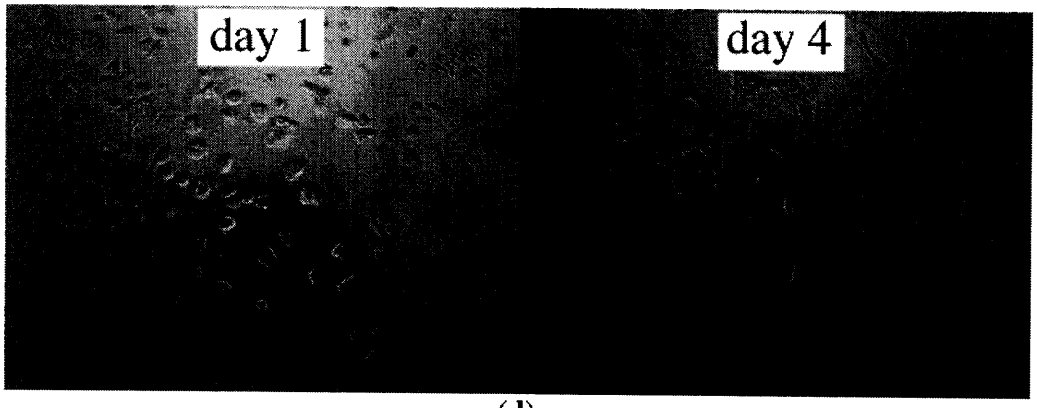

(d)

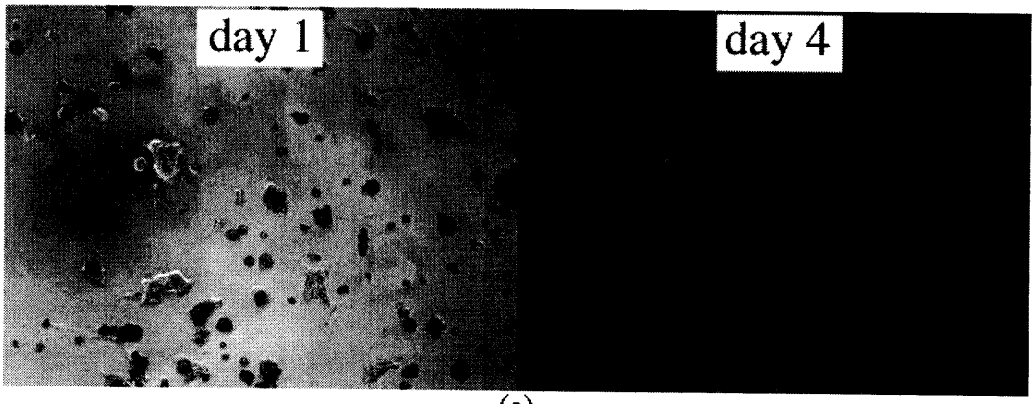

(e)

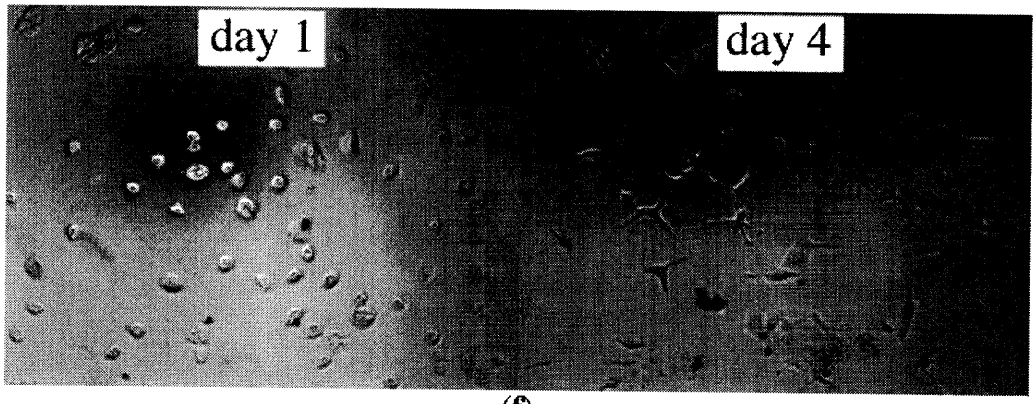

(f)

4 Cellular Mechanisms in Hepatocyte Aggregation and Aggregate Morphogenesis

4.1 Introduction

In chapter 3, the aggregation behavior of hepatocytes *in vitro* was shown to depend primarily on cell seeding density and the concentration of surface-bound ECM. In order to progress in the understanding of this relationship, it is necessary to first determine the cellular mechanisms which underlie hepatocyte aggregation. Once these mechanisms are determined, they themselves can then be studied as functions of the substratum properties on which aggregation is observed.

Reports dealing directly with these mechanisms of hepatocyte aggregation are difficult to find. Processes underlying epithelial cell aggregation in existing literature are often referred to in terms of cell migration, both *in vitro* (6) and *in vivo* (4). It seems logical to presume that cell migration might play a central role in epithelial aggregation since many epithelial cell types have demonstrated an ability to migrate. For hepatocytes, however, this is currently an open question. There have been no explicit reports of hepatocyte migration heretofore, but it has been suggested that these cells can and do migrate. The "streaming liver" model predicts a continuous production of new hepatocytes at the outer rim of the portal space which then migrate along the sinusoid toward the central vein where they are eventually eliminated (153). The observed redistribution of tritiated thymidine-labeled hepatocytes within hepatic plates labeled after partial hepatectomy (4) and during normal postnatal growth of the liver (153) has been used as evidence supporting this hypothesis. However, it has also been suggested that this redistribution actually results from passive hepatocyte movement or the reutilization of label by other cells located nearer the hepatic veins (37). In support of this, experiments similar to those described above but employing ß-galactosidase genetic labeling show no such redistribution (13), suggesting

that these previously reported results were indeed artifactual. Identification within the liver parenchyma of ß-galactosidase-labeled hepatocytes originally transplanted in the spleen has also been used as evidence of hepatocyte migration (99), but this study provides no direct evidence of active migration. These suppositions all share a fundamental weakness in that the conclusions drawn regarding the occurrence of hepatocyte migration are based on the inferences from the displacement of labeled cells and not on direct observation of migration. Therefore, any detailed analysis regarding cellular mechanisms in the aggregation process must involve direct observation of hepatocyte behavior.

The results of the experiments described in this chapter indicate that cell membrane extension, not cell migration, is mechanistically responsible for hepatocyte aggregation. In addition, a cell contraction step appears to be typically involved in this process. This observation leads to the formation of a hypothesis regarding the nature of substratum influence over hepatocyte morphogenesis.

4.2 Results

In order to uncover the mechanisms responsible for hepatocyte aggregation, direct observation of hepatocytes on laminin, fibronectin, or Matrigel-coated substrata was accomplished with the use of time-lapse videomicroscopy over the 4-day culture period. Cells were cultured on a microscope stage incubated petri dish holder and recorded over 12 hour intervals at 1/240th real time. These videotapes were then reviewed and scored for classical cell migration and cell membrane extension. The substrata analyzed were identical to those used in chapter 3 for observations of aggregation phenomena.

4.2.1 Hepatocyte Migration

Because aggregation of epithelial cells may be hypothesized to rely substantially on cell locomotion, the migration behavior of hepatocytes seeded onto the ECM-coated petri

dishes was examined. Classical single-cell locomotion was scored when a cell was observed to move at least one cell-length without contacting another cell during the 12-hour observation period. The reason for using this definition was to distinguish single-cell locomotion from direct cell/cell coupling interactions, which are considered to be aggregation phenomena. Cells were seeded at low (4,000 cells/cm^2) densities, and so typically the area surrounding each cell was sufficiently vacant to allow for unhindered cell migration.

Table 4-1 shows the fraction of observed cells that actively migrated at least one body length as a function of the ECM concentrations on the various substrata. Data are for 12-hour observation periods. At no concentration of any of the ECM substrata were more than 6% of the cells observed to exhibit classical single-cell locomotion Moreover, no significant trends were noted as a function of either type or concentration of the ECM coating proteins.

4.2.2 Hepatocyte Motility

In the course of examining time lapse videotape for classical locomotion behavior, several instances of cell-cell coupling were observed. Coupling is defined as the attachment of one cell membrane to another. As illustrated above, these could not be attributed to classical single cell locomotion. In almost every instance, the observed aggregation was directly attributable to membrane extension in the form of either lamellipodial (short, broad, flattened) or filopodial (long, thin, cylindrical, "needle-like") protrusion. As shown in Figure 4-1, the typical sequence of events in the aggregation process involves membrane-extension driven coupling followed by what appears to be a discrete contractile event which, in some cases, causes a rapid retraction of the peripheral edges of the nascent aggregate.

The key first step in this aggregation process was observed to be membrane extension. Because the subsequent steps occur quickly once cells make membrane-induced contact, membrane extension can be thought of as the rate-limiting step in the aggregation process. Thus the observed degree of aggregation should directly correlate with membrane extension.

In order to quantify this observation, active cell membrane extension was scored during 12-hour observation periods for hepatocytes on 0.01-10 $\mu g/cm^2$ Matrigel. Despite the absence of significant classical locomotion, cells frequently exhibited membrane extensions in the form of long filopodial projections or shorter, "leading edge"- type lamellipodia, which has been reported previously for a number of other epithelial cell types (24). These extensions are prominent and can be easily identified by the presence of a "ruffling" front (70). Movements of cell peripheries which were not accompanied by a ruffling front were not scored as membrane extension. Data for singlets and aggregates were combined as they yielded similar results. Figure 4-2 shows the fraction of cells exhibiting membrane extension as a function of Matrigel concentration. Since it may be hypothesized that the ability of cells to aggregate was dependent on the ability of cells to polarize their membrane extensions in a certain direction (i.e., filopodia or discrete regional lamellipodia), further analysis of the fraction of membrane extensions which were polarized was performed (Figure 4-3). However, chi-square contingency analysis of this data at a significance level of 0.05 indicates that the levels of polarized membrane extension on different Matrigel concentrations were indistinguishable.

ANOVA of Figure 4-2 followed by paired t-tests (both at a significance level of 0.05) indicates that the membrane extension levels present at low seeding densities increase as the Matrigel concentration is increased from the "low" regime (0.01 - 0.1 $\mu g/cm^2$) to the "high" regime (1 - 10 $\mu g/cm^2$). Paired t-tests at a significance level of 0.05 also indicate that cells seeded at high densities (15,000/cm^2 - 45,000/cm^2) on 0.1 and 0.01 $\mu g/cm^2$

Matrigel substrata extend their membranes at a significantly higher level than cells seeded at low densities on the same substrata. Interestingly, the membrane extension levels found in cell populations seeded at high densities on the low Matrigel concentrations were indistinguishable from those found in cells seeded at low densities on the high Matrigel concentrations.

It is obvious from these analyses of Figure 4-2 that cell seeding density plays some role in determining the level of membrane extension present in the culture system. These observations hint that the effects attributed to ECM concentration in the above analysis may simply be due to the number of cells attached to the substratum. However, further statistical analysis of Figure 3-3 indicates that the cell numbers present at low seeding densities on 0.1, 1, and 10 $\mu g/cm^2$ Matrigel are statistically indistinguishable while, as stated above, this is untrue of membrane extension in these cases (cells on 0.1 $\mu g/cm^2$ show significantly less membrane extension than do cells on 1 and 10 $\mu g/cm^2$). Additionally, the number of cells attaching to 0.1 $\mu g/cm^2$ Matrigel at high seeding density is statistically greater than that for any other Matrigel concentration. This trend does not manifest itself in the membrane extension fractions (i.e., the membrane extension level present in these cells is not statistically higher).

It is concluded that, while cell attachment number may play a significant role in promoting membrane extension for cells seeded on identical substrata, this parameter does not independently explain differences in membrane extension for hepatocyte populations seeded onto substrata of differing ECM concentrations.

4.2.3 Motility as a Mechanism of Hepatocyte Aggregation

Since membrane extension was observed to promote hepatocyte aggregation, it became desirable to quantify the relationship between these two parameters. In order to perform such an analysis the effects of cell surface coverage must be taken into account.

This can be accomplished by performing an analysis similar to that of Figure 3-6, now substituting membrane extension as the independent variable. Membrane extension was shown to be a function of ECM concentration and of cell seeding density in Figure 4-2. By further separating the x-axis data from Figure 3-5 into low and high seeding density regimes (i.e., 10 $\mu g/cm^2$ low seeding density, 1 $\mu g/cm^2$ low seeding density, 0.1 $\mu g/cm^2$ low seeding density, 0.1 $\mu g/cm^2$ high seeding density, 0.01 $\mu g/cm^2$ low seeding density, 0.01 $\mu g/cm^2$ high seeding density), these two figures can be combined. The resulting plot is shown in Figure 4-4 and demonstrates a clear relationship between aggregation and membrane extension. Chi squared contingency analysis at the 0.05 significance level indicates that aggregation increases significantly with increasing membrane extension for cells present with low and intermediate surface coverages. Testing of linearity also indicates that the aggregation vs. membrane extension data for these levels of fractional surface coverage and in the membrane extension regimes investigated are linear, and that their slopes are indistinguishable.

In order to determine whether a similar relationship exists for cells seeded onto other types of ECM, the initial aggregation experiments (4,000 cell/cm^2 seeding density) with fibronectin were analyzed for membrane extension and surface coverage and added to Figure 4-2. Fibronectin was chosen as an ECM because adhesion of hepatocytes to fibronectin is mediated by receptors which are different from those mediating the adhesion of hepatocytes to Matrigel. It can be seen in Figure 4-5 that the membrane extension data for fibronectin are indistinguishable (paired t-test; significance level 0.05) from Matrigel data. Figure 4-6 plots aggregation vs. membrane extension for hepatocytes on fibronectin as well as on Matrigel (from Figure 4-4). This analysis illustrates that hepatocyte aggregation on fibronectin is dependent on membrane extension in much the same way as is hepatocyte aggregation on Matrigel, suggesting that the observed relationships are also independent of ECM type.

4.3 Discussion

The studies described in the current chapter serve to provide the first known observations of the mechanisms responsible for hepatocyte aggregation. It seems to be typically assumed that cell migration, if not being solely responsible for, greatly facilitates cell-cell aggregation, although explicit hypotheses in this regard are rarely formulated. Contact inhibition of migration, where the locomotory "machinery" in contacting cells is temporarily paralyzed, is generally thought to be the mechanism by which such aggregation is allowed to occur (81). While no literature reports explicitly describing hepatocyte migration could be found, other epithelial cell types have been observed to migrate *in vitro* (e.g., refs. 8, 17, 110). It has been postulated that hepatocytes are capable of migration (153, 4, 99), and indeed evidence of increased motile functions (e.g., membrane extension through thin polycarbonate filters) under growth factor stimulation has been reported (128). Classical cell locomotion behavior has not been directly observed for hepatocytes, however. We thus employed videomicroscopy to illuminate the nature of hepatocyte motility under the particular conditions of our aggregation experiments.

Observations taken from time lapse videotape of hepatocyte behavior on these ECMs (Table 4-1) show that classical single-cell migration of hepatocytes is essentially negligible under all conditions investigated, despite the fact that aggregation is often times occurring to a significant extent. It is highly unlikely, therefore, that differences in the abilities of various surfaces to support hepatocyte aggregation are brought about by differences in resulting locomotion properties. However, from these same observations, an alternative form of cell motility appears to be more substantially involved. Direct cell-cell coupling was observed over fifty times during the course of this analysis. In these cases, initial contact between the cells occurred almost entirely via membrane extension, after which the cells were able to aggregate. While many of these cells moved more than

one body length, it only occurred after cell/cell contact and so can be considered at least as much a result as a cause of cell aggregation.

It is unclear why hepatocytes do not exhibit classical single-cell locomotion to a significant extent under these conditions. One explanation for why some epithelial cell types would not be able to migrate is that they may lack the ability to form polarized membrane extensions (70). However, we have observed in the course of these studies that hepatocytes are in fact capable of forming such extensions. Another possibility is the presence of focal adhesion contacts, which must be transient in order for cells to migrate (70, 103). Stamatoglou and Hughes (121) have shown that focal contacts develop rapidly at the peripheries of hepatocyte colonies on fibronectin. These focal adhesion regions are capable of circumscribing the colonies and provide an extremely strong cell-surface adhesion strength (146), perhaps substantially greater than the contractile force that these cells are capable of generating.

A correlation between high cell-surface adhesion strength and inhibition of migration has been validated for other (non-epithelial) cell types (23). This might also explain why coupled cells are able to then migrate towards one another. In aggregating hepatocytes, the cytoskeletal actin, which is a key component of focal adhesion complexes (129), reorganizes to circumscribe the entire colony rather than the individual component cells (124). In the process of this reorganization, many of these complexes are likely to be disrupted, decreasing cell-surface adhesion strength and allowing the contractile force of the cell in question or of the new aggregate to now overcome the previously insurmountable force.

At any rate, it is clear from the observations of hepatocyte behavior that membrane extension leading to cell coupling followed by cellular contraction is the typical series of events leading to hepatocyte aggregation. This information, when coupled with the observation that morphogenesis is based in biophysical phenomena, leads to a hypothesis

for hepatocyte aggregate morphogenesis based on cell traction forces and cell-substratum adhesion forces which will be discussed in detail in chapter 5.

Since membrane extension was observed to play a vital role in the coupling and aggregation of hepatocytes, this relationship was analyzed quantitatively. The fraction of cells examined via time lapse videotape on each particular substratum type and concentration were determined. The data obtained for cells on Matrigel substrata are shown in Figure 4-2. These data indicate two trends. First, membrane extension of cells seeded at identical seeding densities increases with increasing Matrigel concentration. Second, increasing hepatocyte seeding density increases membrane extension levels. These observations suggest the possibility that cell attachment number (and not matrix concentration) may ultimately determine levels of cell membrane extension. This in turn would implicate cell secreted factors as stimulants. Hepatocytes secrete a variety of growth factors and ECM molecules, so this is entirely feasible. Further support for this hypothesis is provided by observations made during time lapse videotape analysis that membrane extensions appeared to occur preferentially in the direction of other cells (see Figure 4-1). However, statistical analysis of the data does not support this hypothesis. It is observed that, while cells seeded at low densities on 0.1 $\mu g/cm^2$ Matrigel attach at levels statistically indistinguishable from those seeded at the same densities on higher Matrigel concentrations (Figure 3-3), the levels of membrane extension present in these cells is significantly lower than those attached to the higher concentrations. In addition, the largest number of attached cells was found to occur at high seeding densities on 0.1 $\mu g/cm^2$ Matrigel, but there was no corresponding increase in the membrane extension found in these cells. Furthermore, analysis of the levels of membrane extension with respect to time in culture reveals no uniform increase or decrease in membrane extension levels over time. If secreted molecules (either ECM or growth factor) were entirely responsible for membrane extension such an increase might be expected.

It is not surprising that one simple explanation is insufficient to describe the motility behavior of hepatocytes on these substrata. Membrane protrusions are thought to be driven by localized polymerization of F-actin filaments (137, 129), but the mechanisms by which such polymerization may occur are numerous and are currently open to debate (129). One popular theory which may explain the data in Figure 4-1 is that receptor binding (e.g., to the ECM or to a soluble growth factor) activates polyphosphoinositide synthesis(116), which in turn desequesters actin subunits and uncaps capped filaments, allowing spontaneous F-actin polymerization and elongation to occur (129; 86). Since these events are most likely to occur intracellularly in the vicinity of receptor activation, membrane extension would then occur precisely (and conveniently) in these areas. Subsequent hydrolysis of the polyphosphoinositides could then account for cessation of actin assembly by a reversal of the effects described above (129), accounting for the transience seen in lamellipodial or filopodial extensions.

Experiments in which hepatocytes are seeded onto surfaces coated with 0.001, 0.05, and 1 $\mu g/cm^2$ laminin indicate that the levels of F-actin increase significantly with increasing matrix concentration over the first few hours in culture but then equalize over the next several hours (86). This result was independent of protein secretion as determined by treatment with cycloheximide. Therefore, ECM concentration is indeed capable of affecting the membrane extension activity present in hepatocytes. However, it is also clear from Figure 4-2 that cell attachment density (most likely through a mechanism of protein secretion) will affect hepatocyte membrane extension activity. It is therefore reasonable to conclude that *both* ECM concentration and cell density stimulate hepatocyte membrane extension, which provides a plausible explanation for the behavior seen in Figure 4-2.

With the information provided by Figure 4-2, the relationship between aggregation and membrane extension can now be quantified. This provides a test of the extent to which aggregation is dependent on membrane extension. If surface coverage were the only

important parameter, then the aggregation would be independent of membrane extension. If, as anticipated, membrane extension is a key mechanism in hepatocyte aggregation, then aggregation would show a definite and positive correlation with this parameter. As seen in Figure 4-4, aggregation shows a statistically significant linear relationship with membrane extension in the ranges examined. Therefore, membrane extension does indeed significantly affect the aggregation of hepatocytes, especially at low surface coverage. In addition, the slopes of low and intermediate surface coverage data are indistinguishable from one another. Therefore, the effects of incremental increases in membrane extension levels has the same result in both cases. The agreement with this Matrigel data of data included from cells on fibronectin (Figure 4-6), which recruits different receptors than those recruited by Matrigel for hepatocyte adhesion, suggests that this is independent of ECM type. Again, this result is not surprising; the data here are concerned strictly with events leading to hepatocyte aggregation.

These results are significant in that they indicate that the aggregation of hepatocytes relies on a mechanism by which membrane extension leads to cell-cell coupling. This mechanism is dependent on substratum properties only insofar as these parameters influence the levels of membrane extension present in the cell population. Moreover, the substratum should support a sufficiently high degree of initial cell attachment and spreading if aggregation is desired. These parameters can be controlled by variation in ECM concentration.

In chapter 3 it was suggested that the substratum dictates the morphological fate of a hepatocyte aggregate through biophysical means. It was unclear, however, what these biophysical means involved. Having established that membrane extension leads to cell coupling followed by a cellular contraction, a hypothesis can be formulated regarding the nature of substratum control over hepatocyte aggregate morphogenesis. Since cellular contraction appears to be responsible for the detachment of peripheral aggregate borders, it

is suggested that morphogenesis is determined by the ability of this contractile event to overcome cell-substratum affinity that would ultimately determine whether spheroids could form or whether monolayers would instead be present. Thus, a low cell-substratum adhesion force would permit cellular contractile forces to influence morphogenesis and spheroids would result. A high cell-substratum adhesion force would prove insurmountable for cellular contractile forces and so monolayered aggregates would result. This hypothesis, shown schematically in Figure 4-7, forms a basis for the studies performed in chapter 5.

ECM conc.	Matrigel	Laminin	Fibronectin
10 $\mu g/cm^2$	9 / 117	-	-
1 $\mu g/cm^2$	4 / 104	1 / 190	1 / 77
0.1 $\mu g/cm^2$	1 / 192	1 / 144	1 / 80
0.01 $\mu g/cm^2$	0 / 171	1 / 118	0 / 84

Table 4-1. Dependence of hepatocyte migration on composition of the extracellular matrix substratum. The number of cells observed to locomote during 12-hour tracking periods is given for the various surface-coating concentrations of Matrigel, laminin, and fibronectin

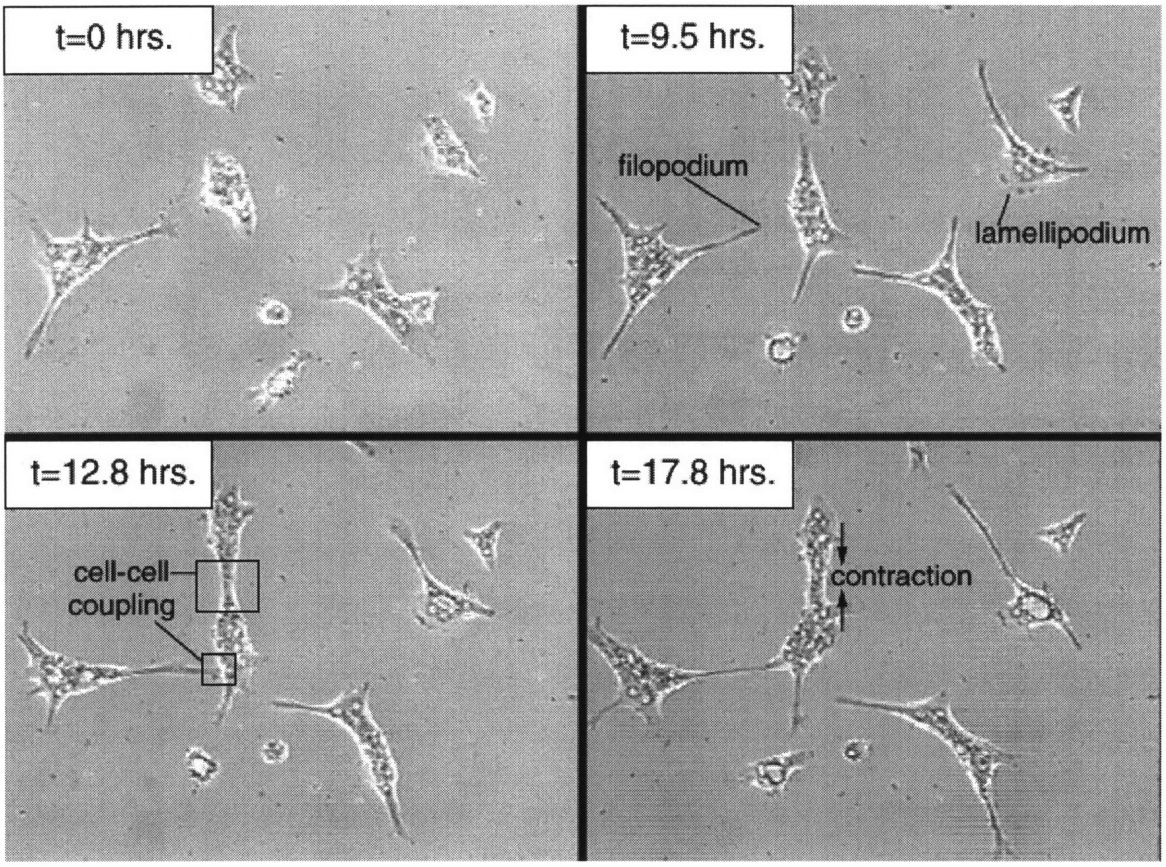

Figure 4-1. Photographs of aggregating hepatocytes during a 17.8 hour interval. The sequence illustrates the processes of membrane extension, cell-cell coupling, and cytoskeletal contraction. Cell migration can also be seen in one of the non-aggregating cells. Time zero represents day 2, approximately 48 hours after seeding.

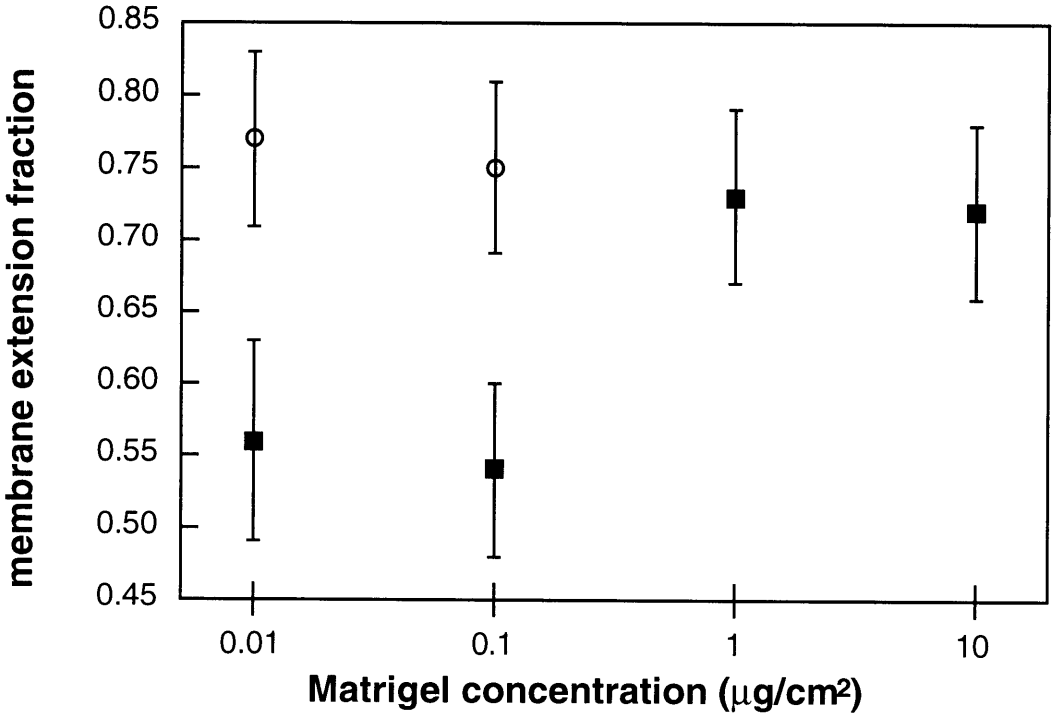

Figure 4-2. Dependence of hepatocyte membrane extension activity on cell seeding density. The fraction of cells observed to exhibit membrane extension is plotted as a function of substratum Matrigel concentration for low (4000 cells/cm^2 - 8000 cells/cm^2) (■) and high (15,000 cells/cm^2 - 45,000 cells/cm^2) (O) seeding densities.

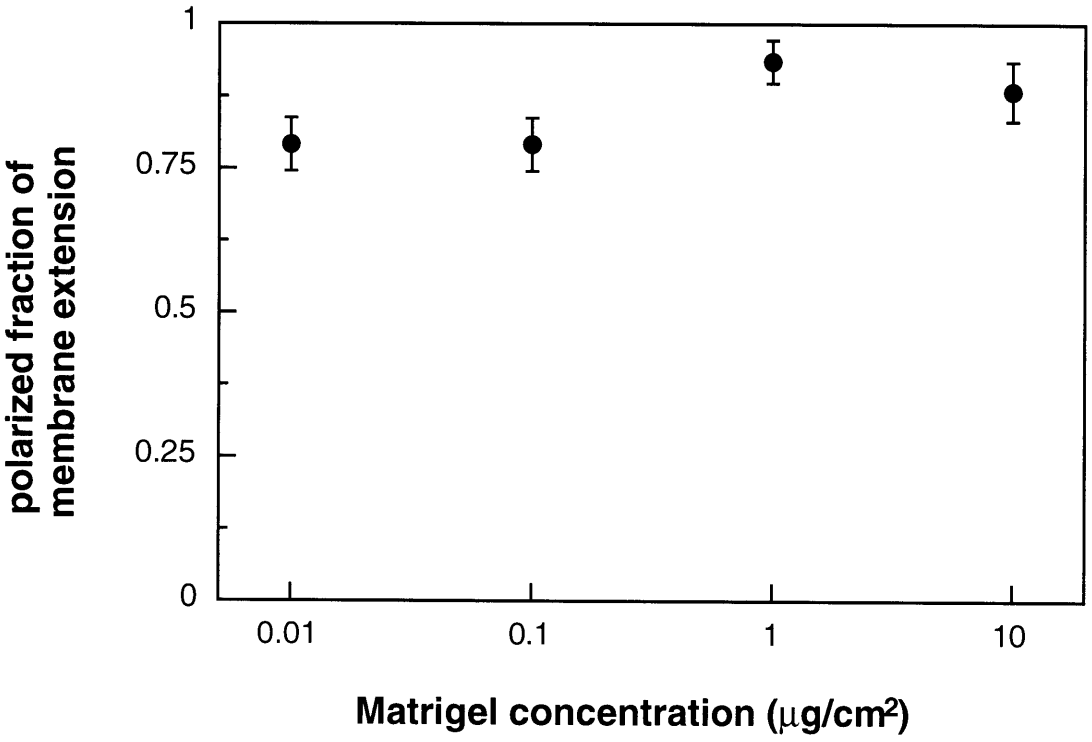

Figure 4-3. Dependence of polarized membrane extension activity on Matrigel concentration. The fraction of membrane extending cells which exhibit polarized membrane extension is plotted as a function of substratum Matrigel concentration.

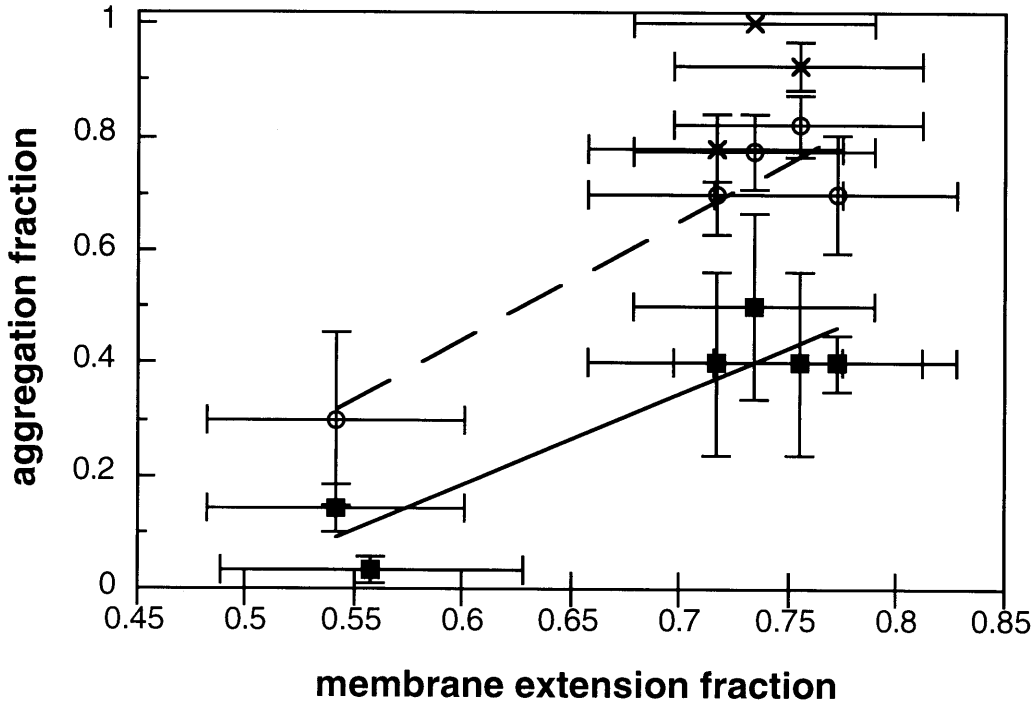

Figure 4-4. Dependence of hepatocyte aggregation on membrane extension. The fraction of observed fields exhibiting macroscopic aggregation is plotted as a function of the fraction of observed cells exhibiting membrane extension on Matrigel substrata for low (0.01 - 0.08) (■), medium (0.09 - 0.16) (○), and high (0.17 - 0.24) (×) ranges of fractional surface coverage.

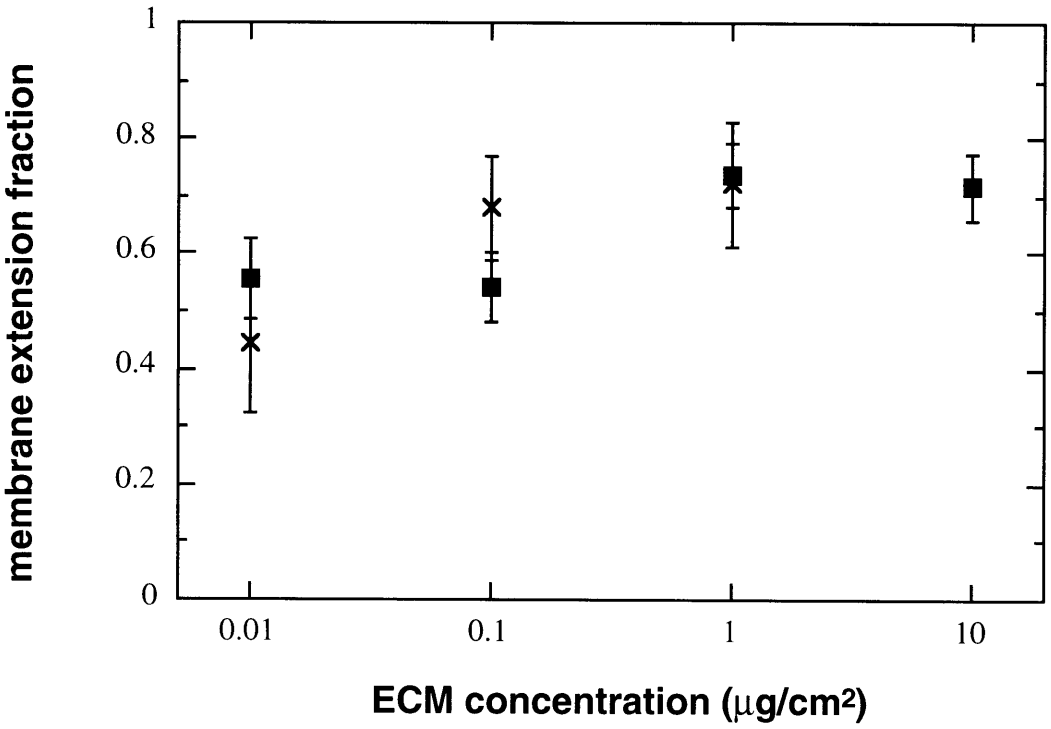

Figure 4-5. Dependence of hepatocyte membrane extension on ECM type. The fraction of observed cells exhibiting membrane extension is plotted as a function of ECM concentration for Matrigel (■) and fibronectin (✕) substrata.

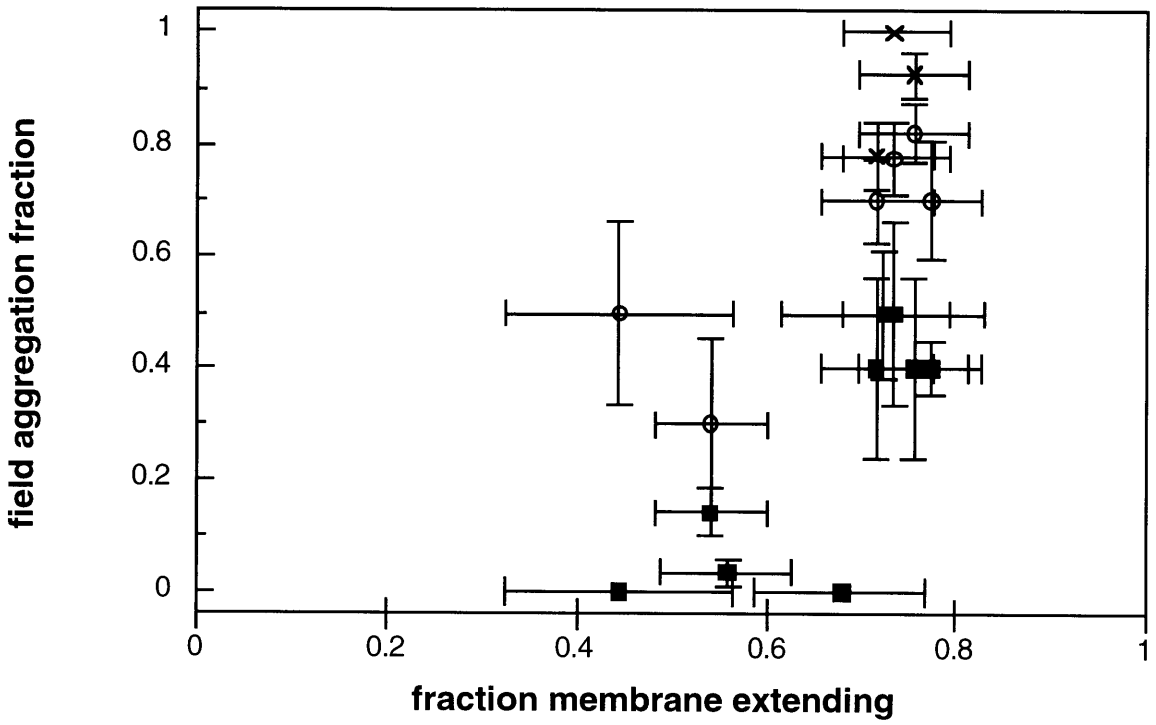

Figure 4-6. Dependence of the aggregation of hepatocytes cultured on different ECM substrata on membrane extension. The fraction of observed fields exhibiting macroscopic aggregation is plotted as a function of the fraction of observed cells exhibiting membrane extension on Matrigel and fibronectin substrata for low (0.01 - 0.08) (■), medium (0.09 - 0.16) (O), and high (0.17 - 0.24) (✕) ranges of fractional surface coverage.

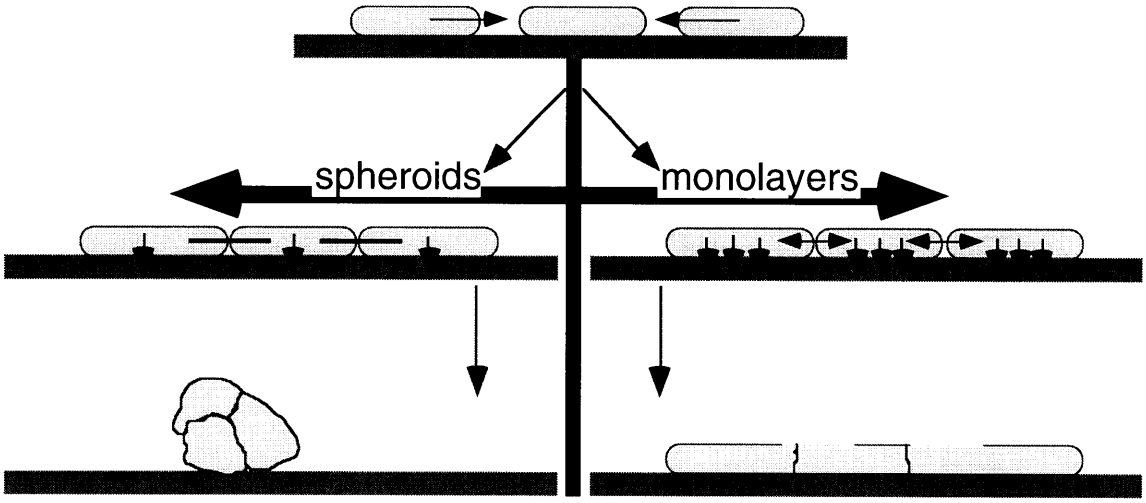

Figure 4-7. Schematic diagram of the proposed morphogenesis hypothesis.

5 The Biophysical Nature of Substratum Control of Hepatocyte Aggregate Morphogenesis

5.1 Introduction

In chapter 3 it was observed that low ECM concentrations appeared to support spheroidal aggregation, while monolayers formed at the highest ECM concentrations. It was also observed in these studies that, although these cells typically do not exhibit classical migration to a significant extent while aggregating, coupled hepatocytes are capable of contracting with forces large enough to pull towards one another as they form nascent aggregates, breaking cell-substratum attachments in the process.

Based on these observations, the hypothesis proposed in the previous chapter states that aggregate morphology is in large part governed by a balance between cell contraction forces and cell-surface adhesion forces. When cell-surface adhesion forces are relatively weak in comparison with cell contractile forces, the cells can reorganize to form into spheroids; when these cell-surface forces cannot be overcome by cell contraction, monolayered aggregation results. While it has been postulated that the condition of weak cell-substratum interactions increases the likelihood of spheroid formation (71, 64, 138), this effect has never been quantitatively verified. Moreover, the relation of cell-substratum adhesion to cell contractile forces are generally not mentioned explicitly. Therefore, in these studies this hypothesis was tested by systematically varying the morphology of hepatocellular aggregates by varying the amount of ECM on the substratum, and measured the corresponding cell-substratum adhesion strengths for each condition using a shear-flow detachment assay.

5.2 Results

5.2.1 Cell-Substratum Attachment Forces on Matrigel Substrata

In order to understand the biophysical nature of hepatocyte-substratum interactions, shear flow detachment assays were performed on hepatocytes 24 hours after seeding onto each surface. Well-defined distractive forces were applied to the cells via shear flow and the levels of cell detachment measured. Figure 5-1 shows the fraction of cells detached at each shear stress. Due to the dichotomous nature of the detachment fractions, error bars were calculated based on sampling from a binomial population (154). It is immediately apparent that the data for cells cultured on 0.1 $\mu g/cm^2$ and 0.01 $\mu g/cm^2$ Matrigel are similar, and are lower than the shear stress required to detach cells cultured on 1 $\mu g/cm^2$ Matrigel . A chi-square contingency test verifies this observation at significance level of 0.05. These trends are consistent with the hypothesis that spheroids form at lower levels of cell-substratum adhesion strengths while monolayers form at higher levels.

It should be noted here that, while a large majority of the hepatocytes observed in the adhesion assays existed as single cells, there were some cell aggregates that were inadvertently included. An analysis of the effects that these aggregates had on the results can be conducted by comparing the cell-to-track ratios (i.e., average number of cells per track) before and after exposure to shear flow for each of the three Matrigel concentrations examined. A t-test performed at a significance level of 0.05 indicates that there is no statistical difference between these ratios for hepatocytes on any of the Matrigel concentrations examined and therefore that these results were not biased in any way by the presence of cell aggregates.

While these data relating cell detachment to surface shear stress provide insight into the relationship between Matrigel coating concentration and cell attachment, they are inadequate estimators of the true strengths of cell attachment. Since the actual detachment *force* applied to a cell is dependent on both shear stress *and* cell morphology, the possible differences in morphologies must be accounted for and shear forces explicitly determined.

Values for applied force were obtained from the shear stress data by modeling the cells in various states of spreading as hemispherical caps of constant volume. This appears to be the most reasonable estimation of hepatocyte morphology based on scanning electron micrographs of hepatocytes attached to a variety of extracellular matrix types and concentrations (11, 46). For a sphere in xyz coordinates centered around the origin, a hemispherical cap can be represented by that section of the sphere contained within the limits of $z=\rho$ to $z=R$, where $0 \leq \rho < R$. To obtain the shear force acting on a hemispherical cap with a base of radius r_ρ, the solution for shear force on a hemisphere was modified by Truskey and Proulx to yield $F_S = 2.15\pi(r_\rho^2 + h^2)\tau_w$ (141). Therefore, both parameters must be calculated from measured quantities. Average cell areas were measured as a function of Matrigel concentration and obtained corresponding values for radii based on an assumption of circular spreading areas. The height of each cap was then determined by using this radius and assuming that cell volume remains constant, independent of the degree of spreading. Table 5-1 shows values for cell spreading areas, and the corresponding radius and height estimations calculated for cells on each of the Matrigel surface concentrations examined.

The plot of cell detachment vs. calculated shear force is given in Figure 5-2. These results show that the force required to detach hepatocytes from 1 $\mu g/cm^2$ Matrigel surfaces is statistically greater than the force required to detach the cells from 0.01 $\mu g/cm^2$ and 0.1 $\mu g/cm^2$ Matrigel as determined by a chi-square contingency test performed at a significance level of 0.05. The curves shown in this plot represent the integrals of lognormal probability density function (PDF) distributions which have been fit to the hepatocyte track adhesion strength data (see Appendix B for calculations). A lognormal PDF integral has been applied successfully to shear flow detachment data for fibroblasts (140) and fits the present hepatocyte data quite well as determined by chi-square goodness of fit tests. These curve fits provide further illustration of the disparity between the cells on high (1 $\mu g/cm^2$) and low (0.01 $\mu g/cm^2$, 0.1 $\mu g/cm^2$) Matrigel concentrations. With the parameters obtained

from these curve fits (mean, variance), the lognormal PDF distributions can now be plotted (Figure 5-3), which also show clear distinction between these two sets of data.

5.2.2 Effects of Changing Adhesion Strength on Aggregate Morphology

Since hepatocytes have been shown to synthesize and secrete matrix *in vitro* (135, 131, 123), it is possible that changes in substratum ECM concentration occur due to secretion of new matrix or degradation of existing matrix over the four day culture period. In order to investigate the effects of possible matrix secretion, spheroids were allowed to form on 0.1 $\mu g/cm^2$ Matrigel substrata. At days 2 and 3 after initial seeding some of these spheroids were transferred to freshly prepared dishes which had been coated with either 0.1 or 1 $\mu g/cm^2$ Matrigel. Those aggregates which were added to the 1 $\mu g/cm^2$ dish formed into monolayer-type structures within 24 hours, while aggregates in the initial cultures as well as those transferred to freshly prepared 0.1 $\mu g/cm^2$ dishes remained as spheroids for the duration of the experiment (up to 4 days after initial culture). This analysis demonstrates that the morphology of hepatocyte aggregates is continually sensitive to substratum ECM concentration.

5.3 Discussion

The purpose of the studies detailed in this chapter is to test the hypothesis that hepatocyte aggregate morphogenesis is based in biophysical phenomena. The hypothesis states that aggregate morphology evolves due to the interplay between cell-substratum adhesion and cell-cell contraction forces.

It has been shown that the strength of adhesion of human smooth muscle cells to collagen IV- and fibronectin-coated substrata increases with increasing ECM concentration (23). While observations that hepatocyte spreading can be controlled by surface ECM concentrations have been reported (11, 85), no quantitative data relating adhesion to morphology were presented. By varying the surface density of adsorbed ECM molecules,

cell-substratum adhesion strength can presumably be varied independent of the type(s) of adhesion receptors involved. To critically test the hypothesis regarding the relationship between cell-substratum adhesion and aggregate morphology, it is then essential to quantify cell-substratum adhesion strength at the different ECM coating densities.

Hepatocyte cell-substratum adhesion strength was assessed using a shear flow detachment assay performed 24 hours after the seeding of hepatocytes. This time point was chosen because observations from the 4 day aggregation studies show that macroscopic aggregates of hepatocytes -- regardless of resulting aggregate morphology -- are just beginning to form after 24 hours in culture. Most cells at this time remain unaggregated, allowing for relatively unambiguous interpretation of cell-substratum adhesion data, and yet these cells are on the verge of aggregation, suggesting that the adhesion strength measured at this point is crucial in ultimately determining aggregate morphology. Even those cells which were seeded as aggregates do not generally begin to exhibit their final morphology until after 24 hrs. (e.g., Figure 2-2). From Figure 5-1, which shows the fraction of cells detached from each Matrigel concentration as a function of shear stress, it is evident that the cells are more easily detached from lower ECM density (0.01 $\mu g/cm^2$ and 0.1 $\mu g/cm^2$ Matrigel) than they are from higher ECM density (1 $\mu g/cm^2$ Matrigel). However, since cell morphology is also a function of ECM surface density, these morphological differences will cause different resultant forces to act on cells exposed to identical shear stresses. These morphologies, therefore, must be accounted for to allow a true comparison of cell-substratum adhesion strengths.

Shear forces can be calculated from the shear stress data by allowing for estimations of cellular morphology (45, 141). It is assumed here that the morphologies of the hepatocytes in the various stages of spreading can be approximated by hemispherical caps. The resultant data (i.e., fraction of cells detached for specific values of force) represent the probability that a cell adheres to the surface with a force less than or equal to the force in question. This curve then is simply the integral of a probability density function for cell-

substratum adhesion strength (i.e., the probability of a cell adhering to the substratum with a particular strength). The data for hepatocyte detachment were fit to lognormal PDF distributions (Figures 5-2 and 5-3). By presenting the data in this format, it can be clearly seen that spheroidal aggregation occurs at low levels of cell substratum adhesion strength, while monolayers form at higher levels. This analysis illustrates that there is effectively no difference between the trends observed from the shear stress data (Figure 5-1) and the trends obtained by transformation of the shear stress data to shear force data (Figure 5-2).

In order to determine whether the data obtained for shear flow detachment of hepatocytes is reasonable, comparison with shear stresses required to detach other cell types is helpful. Hubbe (45) has reported that exposure to a 7.5 Pa shear stress for 2 minutes will detach 9-29% of attached HeLa cells. van Kooten *et al.* (145) have reported that 50% detachment of human skin fibroblasts occurs with 30 min. exposure to a 26.3 Pa shear or 140 min. exposure to a 17.6 Pa shear. These results indicate that a reasonable maximum shear stress necessary for detachment of the our cells is in the range of 10-100 Pa, which is consistent with the data in Figure 5-1.

Since these adhesion data are taken at the 24 hour time point, it is possible that changes in adhesion strength over the remaining three days of observation could occur due to secretion of new matrix or degradation of existing matrix. Experiments in which spheroids were added to both 1 $\mu g/cm^2$ and 0.1 $\mu g/cm^2$ Matrigel substrata indicate that the spheroids will remodel to form monolayers on 1 $\mu g/cm^2$ substrata, but not on 0.1 $\mu g/cm^2$ substrata. Therefore, the maintenance of spheroidal aggregates was shown to be sensitive to matrix concentration. If a significant amount of matrix were being deposited onto the 0.1 or 0.01 $\mu g/cm^2$ Matrigel substrata, the spheroids present on these surfaces could be expected to reform into monolayered aggregates. This is clearly not the case. In addition, it was observed that the proteolysis of receptors and/or ligands due to trypsin exposure causes rapid (i.e., <15 min.) rounding of initially spread cells (e.g., hepatocytes cultured on 1 $\mu g/cm^2$ Matrigel). This indicates that a significant loss in receptor-ligand bond

number might also cause monolayered cells to convert to a spheroidal morphology. These observations support the idea that any changes in matrix concentration which occur during the course of these experiments do not significantly affect cell-substratum adhesion, and that the adhesion data taken on day 1 is a valid parameter for use in the biophysical analysis of aggregate morphogenesis.

These results provide quantitative proof of the hypothesis that cell-substratum adhesion strengths correlate with hepatocyte aggregate morphology, but they do not account for the mechanism(s) by which aggregates evolve. There are two potential mechanisms that can be identified:

(1) Aggregate morphology evolves through a mechanism akin to that of the free energy minimization phenomenon described by Steinberg (126). In this scenario, aggregate morphogenesis is guided by the near-equilibrium fluctuations of cell-cell and cell-substratum molecular (i.e., receptor-based) interactions. As cells aggregate, physical remodeling results from small perturbations in the local molecular equilibrium as the nascent aggregate attempts to increase high adhesion (either cell-cell or cell-substratum) contact regions. Random cell motility also contributes to increased formation of desirable (i.e., more adhesive) cell-cell or cell-substratum interactions as an aggregate progresses towards a minimum free energy (equilibrium) state. Therefore, when cell-substratum attachment sites are sparse, surface free energy is minimized by maximizing the more highly adhesive intercellular adhesions, and spheroids result. Conversely, when cell-substratum attachment sites are plentiful, surface free energy is minimized by maximizing the number of cell-substratum adhesion bonds, resulting in monolayers. Active, directional activation of the cytoskeletal machinery does not play a role in this process. In this sense, morphogenesis occurs through a passive mechanism, with the relative strengths of cell-cell versus cell-substratum adhesive interactions ultimately determining the outcome.

(2) Aggregate morphogenesis is dependent on the active and directed mobilization of cytoskeletal machinery. In this mechanism, cell-cell contact initiates an (unspecified) intracellular contraction signal which actively promotes retraction of the peripheral regions of the aggregate. While further cellular reorganization may occur due to the free energy minimization process described above, it is the kinetic ability (or inability) of this active (or energy requiring) contractile event to overcome the cell-substratum adhesiveness which defines the morphological destiny of an aggregate. Thus, cell-substratum adhesion strength still plays an integral role in morphogenesis, but it is the relative strength of cell contractile forces versus cell-substratum adhesion strength that serves as the primary determinant of hepatocyte aggregate morphology.

Using time-lapse videomicroscopy, it was observed in chapter 4 that hepatocyte aggregation occurs in the following sequential steps: (1) membrane extension (lamellipodial or filopodial); (2) contact of membrane extension with an adjoining cell and establishment of intercellular adhesions; (3) contraction of joined cells and partial to extensive rearrangement or release of cell-substratum adhesions. The time scale for completion of steps 2-3 is generally on the order of 2-6 hours. In formation of spheroidal aggregates, contraction (step 3) occurs as a series of discrete steps, typically involving a rapid retraction of distal cellular extensions and peripheral attachments. Membrane extension or spreading of one cell onto the top of another cell was not observed at any point during the extensive time lapse videotape analysis performed (i.e., cells did not form directly into multilayered aggregates), although rearrangement of aggregates into multilayer spheroids occurred over 24-48 hr. The initiation of morphogenesis is thus consistent with the second of the above mechanisms, while maturation of aggregate morphology into multi-layer spheroids is likely to be at least partially due to the first mechanism. Further support for this mechanism is provided by preliminary observations of F-actin organization in spheroidal and monolayered hepatocyte aggregates (Appendix C).

Therefore, since the steps which initiate morphogenesis appear to be dependent on the second of the proposed mechanisms, it is suggested that hepatocyte aggregate morphology is ultimately determined by the relationship between cell contractile forces and cell-substratum adhesion forces. When the contractile force exceeds the cell-substratum adhesion force the cells will be able to "pull" themselves from the surface, breaking cell-substratum attachments, to form into spheroids. When the latter exceeds the former, the cells are unable to detach themselves from the substratum, resulting in monolayer formation with only slight rearrangement of cell-substratum attachment.

While there is currently no direct information on the contractile forces that hepatocytes are capable of generating, the magnitude of such forces can be estimated from studies of other cell systems and behaviors. As observed by time-lapse videomicroscopy, the process of cell contraction during aggregation appears similar to migration of a single cell in a preferred direction (100). Generation of force during cell migration occurs by contraction of actin-based cytoskeleton which is ultimately linked to integrins and other receptors for ECM proteins (73). Cell movement in a single direction results from an asymmetry in cell-substratum adhesion strength between the leading and trailing edge of the cell (117), which allows the rear of the cell to detach when the cell contracts, transmitting a traction force to the substratum. One manifestation of asymmetry is a weaker link of the integrin receptors to the cytoskeleton at the rear (113), although the signaling mechanism causing such asymmetry is unknown. The contact of two adjacent hepatocytes during aggregation may result in generation of signals which result in adhesion asymmetries analogous to those in migration, inducing directional movement of the cell towards the aggregate. In cell-cell aggregation, the 'leading edge', then, is the edge touching the other cell. Traction forces measured for cells migrating on two-dimensional substrata may therefore provide reasonable estimates of the traction forces generated by contracting hepatocytes during cell aggregation. Since traction force represents the part of the total contractile force transmitted to the substratum (73), comparison of traction forces with

measured adhesion forces should allow prediction of which cells will be able to detach and form spheroidal aggregates.

Traction forces exerted by locomoting cells on deformable 2-dimensional substrata have been measured for a few cell types (for review see ref. 93). These forces range from a maximum of ~ 8 x 10^{-9} N - 2.5 x 10^{-8} N for keratocytes (76) to ~20 x 10^{-8} N for fibroblasts (93). Fibroblasts are perhaps the best characterized cell type in terms of their ability to migrate and they exhibit highly contractile actin filament bundles parallel to the substratum surface called stress fibers (70). Keratocytes do not appear to form such fibers (75). At short time periods (<24 hours) hepatocytes exhibit thick actin bands around their periphery but not fibroblast-like stress fibers (89, 125, 121). The formation of stress fibers in hepatocytes on 1 $\mu g/cm^2$ Matrigel substrata was observed, but these did not appear to be extensive until day 4, well after aggregation occurs. Based on this information, it can be plausibly inferred that the traction forces generated by the hepatocytes in these studies fall somewhere in-between the measured traction forces of keratocytes and fibroblasts.

Adhesion data PDFs, e.g. Figure 5-3, allow for simple comparison between cell-surface attachment forces and estimates of cell contractile forces -- a visual test of the hypothesis that hepatocyte aggregate morphology is determined by the balance between these two forces. Figure 5-4 shows the traction force values for these cell types in conjunction with the hepatocyte cell-substratum adhesion distributions from Figure 5-3. It is evident that the traction forces generated by keratocytes are in the same range as the cell-substratum adhesion forces of those cells that form into spheroids (0.1 $\mu g/cm^2$, 0.01 $\mu g/cm^2$ Matrigel nominal concentrations) but are much less than the adhesion forces of most of the cells on 1 $\mu g/cm^2$ Matrigel. Conversely, fibroblast traction forces exceed the cell-substratum adhesion forces of almost all of the cells on 0.1 $\mu g/cm^2$ and 0.01 $\mu g/cm^2$ Matrigel but not of cells on 1 $\mu g/cm^2$ Matrigel. In other words, since the traction forces for fibroblasts and keratocytes form reasonable upper and lower bounds for the traction forces capable of being generated by hepatocytes, spheroids form when cell traction forces can

exceed cell-surface adhesion forces, while monolayers form when traction forces fall below cell-surface adhesion forces. These results provide strong support for the hypothesis that hepatocyte aggregate morphology is governed by biophysical phenomena.

It has been assumed in this analysis that the primary cellular biophysical parameter influenced by ECM concentration is cell-substratum adhesion strength, and there are at present no data bearing on whether hepatocyte contractile strength is a function of the adsorbed Matrigel concentration. Cellular F-actin, which is responsible for cytoskeletal tension generation, is present in similar levels in hepatocytes attached to a wide range of extracellular matrix concentrations (86), so it is unlikely that any differences in contractile strengths can be attributed to differences in F-actin mass. It has been shown that increasing serum concentration in the medium will stimulate a higher extent of contraction in gel matrices imbedded with cells (61), and that thrombin stimulates increased contraction of fibroblasts and endothelial cells in collagen matrices (66), but it is not known whether this is due to increases in cellular contraction or in cell-matrix adhesion strength. In fibroblasts, an increase in the ECM concentration may contribute to increased focal adhesion formation, which is associated with an increase in stress fiber formation (70). Observations of hepatocytes on 1 $\mu g/cm^2$ Matrigel indicate that stress fibers do indeed form in some cases (Figure C-4), suggesting that hepatocytes may be able to generate contractile strengths approaching those of fibroblasts. Regardless, the adhesion strength demonstrated by most hepatocytes on a 1 $\mu g/cm^2$ Matrigel substratum (Figure 5-4) is greater than even this upper bound estimate of contractile strength. Thus, according to the hypothesis, it would be expected that the aggregates that form on a 1 $\mu g/cm^2$ Matrigel substratum will be monolayer rather than spheroid in morphology, and indeed they are.

It is also possible that cell-cell adhesion is influenced by ECM concentration. Stable hepatocyte cell-cell adhesions are formed within a few hours of contact; within 48 hours, typical epithelial junctions (i.e., tight junctions, bile canaliculus-like structures and zonula adherens-type junctions) are observed (82). While the effects of ECM concentration

on these phenomena are not well characterized, time lapse videotape analysis of aggregating hepatocytes allows for analysis of this relationship. Data were obtained from 12 hour videotaped segments for the frequency of contact between independent hepatocyte singlets and/or aggregates and the subsequent event of either remaining in contact or separating. These data show that a similarly large majority of the cells remain adhered to one another for all three Matrigel concentrations, suggesting that cell-cell adhesions are not significantly affected by ECM concentrations.

It is concluded that cell-substratum adhesion strength is a determinant of hepatocyte aggregate morphology, and suggested that this parameter manifests itself in morphogenesis through biophysical interplay with cell contractile strength.

Matrigel conc.	mean spreading area	radius	height
1 $\mu g/cm^2$	2066 μm^2	25.6 μm	6.3 μm
0.1 $\mu g/cm^2$	861 μm^2	16.6 μm	12.8 μm
0.01 $\mu g/cm^2$	677 μm^2	14.7 μm	14.7 μm

Table 5-1. The mean cell spreading areas and calculated radius and height values for hepatocytes on 1 $\mu g/cm^2$, 0.1 $\mu g/cm^2$, and 0.01 $\mu g/cm^2$ Matrigel substrata.

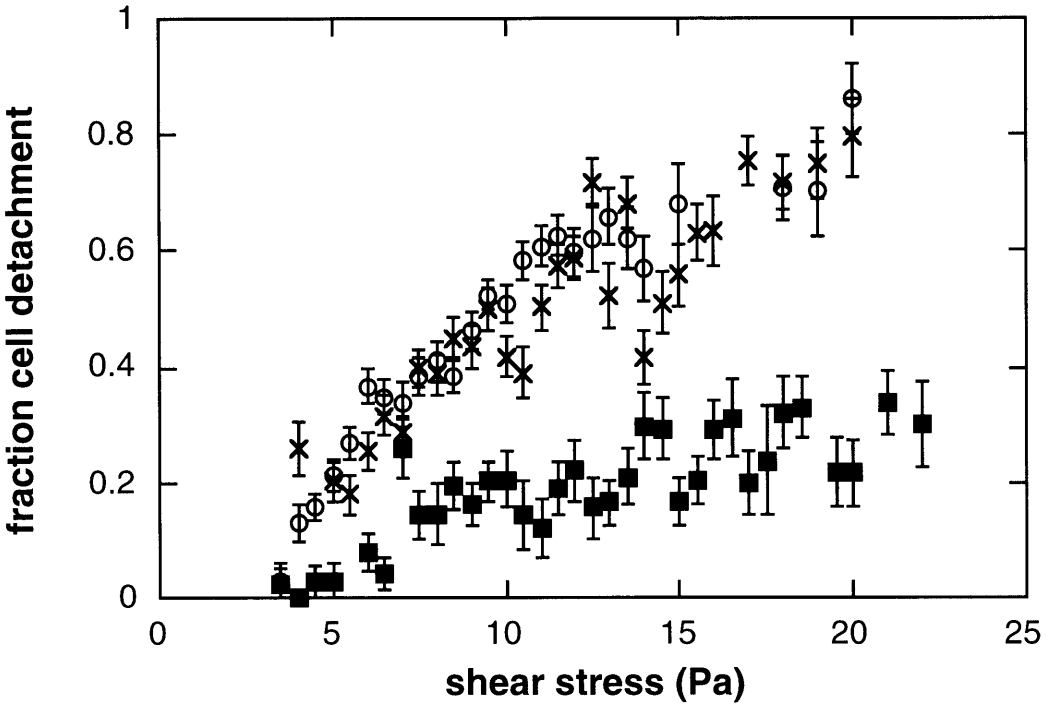

Figure 5-1. Dependence of hepatocyte detachment on the applied shear stress. The fraction of cells detached is plotted as a function of the shear stress to which the cells are exposed for 1 μg/cm^2 (■), 0.1 μg/cm^2 (○), and 0.01 μg/cm^2 (×) Matrigel substrata.

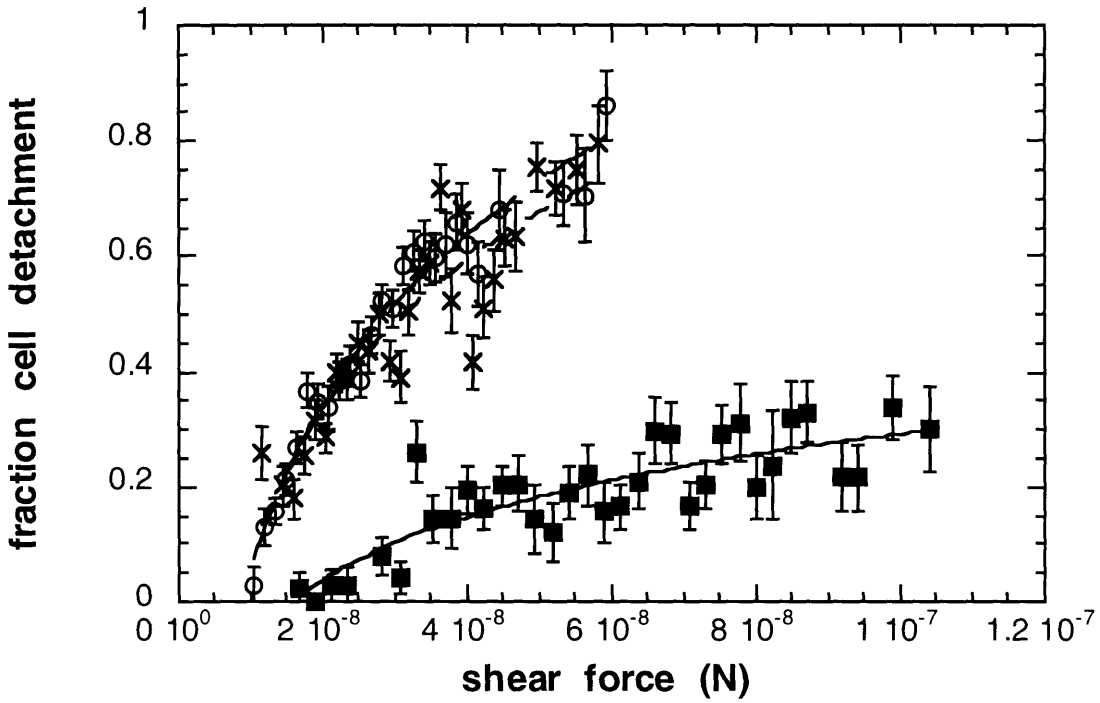

Figure 5-2. Dependence of hepatocyte detachment on the applied shear force. The fraction of cells detached is plotted as a function of the calculated shear force present on the cells for 1 μg/cm^2 (—■—), 0.1 μg/cm^2 (—Θ -), and 0.01 μg/cm^2 (— ✕ -) Matrigel substrata. Curve fits are generated from the integral of a lognormal probability density function.

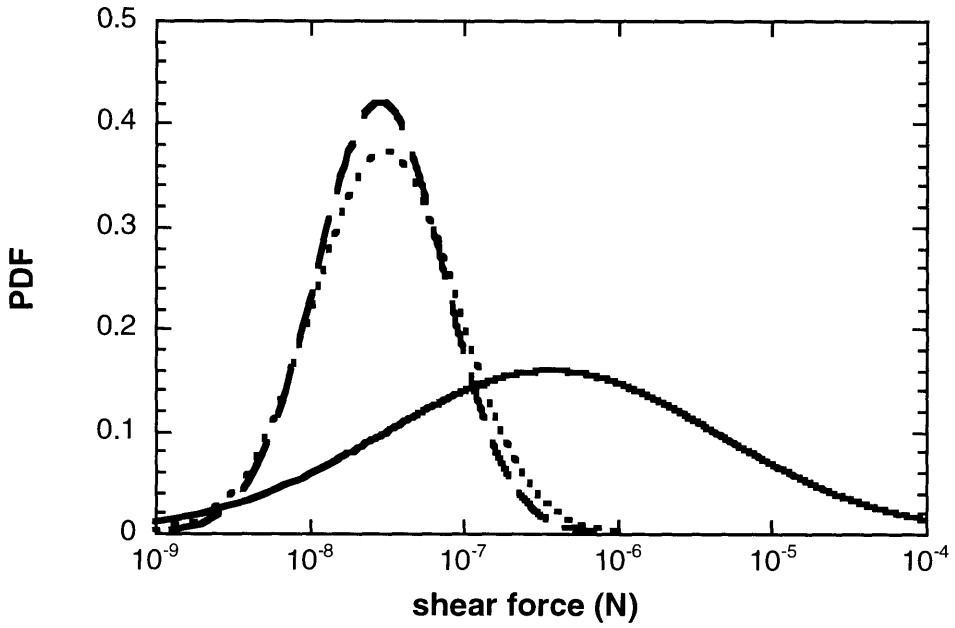

Figure 5-3. The probability density function of the shear force required to detach hepatocytes from 1 μg/cm^2 (———), 0.1 μg/cm^2 (— —), and 0.01 μg/cm^2 (- — -) Matrigel substrata.

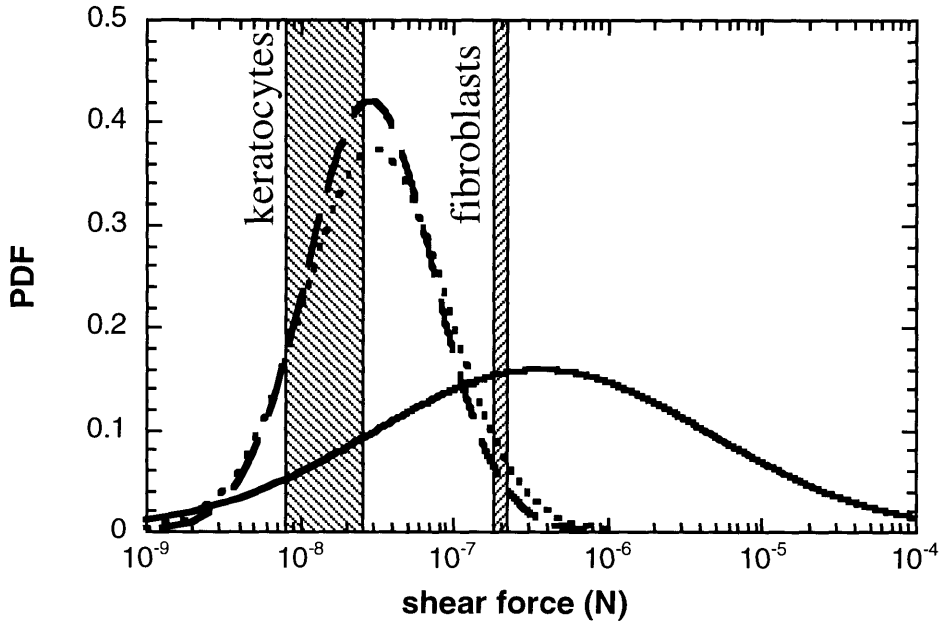

Figure 5-4. A comparison of adhesive and contractile forces. The probability density function of the shear force required to detach hepatocytes from 1 μg/cm^2 (———), 0.1 μg/cm^2 (— —), and 0.01 μg/cm^2 (- — -) Matrigel substrata is plotted along with the maximum measured traction forces generated by keratocytes and fibroblasts.

6 Conclusions

6.1 Summary

This thesis investigated the nature of substratum control over hepatocyte aggregation and aggregate morphogenesis. The initial studies investigated the effects of variation in biophysical and biochemical substratum properties on hepatocyte aggregation and aggregate morphology. Following this analysis, the cellular mechanisms underlying hepatocyte aggregation were identified and employed in the formulation of a hypothesis of the biophysical nature of substratum control over hepatocyte aggregate morphology. The final phase of the thesis involved the verification of this hypothesis through observations of cellular behavior in conjunction with quantification of the principal biophysical parameters of interest.

The aggregation of primary rat hepatocytes dispersed in culture was shown to depend in large part on the degree of surface coverage by these cells. In addition, the substratum ECM concentration significantly affected the ability of these cells to aggregate, most notably at low cell surface coverages. ECM type (Matrigel, laminin, fibronectin) did not appear to influence aggregation behavior. By day four in culture, these hepatocellular aggregates exhibited vastly different morphologies, again depending on the substratum ECM concentration. Spheroids formed at low matrix concentrations independent of ECM type, while monolayers formed at high matrix concentrations. Similar behavior was observed for all ECM types examined (Matrigel, laminin, fibronectin, type I collagen). These results suggest that the biophysical properties of a substratum play an important role in both the ability of hepatocytes to aggregate and the morphology assumed upon aggregation.

In order to further assess the effects of substratum properties on these phenomena it was necessary to gain an understanding of the cellular mechanisms which are involved in hepatocyte aggregation and the ensuing events. Time-lapse microscopy of hepatocytes in

culture indicates that cell membrane extension is the primary mechanism by which cell aggregation occurs. The initial assumption that cell migration via the "crawling" mechanism by which mammalian cells typically translocate was responsible for hepatocyte aggregation proved incorrect. Rather, aggregation is initiated primarily by a mechanism which involves cell membrane extension. This membrane extension appears to be stimulated by increases in both ECM concentration and cell seeding density and is not affected by exposure to different types of ECM. These results indicate that a substratum can be designed to elicit the desired degree of hepatocyte aggregation simply by varying the substratum ligand concentration and the initial density at which these cells are seeded.

Observations of hepatocyte behavior following cell-cell contact indicate that a cellular contraction event often occurs which pulls the coupled cells towards one another. Since the morphology of hepatocyte aggregates was observed to depend on ECM concentration, a hypothesis was formulated that aggregate morphology is dictated by the relative strengths of cellular contraction and cell-substratum adhesion: monolayers form when cell-substratum adhesion is dominant, spheroids result when cellular contraction is dominant.

Verification of this hypothesis requires a quantitative analysis of hepatocyte adhesion strength on substrata of different ligand concentrations. Quantification of cell-substratum adhesion strengths indicates that, indeed, monolayers form at high cell-substratum adhesion strengths, spheroids form at low cell-substratum adhesion strengths. Literature values of cell traction forces fall in-between the measured values of cell-substratum adhesion strengths, providing strong support for the proposed hypothesis.

Since the morphology exhibited by hepatocyte aggregates has been shown to correlate with the ability of these cells to attain states of differentiation or growth, these results provide an effective method for controlling cell behavior by variation in the biophysical properties of the substratum. This information provides a rational basis for the

design and modification of biomaterials to be used in hepatic tissue engineering applications.

6.2 Future Work

Since a functioning liver consists not only of hepatocytes, but also of a variety of other cell types (e.g., sinusoidal endothelial cells, bile duct epithelia), it is imperative to next consider the effects of the biophysical parameters outlined in this thesis on the sorting and morphogenesis of co-cultures of hepatocytes and non-parenchymal cells. Sinusoidal endothelia are the most logical candidates for analysis in co-culture with hepatocytes as these cells are found adjacent to one another in the vascular bed *in vivo*.

Co-culture of hepatocytes with sinusoidal endothelial cells (SEC) adds another level of complexity to the analysis performed in this thesis, as three types of cell-cell interactions (hepatocyte-hepatocyte, SEC- SEC, hepatocyte- SEC) and two types of cell-substratum interactions (hepatocyte-substratum, SEC-substratum) must now be accounted for. In addition to the types of experiments performed in this thesis (quantification of the hepatocyte- and SEC-substratum adhesion strength), a suggested research strategy for such experiments involves the use of SECs which, through genetic modification, differ in the expressed amounts of cell-cell adhesion molecules (e.g., cadherins) and subsequent observation of differences in organization and pattern formation. The use of cadherin antibodies, both in solution and bound to the substratum, would also be of help in elucidating the effects of biophysical adhesion events in the observed morphogenetic behavior.

Effective analysis of relative strengths of cell-cell interactions can be accomplished by seeding mixtures of cells into cell suspension spinner vessels at different total concentrations and different cell type ratios (from 100% SECs to 100% hepatocytes). Inspection of the resulting aggregates at different time points allows for determination of the relative strengths of homotypic and heterotypic binding as well as insight into the

kinetic behavior of these associations. This information can then be correlated with the morphogenetic behavior observed in co-culture on substrata of various adhesivities.

One attractive candidate for substrata to be used in the co-culture of hepatocytes and endothelial cells is a surface utilizing ligands which are specific for hepatocytes (e.g., galactose). By allowing endothelial cells to associate only with other cells (i.e., not the substratum), cell-sorting is more efficiently achieved through selective substratum adhesive interactions with hepatocytes. In this scenario, substratum ligand density is optimized for hepatocytes based on the criteria established in this thesis, while cell-cell interactions could be assessed through both co-culture with hepatocytes on these substrata and the cell suspension method described above.

APPENDICES

Appendix A: Additional Surface Characterization

In addition to the XPS surface characterization detailed in chapter 2, three other protein assays were also used in an attempt to analyze adsorbed protein concentrations: a micro bicinchoninic acid (BCA) assay, a NanoOrange™ assay, and an o-phthalaldehyde (OPA) assay. Each of these assays was used to measure the protein concentration of the solution removed from the petri dish (i.e., the unadsorbed protein concentration). Adsorbed protein concentrations were then calculated from differences between initial and final solution concentrations. All proteins were adsorbed to 35mm petri dishes as described in section 2.2.1. Protein standards were prepared by diluting the stock protein solution (which is of known concentration) to the desired final concentration in PBS. All procedures were performed at ambient temperature unless otherwise specified.

A.1 BCA Assay

The determination of protein concentration with BCA is initiated by the biuret reaction, in which peptide bonds and individual amino acid side chains (primarily cysteine, cystine, tryptophan and tyrosine) react with Cu^{2+} in an alkaline medium to produce Cu^{+}. A purple reaction product is then produced by the interaction of two molecules of BCA with one cuprous ion (Cu^{+}), which allows for spectrophotometric determination of protein in aqueous solutions.

BCA protein assays were performed with the use of a micro BCA protein assay reagent kit (product #23235; Pierce Chemical Co.; Rockford, IL). Standards, samples and blanks (100 µl aliquots) were added to designated wells of a 96 well microtiter plate, after which 100 µl of BCA working reagent was added to each well. The microtiter plate was then covered and incubated overnight at 37° C. The absorbance of each well was then measured at 562 nm with a Spectramax 250 microplate spectrophotometer (Molecular Devices; Sunnyvale, CA). Due to the relatively low sensitivity this assay provides, only

data for 1μg/cm^2 nominal Matrigel concentrations were obtainable. The results from these experiments indicate that 0.4 ± 0.1 μg/cm^2 Matrigel adsorbs to the surfaces at 1μg/cm^2 nominal Matrigel concentration, which agrees closely with XPS measurements.

A.2 NanoOrange™ Assay

The NanoOrange™ protein assay reagent fluoresces upon association with various detergents. Denaturation of proteins via addition of dimethyl sulfoxide (DMSO) followed by addition of NanoOrange™ reagent allows for quantitation of protein concentrations. The assay was begun by mixing 1 ml of protein solution with 2.5 ml NanoOrange working reagent in 15 ml polypropylene centrifuge tubes. This mixture was then incubated for 10 min. at 90° C and subsequently allowed to cool to room temperature for 20 min. Fluorescence readings were recorded through the use of an RF5000U spectrofluorophotometer (Shimadzu Corporation; Kyoto, Japan) with excitation wavelength set for 470 nm and emission wavelength set for 570 nm. The adsorption of Matrigel at a 1 μg/cm^2 nominal protein density was determined using this method and measured as 0.7 ± 0.3 μg/cm^2, which is of the same order of magnitude as XPS measurements. This assay was unable to detect adsorbed protein concentrations below those of the 1 μg/cm^2 nominal protein concentrations.

A.3 OPA Assay

OPA detects protein concentrations by reacting with primary amines in the presence of mercaptoethanol, yielding a blue colored fluorescent product with a maximum wavelength of excitation at 340 nm and emission at 455 nm. Standards, samples and blanks were prepared for analysis by adding 2 ml solution to a 3 ml polystyrene cuvette (VWR Scientific). Immediately prior to fluorescence analysis, 0.5 ml Fluoraldehyde™ OPA reagent (product #23255X; Pierce Chemical Co. Rockford, IL) was added to the cuvette and mixed vigorously. The cuvette was then placed in an RF5000U

spectrofluorophotometer (Shimadzu Corporation; Kyoto, Japan) with excitation wavelength set for 340 nm and emission wavelength set for 455 nm. The intensity of emitted light was tracked for 5 min. and the peak value recorded. The OPA assay was not sensitive enough to give reproducible protein adsorption data at 1 $\mu g/cm^2$ nominal Matrigel concentrations, and so data are not reported here.

Appendix B: Lognormal Probability Density Function Integral

In order to calculate the integral of the lognormal probability density function, $\int_{-\infty}^{\ln z} \frac{1}{\sqrt{2\pi}\sigma}\left(e^{-\left[(x-\mu)^2/2\sigma^2\right]}\right)dx$, it is helpful to first expand the exponential term using the appropriate series expansion. This expression can then be directly integrated:

$$\int_{-\infty}^{\ln z} \frac{1}{\sqrt{2\pi}\sigma}\left(e^{-\left[(x-\mu)^2/2\sigma^2\right]}\right)dx$$

$$= \int_{-\infty}^{\ln z} \frac{1}{\sqrt{2\pi}\sigma}\left[1 - \frac{(x-\mu)^2/(2\sigma^2)}{1!} + \frac{(x-\mu)^4/(4\sigma^4)}{2!} - \ldots\right]dx \qquad \text{Eqn. B.1}$$

$$= \frac{1}{\sqrt{2\pi}\sigma}\left[x + \sum_{i=1}^{\infty}\left(-1^i \frac{(x-\mu)^{2i+1}}{i!(2i+1)\left(\sqrt{2}\sigma\right)^{2i}}\right)\right]_{-\infty}^{\ln z} \qquad \text{Eqn. B.2}$$

$$= \frac{1}{\sqrt{\pi}}\left[\frac{\mu}{\sqrt{2}\sigma} + \sum_{i=0}^{\infty}\left(-1^i \frac{(x-\mu)^{2i+1}}{i!(2i+1)\left(\sqrt{2}\sigma\right)^{2i+1}}\right)\right]_{-\infty}^{\ln z} \qquad \text{Eqn. B.3.}$$

Now, evaluating Eqn. B.3 at $x = -\infty$ and with finite μ, σ:

$$\frac{1}{\sqrt{\pi}}\left[\frac{\mu}{\sqrt{2}\sigma}+\sum_{i=0}^{\infty}\left(-1^{i}\left\{\left(\frac{-\infty}{\sqrt{2}\sigma}\right)^{2i+1}\Big/(i!(2i+1))\right\}\right)\right]$$

$$=\frac{1}{\sqrt{\pi}}\left[\frac{\mu}{\sqrt{2}\sigma}\right]+\frac{1}{2}\operatorname{erf}\left[\frac{-\infty}{\sqrt{2}\sigma}\right] \qquad \text{Eqn. B.4}$$

$$=\frac{1}{\sqrt{\pi}}\left[\frac{\mu}{\sqrt{2}\sigma}\right]-\frac{1}{2} \qquad \text{Eqn. B.5.}$$

Substituting Eqn. B.5 into Eqn. B.3,

$$\int_{-\infty}^{\ln z}\frac{1}{\sqrt{2\pi}\sigma}\left(e^{-\left[(x-\mu)^{2}/2\sigma^{2}\right]}\right)dx$$

$$=\left\{\frac{\mu}{\sqrt{2\pi}\sigma}+\frac{1}{\sqrt{\pi}}\sum_{i=0}^{\infty}\left(-1^{i}\frac{(\ln z-\mu)^{2i+1}}{i!(2i+1)(\sqrt{2}\sigma)^{2i+1}}\right)\right\}-\left\{\frac{\mu}{\sqrt{2\pi}\sigma}+\frac{1}{2}\right\} \qquad \text{Eqn. B.6}$$

$$=\frac{1}{2}+\frac{1}{\sqrt{\pi}}\sum_{i=0}^{\infty}\left(-1^{i}\frac{(\ln z-\mu)^{2i+1}}{i!(2i+1)(\sqrt{2}\sigma)^{2i+1}}\right) \qquad \text{Eqn. B.7.}$$

Therefore, if ln z is a normally distributed variable (i.e., z is a lognormally distributed variable), the integral of the probability density function is given by Eqn. B.7.

Appendix C: Cytoskeletal Structure and Organization

C.1 Introduction

In chapter 5, cellular contractile force is implicated as a primary determinant of hepatocyte aggregate morphology. The ability of cells to generate such forces is dependent on the cytoskeleton, a complex network of protein filaments that extends throughout the cytoplasm. The cytoskeleton is composed of three principal types of filaments: tubulin containing microtubules, actin containing microfilaments and intermediate filaments. It is generally accepted that, while all three of these filaments serve to provide structural support, the actin microfilaments (or F-actin) are responsible for cell or membrane movement, contractile events and generation of cytomechanical force. Since microfilaments have also been shown to associate with the zonulae adherens of the epithelial junctional complex, it is particularly important to understand the role that these cytoskeletal components may play in hepatocyte aggregation and morphogenesis.

Actin microfilaments are rod-like double helical polymers which form spontaneously from globular actin (G-actin) monomers. F-Actin can exist intracellularly as linear bundles, two-dimensional networks, and three-dimensional gels. The physical state of actin in the cell is governed to a large extent by the actions of actin-binding proteins. There are at least 20 known actin binding proteins found intracellularly some of which can induce such events as stiffening, contraction, gelation, bundling, capping, severing, and polymerization/depolymerization of filaments (14, 69, 129).

An important function of F-actin pertaining to these studies clearly involves the generation of tension or traction forces. Cytoskeletal contraction generates tension throughout the cell, placing stress on points of cell-substratum attachment and defining a new biomechanical force balance. This force balance can in turn affect the architecture of the F-actin network and the cytoskeleton as a whole (53). When the cytoskeletal tension

generation is insufficient to deform the substratum or break cell-substratum attachments, actin stress fibers are likely to result (94). These are linear bundles of F-actin microfilaments and will tend to orient along the direction of stress (98). Interestingly, stress fibers which form in cells on rigid collagen gels collapsed after these gels were "relaxed" and made deformable (83). Inspection of cytoskeletal architecture can therefore be of assistance in understanding the biophysical nature of interaction between cells and substrata.

In hepatocytes, cytoskeletal organization is similar to that of other epithelial cell types. *In vivo*, F-actin is localized at lateral junctional complexes in hepatocytes, reminiscent of adherens junction type structures. *In vitro*, hepatocyte F-actin has been shown to organize either at cellular junctions or in stress fiber-type arrangements, depending on the physical properties of the matrix to which the cells are attached (84).

Since it is the cytoskeleton which is responsible for the generation of cellular contractile events, further analysis of the balance between cell-substratum adhesion forces and cell contractile forces can be achieved by observation of differences in cytoskeletal phenotype in spheroidal and monolayer hepatocyte aggregates.

C.2 Experimental Methods

The organization of F-actin, the cytoskeletal component responsible for generation of tension/contraction, was observed via confocal microscopy. Hepatocytes were cultured on 1cm x 1cm polystyrene sections as described in section 2.2.2. All procedures were done at ambient temperature. Cells were fixed at various time points using 4% paraformaldehyde in PBS pH 7.4 for 30 min., rinsed twice in PBS, and permeabilized for 20 min. in 0.1% Triton X-100. The cells were then washed three times and stored in PBS until staining.

Cells were stained for 30 min. with 0.8 μm FITC-phalloidin (SIGMA Chemicals) and then washed four times with PBS. A drop of 10 mg/ml n-propyl gallate in a solution

of glycerol and 10 mM Tris pH 8.5 was added to each of the polystyrene sections to minimize photobleaching, after which they were placed on glass microscope slides and held stationary with nail polish.

All samples were analyzed in a laser confocal microscope (Bio-Rad MRC 600; Bio-Rad Microsciences, Cambridge, MA) attached to an inverted microscope equipped with a 20X lens. Confocal images (768 x 512 pixels) were obtained using Bio-Rad COMOS software.

C.3 Results and Implications

The actin microfilament distributions in hepatocytes seeded onto 1 $\mu g/cm^2$, 0.1 $\mu g/cm^2$, and 0.01 $\mu g/cm^2$ Matrigel substrata were qualitatively analyzed at 3 hrs., 24 hrs., and 4 days after seeding.

All cells, regardless of the substratum, showed a diffuse, cortical actin distribution 3 hrs. after seeding (Figure C-1). At 24 hrs., the same diffuse pattern was seen in single hepatocytes on all substrata, as well as in cells which appear to have coupled shortly before fixing (Figure C-2). The microfilaments in those cells which had formed into aggregates by this time point, however, appeared to be organizing into distinct patterns (Figure C-3). In spheroidal aggregates (aggregates on 0.1 $\mu g/cm^2$ and 0.01 $\mu g/cm^2$ Matrigel substrata), actin filaments localized subjacent to individual membranes and at areas of cell-cell contact. This arrangement suggests a lack of opposition to the contractile forces provided by the actin network (94, 119, 52), and is reminiscent of the apical ring of microfilaments which is a prominent feature of *in vivo* epithelia (122). However, these structures do not appear to form in monolayer aggregates (aggregates on 1 $\mu g/cm^2$ Matrigel substrata). Instead, the microfilaments begin to form long fibers oriented linearly within these cells. These bundles of microfilaments, known as stress fibers, are connected with the substratum through a series of intermediates typically including talin, vinculin, and integrin receptors (70, 16). By day 4, these stress fibers can become quite prominent (Figure C-4). It has been demonstrated that stress fibers often form due to the type of strong physical resistance to

cytoskeletal contraction provided by highly adhesive substrata (94, 119, 52) and are disrupted when an unyielding substratum is suddenly "relaxed" (83). The hepatocyte behavior in Figure C-4 therefore suggests that the absence of retraction in peripheral regions of these aggregates is due at least in part to the failure of the contractile actin filaments to overcome cell-substratum adhesion forces in these regions. These observations provide further validity for the cell contraction component of the hypothesis which was proposed in chapter 4 and analyzed in chapter 5.

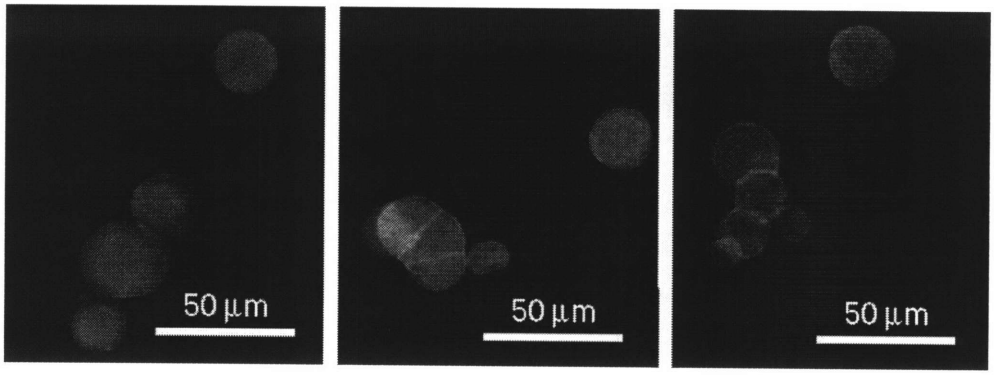

Figure C-1. Confocal micrographs of hepatocytes 3 hrs. post seeding on (a) 0.01 µg/cm^2; (b) 0.1 µg/cm^2; (c) 1 µg/cm^2 Matrigel substrata

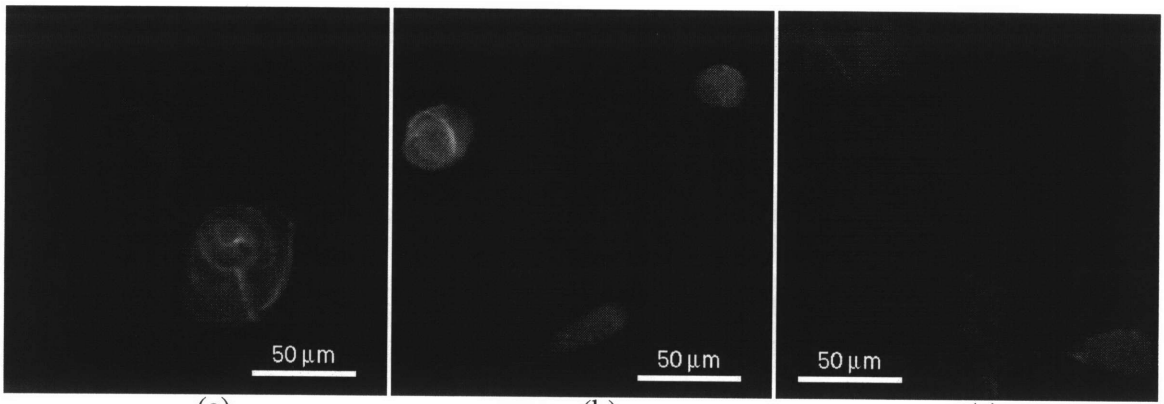

Figure C-2. Confocal micrographs of hepatocytes 24 hrs. post seeding on (a) 0.01 µg/cm^2; (b) 0.1 µg/cm^2; (c) 1 µg/cm^2 Matrigel substrata

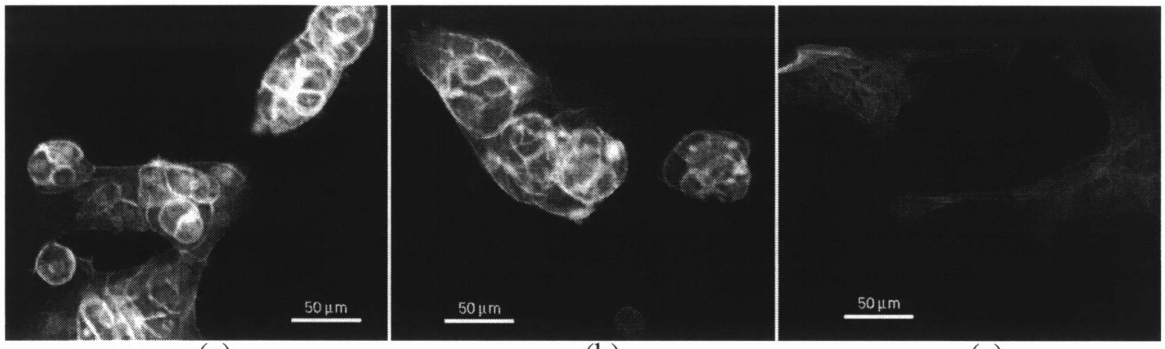

(a) (b) (c)

Figure C-3. Confocal micrographs of well-aggregated hepatocytes 24 hrs. post seeding on (a) 0.01 µg/cm^2; (b) 0.1 µg/cm^2; (c) 1 µg/cm^2 Matrigel substrata

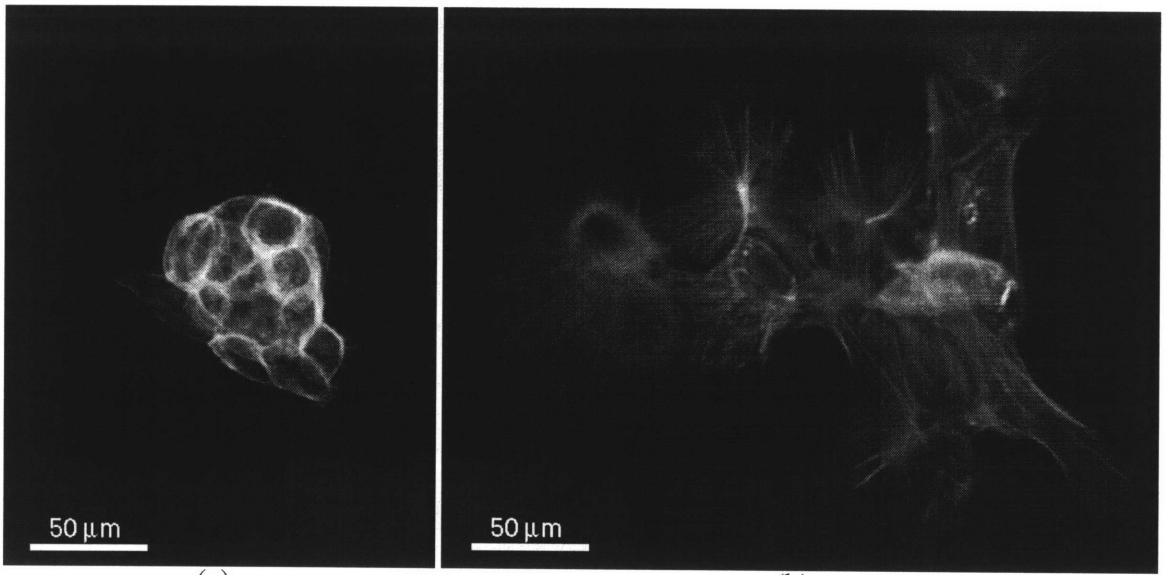

(a) (b)

Figure C-4. Confocal micrographs of hepatocytes 4 days post seeding on (a) 0.01 µg/cm^2 and (b) 1 µg/cm^2 Matrigel substrata

REFERENCES

1. Akiyama, S.K., Yamada, S.S., Chen, W. and Yamada, K.M. (1989). "Analysis of fibronectin receptor function with monoclonal antibodies: roles in cell adhesion, migration, matrix assembly, and cytoskeletal organization." *J. Cell Biol.* **109**: 863-875.

1a. Alberts, B., Bray, D., Lewis, J., Raff, M., Roberts, K. and Watson, J.D. (1989). *Molecular Biology of the Cell*l. New York, Garland Publishing.

2. Albelda, S.M. and Buck, C.A. (1990). "Integrins and other cell adhesion molecules." *FASEB J.* **4**: 2868-2880.

3. Allgor, S. (1996). Linear and star-shaped poly (ethylene oxide) grafted surfaces: grafting density and protein adsorption. Cambridge, MA, USA, Massachusetts Institute of Technology.

4. Arber, N., Zajicek, G. and Ariel, I. (1988). "The streaming liver. II. Hepatocyte life history." *Liver* **8**: 80-87.

5. Asano, K., Koide, N. and Tsuji, T. (1989). "Ultrastructure of multicellular rat spheroids formed in the primary culture of adult rat hepatocytes." *J. Clin. Electron Microsc.* **22**: 243-252.

6. Bade, E.G. and Feindler, S. (1988). "Liver epithelial cell migration induced by epidermal growth factor or transforming growth factor alpha is associated with changes in the gene expression of secreted proteins." *In Vitro Cell. Dev. Biol.* **24**(2): 149-154.

7. Bard, J. (1990). *Morphogenesis*. New York, Cambridge University Press.

8. Barrandon, Y. and Green, H. (1987). "Cell migration is essential for sustained growth of keratinocyte colonies: the roles of transforming growth factor-α and epidermal growth factor." *Cell* **50**: 1131-1137.

9. Ben-Ze'ev, A., Robinson, G.S., Bucher, N.L.R. and Farmer, S.R. (1988). "Cell-cell and cell-matrix interactions differentially regulate the expression of hepatic and cytoskeletal genes in primary cultures of rat hepatocytes." *Proc. Natl. Acad. Sci. USA* **85**: 2161-2165.

10. Bissell, D.M., Arenson, D.M., Maher, J.J. and Roll, F.J. (1987). "Support of cultured hepatocytes by a laminin-rich gel." *J. Clin. Invest.* **79**: 801-812.

11. Bissell, D.M., Stamatoglou, S.C., Nermut, M.V. and Hughes, R.C. (1986). "Interactions of rat hepatocytes with type IV collagen, fibronectin, and laminin matrices. Distinct matrix-controlled modes of attachment and spreading." *Eur. J. Cell Biol.* **40**: 72-78.

12. Bissell, M.J., Hall, H.G. and Parry, G. (1982). "How does the extracellular matrix direct gene expression?" *J. Theor. Biol.* **99**: 31-68.

13. Bralet, M., Branchereau, S., Brechot, C. and Ferry, N. (1994). "Cell lineage study in the liver using retroviral mediated gene transfer." *Am. J. Pathol.* **144**(5): 896-905.

14. Bray, D. (1992). *Cell Movements.* New York, Garland Publishing, Inc.

15. Buck, C.A. and Horwitz, A.F. (1987). "Cell surface receptors for extracellular matrix molecules." *Ann. Rev. Cell Biol.* **3**: 179-205.

16. Burridge, K., Fath, K., Kelly, T., Nuckolls, G. and Turner, C. (1988). "Focal adhesions: transmembrane junctions between the extracellular matrix and the cytoskeleton." *Ann. Rev. Cell Biol.* **4**: 487-525.

17. Cameron, J.D., Hagen, S.T., Waterfield, R.R. and Furcht, L.T. (1988). "Effects of matrix proteins on rabbit corneal epithelial cell adhesion and migration." *Curr. Eye Res.* **7**(3): 293-301.

18. Carlsson, R., Engvall, E., Freeman, A. and Ruoslahti, E. (1981). "Laminin and fibronectin in cell adhesion: enhanced adhesion of cells from regenerating liver to laminin." *Proc. Natl. Acad. Sci. USA* **78**(4): 2403-2406.

19. Clement, B., Segui-Real, B., Hassell, J.R., Martin, G.R. and Yamada, Y. (1989). "Identification of a cell surface-binding protein for the core protein of the basement membrane proteoglycan." *J. Biol. Chem.* **264**: 12467-12471.

20. Clement, B., Segui-Real, B., Savagner, P., Kleinman, H.K. and Yamada, Y. (1990). "Hepatocyte attachment to laminin is mediated through multiple receptors." *J. Cell Biol.* **110**: 185-192.

21. Demitriou, A.A., Levenson, S.M., Novikoff, P.M., Novikoff, A.B., Chowdhury, N.R., Whiting, J., Reisner, A. and Chowdhury, J.R. (1986). "Survival, organization, and function of microcarrier-attached hepatocytes transplanted in rats." *Proc. Natl. Acad. Sci. USA* **83**: 7475-7479.

22. DiMilla, P.A., Barbee, K. and Lauffenburger, D.A. (1991). "Mathematical model for the effects of adhesion and migration on cell migration speed." *Biophys. J.* **60**: 15-37.

23. DiMilla, P.A., Stone, J.A., Albelda, S.M., Lauffenburger, D.A. and Quinn, J.A. (1993). "Maximal migration of human smooth muscle cells on fibronectin and type IV collagen occurs at an intermediate attachment strength." *J. Cell Biol.* **122**(3): 729-737.

24. DiPasquale, A. (1975). "Locomotory activity of epithelial cells in culture." *Exp. Cell Res.* **94**: 191-215.

25. DiPersio, C.M., Jackson, D.A. and Zaret, K.S. (1991). "The extracellular matrix coordinately modulates liver transcription factors and hepatocyte morphology." *Mol. Cell. Biol.* **11**(9): 4405-4414.

26. Emerman, J.T. and Pitelka, D.R. (1977). "Maintenance and induction of morphological differentiation in dissociated mammary epithelium on floating collagen membranes." *In Vitro* **13**: 316-328.

27. Engel, J. (1991). "Common structural motifs in proteins of the extracellular matrix." *Curr. Opin. Cell Biol.* **3**: 779-785.

28. Enrich, C., Evans, W.H. and Gahmberg, C.G. (1988). "Fibronectin isoforms in plasma membrane domains of normal and regenerating rat liver." *FEBS Letters* **228**(1): 135-138.

29. Farquhar, M.G. and Palade, G.E. (1963). "Junctional complexes in various epithelia." *J. Cell Biol.* **17**: 375-412.

30. Flaherty, P. and Tadmor, B. (1995). "Matrigel matrix-based culture systems for primary hepatocytes." *J. NIH Res.* **7**: 74.

31. Folkman, J. and Greenspan, H.P. (1975). "Influence of geometry and control of cell growth." *Biochim. Biophys. Acta* **417**: 211-236.

32. Folkman, J. and Moscona, A. (1978). "Role of cell shape in growth control." *Nature* **273**(5661): 345-349.

33. Forsberg, E., Paulsson, M., Timpl, R. and Johansson, S. (1990). "Characterization of a laminin receptor on rat hepatocytes." *J. Biol. Chem.* **265**(11): 6376-6381.

34. Gail, M.H. and Boone, C.W. (1972). "Cell-substrate adhesivity. A determinant of cell motility." *Exp. Cell Res.* **70**: 33-40.

34a. Gordon, M.K. and Olson, B.R. (1990). "The contribution of collagenous proteins to tissue specific matrix assemblies." *Curr. Opin. Cell Biol.* **2**:833-838

35. Gospodarowicz, D., Greenburg, G. and Birdwell, C.R. (1978). "Determination of cellular shape by extracellular matrix and its correlation with the control of cellular growth." *Cancer Res.* **38**: 4155-4171.

36. Grant, D.S., Kleinman, H.K., Leblond, C.P., Inoue, S., Chung, A.E. and Martin, G.R. (1985). "The basement-membrane-like matrix of the mouse EHS tumor: II. Immunohistochemical quantitation of six of its components." *J. Anat.* **174**: 387-398.

37. Grisham, J.W. (1994). "Migration of hepatocytes along hepatic plates and stem cell-fed hepatocyte lineages." *Am. J. Pathol.* **144**(5): 849-854.

38. Grossman, M., Raper, S.E., Kozarsky, K., Stein, E.A., Engelhardt, J.F., Muller, D., Lupien, P.J. and Wilson, J.M. (1994). "Successful *ex vivo* gene therapy directed to liver in a patient with familial hypercholesterolaemia." *Nature Gen.* **6**: 335-341.

39. Guan, J.L., Trevethick, J.E. and Hynes, R.O. (1991). "Fibronectin/integrin interaction induces tyrosine phosphorylation of a 120 kD protein." *Cell Regul.* **2**: 951-964.

40. Gullberg, D., Gehlsen, K.R., Turner, D.C., Ahlen, K., Zijenah, L.S., Barnes, M.J. and Rubin, K. (1992). "Analysis of $\alpha_1\beta_1$, $\alpha_2\beta_1$ and $\alpha_3\beta_1$integrins in cell-

collagen interactions: identification of conformation dependent $\alpha_1\beta_1$ binding sites in collagen type I." *EMBO J.* **11**(11): 3865-3873.

41. Hanski, C., Huhle, T. and Reutter, W. (1985). "Involvement of plasma membrane dipeptidyl peptidase IV in fibronectin-mediated adhesion of cells on collagen." *Biol. Chem. Hoppe-Seyler* **366**: 1169-1176.

42. Hay, E.D., Ed. (1991). *Cell Biology of Extracellular Matrix.* New York, Plenum Press.

43. Hogervorst, F., Kuikman, I., Kessel, A.G.v. and Sonnenberg, A. (1991). "Molecular cloning of the human alpha6 subunit. Alternative splicing of alpha6 mRNA and chromosomal localization of the alpha6 and beta4 genes." *Eur. J. Biochem.* **199**: 425-433.

44. Hoofnagle, J.H., R.L. Carithers, J., Shapiro, C. and Ascher, N. (1995). "Fulminant hepatic failure: summary of a workshop." *Hepatol.* **21**(1): 240-252.

45. Hubbe, M.A. (1981). "Adhesion and detachment of biological cells *in vitro*." *Prog. Surf. Sci.* **11**: 65-138.

46. Hughes, R.C. and Stamatoglou, S.C. (1987). "Adhesive interactions and the metabolic activity of hepatocytes." *J. Cell Sci. Suppl.* **8**: 273-291.

47. Hynes, R.O. (1986). "Fibronectins." *Scientific American* **254**(6): 42-51.

48. Hynes, R.O. (1987). "Integrins, a family of cell surface receptors." *Cell* **48**: 549-555.

49. Hynes, R.O. and Yamada, K.A. (1982). "Fibronectins: multifunctional modular glycoproteins." *J. Cell Biol.* **95**: 369-377.

50. Ingber, D.E. (1990). "Fibronectin controls capillary endothelial cell growth by modulating cell shape." *Proc. Natl. Acad. Sci. USA* **87**: 3579-3583.

51. Ingber, D.E. (1991). "Integrins as mechanochemical transducers." *Curr. Opin. Cell Biol.* **3**: 841-848.

52. Ingber, D.E. (1993). "Cellular tensegrity: defining new rules of biological design that govern the cytoskeleton." *J. Cell Sci.* **104**: 613-627.

53. Ingber, D.E. (1993). "The riddle of morphogenesis: a question of solution chemistry or molecular cell engineering?" *Cell* **75**: 1249-1252.

54. Ingber, D.E., Madri, J.A. and Jamieson, J.D. (1981). "Role of basal lamina in the neoplastic disorganization of tissue architecture." *In Vitro Cell Develop. Biol.* **23**: 387-394.

55. Ingber, D.E., Prusty, D., Frangioni, J.V., Cragoe, E.J., Lechene, C. and Schwartz, M.A. (1990). "Control of intracellular pH and growth by fibronectin in capillary endothelial cells." *J. Cell Biol.* **110**: 1803-1811.

56. Jauregui, H.O., Mullon, C.J., Trenkler, D., Naik, S., Santangini, H., Press, P., Muller, T.E. and Solomon, B.A. (1995). "*In vivo* evaluation of a hollow fiber liver assist device." *Hepatol.* **21**(2): 460-469.

57. Juliano, R.L. and Haskill, S. (1993). "Signal transduction from the extracellular matrix." *J. Cell Biol.* **120**(3): 577-585.

58. Kamlot, A., Rozga, J., Watanabe, F.D. and Demetriou, A.A. (1996). "Review: artificial liver support systems." *Biotechnol. Bioeng.* **50**: 382-391.

59. Kane, R.E., Tector, J., Brems, J.J., Li, A. and Kaminski, D. (1991). "Sulfation and glucuronidation of acetaminophen by cultured hepatocytes reproducing *in vivo* sex-differences in conjugation on Matrigel and type 1 collagen." *In Vitro Cell. Dev. Biol.* **27A**: 953-960.

60. Kanner, S.B., Reynolds, A.B., Vines, R.R. and Parsons, J.T. (1990). "Monoclonal antibodies to individual tyrosine kinase phosphorylated protein substrates of oncogene encoded tyrosine kinases." *Proc. Natl. Acad. Sci. USA* **87**: 3328-3332.

61. Kitamura, M., Maruyama, N., Yoshida, H., Nagasawa, R., Mitarai, T. and Sakai, O. (1991). "Extracellular matrix contraction by cultured mesangial cells: an assay system for mesangial cell-matrix interaction." *Exp. Mol. Path.* **54**: 181-200.

62. Kleinman, H.K., Klebe, R.J. and Martin, G.R. (1981). "Role of collagenous matrices in the adhesion and growth of cells." *J. Cell Biol.* **88**: 473-485.

63. Klymkowsky, M.W. and Parr, B. (1995). "The body language of cells: the intimate connection between cell adhesion and behavior." *Cell* **83**: 5-8.

64. Koide, N., Sakaguchi, K., Koide, Y., Asano, K., Kawaguchi, M., Matsushima, H., Takenami, T., Shinji, T., Mori, M. and Tsuji, T. (1990). "Formation of multicellular spheroids composed of adult rat hepatocytes in dishes with positively charged surfaces and under other nonadherent environments." *Exp. Cell Res.* **186**(2): 227-235.

65. Koide, N., Shinji, T., Tanabe, T., Asano, K., Kawaguchi, M., Sakaguchi, K., Koide, Y., Mori, M. and Tsuji, T. (1989). "Continued high albumin production by multicellular spheroids of adult rat hepatocytes formed in the presence of liver-derived proteoglycans." *Biochem. Biophys. Res. Commun.* **161**(1): 385-391.

66. Kolodney, M.S. and Wysolmerski, R.B. (1992). "Isometric contraction by fibroblasts and endothelial cells in tissue culture: a quantitative study." *J. Cell Biol.* **117**(1): 73-82.

67. Kornberg, L., Earp, H.S., Parsons, J.T., Schaller, M. and Juliano, R.L. (1992). "Cell adhesion of integrin clustering increases phosphorylation of a focal adhesion associated tyrosine kinase." *J. Biol. Chem.* **267**: 23439-23442.

68. Kornberg, L., Earp, H.S., Turner, C., Prokop, C. and Juliano, R.L. (1991). "Signal transduction by integrins: increased protein tyrosine phosphorylation caused by clustering of beta1 integrins." *Proc. Natl. Acad. Sci. USA* **88**: 8392-8396.

69. Kreis, T. and Vale, R., Eds. (1993). *Guidebook to the cytoskeletal and motor proteins*. New York, Oxford University Press.

70. Lackie, J.M. (1986). *Cell Movement and Cell Behaviour*. London, Allen and Unwin.

71. Landry, J., Bernier, D., Ouellet, C., Goyette, R. and Marceau, N. (1985). "Spheroidal aggregate culture of rat liver cells: histotypic reorganization, biomatrix deposition, and maintenance of functional activities." *J. Cell Biol.* **101**: 914-923.

72. Langer, R.S. and Vacanti, J.P. (1993). "Tissue engineering." *Science* **260**: 920-926.

73. Lauffenburger, D.A. and Horwitz, A.F. (1996). "Cell migration: a physically integrated process." *Cell* **84**: 359-369.

74. Lauffenburger, D.A. and Linderman, J.J. (1993). *Receptors*. New York, Oxford University Press.

75. Lee, J., Ishihara, A., Theriot, J.A. and Jacobson, K. (1993). "Principles of locomotion for simple-shaped cells." *Nature* **362**: 167-171.

76. Lee, J., Leonard, M., Oliver, T., Ishihara, A. and Jacobson, K. (1994). "Traction forces generated by locomoting keratocytes." *J. Cell Biol.* **27**(6): 1957-1964.

77. Linblad, W.J., Scheutz, E.G., Redford, K.S. and Guzelian, P.S. (1991). "Hepatocellular phenotype *in vitro* is influenced by biophysical features of the collagenous substratum." *Hepatol.* **13**(2): 282-288.

78. Maher, J.J. and Bissell, D.M. (1993). "Cell-matrix interactions in liver." *Sem. Cell Biol.* **4**: 189-201.

79. Martinez-Hernandez, A., Delgado, F.M. and Amenta, P.S. (1991). "The extracellular matrix in hepatic regeneration." *Lab. Invest.* **64**(2): 157-166.

80. Michalopoulos, G.K., Bowen, W., Nussler, A.K., Becich, M.J. and Howard, T.A. (1993). "Comparative analysis of mitogenic and morphogenic effects of HGF and EGF on rat and human hepatocytes maintained in collagen gels." *J. Cell. Physiol.* **156**: 443-452.

81. Middleton, C.A. and Sharp, J.A. (1984). *Cell Locomotion In Vitro*. Berkeley, CA, University of California Press.

82. Miettinen, A., Virtanen, I. and Linder, E. (1978). "Cellular actin and junction formation during reaggregation of adult rat hepatocytes into epithelial cell sheets." *J. Cell Sci.* **31**: 341-353.

83. Mochitate, K., Pawelek, P. and Grinnell, F. (1991). "Stress relaxation of contracted collagen gels: disruption of actin filament bundles, release of cell surface fibronectin, and down-regulation of DNA and protein synthesis." *Exp. Cell Res.* **193**: 198-207.

84. Moghe, P.V., Berthiaume, F., Ezzell, R.M., Toner, M., Tompkins, R.G. and Yarmush, M.L. (1996). "The role of culture matrix configuration and composition in maintenance of hepatocyte polarity and function." *Biomaterials* **17**(3).

85. Mooney, D., Hansen, L., Vacanti, J., Langer, R., Farmer, S. and Ingber, D. (1992). "Switching from differentiation to growth in hepatocytes: control by extracellular matrix." *J. Cell. Phys.* **151**: 497-505.

86. Mooney, D.J., Langer, R. and Ingber, D.E. (1995). "Cytoskeletal filament assembly and the control of cell spreading and function by extracellular matrix." *J. Cell Sci.* **108**(6): 2311-2320.

87. Mueller, S.C., Kelly, T., Dai, M., Dai, H. and Chen, W.-T. (1989). "Dynamic cytoskeletal-integrin associations induced by cell binding to immobilized fibronectin." *J. Cell Biol* **109**: 3455-3464.

88. Nelson, W.J. and Warren, S.L. (1988). Modulation of intercellular adhesion in epithelia: consequences on the formation of three-dimensional multicellular structures. *Signal Transduction in Cytoplasmic Organization and Cell Motility*. P. Satir, J. Condeelis and E. L. Zarides. New York, Alan R. Liss, Inc.

89. Nermut, M.V., Green, N.M., Eason, P., Yamada, S.S. and Yamada, K.M. (1988). "Electron microscopy and structural model of human fibronectin receptor." *EMBO J.* **7**(13): 4093-4099.

90. Ng-Sikorski, J., Andersson, R., Patarroyo, M. and Andersson, T. (1991). "Calcium signaling capacity of the CD11b/CD18 integrin on human neutrophils." *Exp. Cell Res.* **195**: 504-508.

91. Nyberg, S.L., Shirabe, K., Peshwa, M.V., Sielaff, T.D., Crotty, P.L., Mann, H.J., Remmel, R.P., Payne, W.D., Hu, W.S. and Cerra, F.B. (1993). "Extracorporeal application of a gel-entrapment bioartificial liver: demonstration of drug metabolism and other biochemical functions." *Cell Transplant.* **2**(6): 441-452.

92. Odell, G., Oster, G., Burnside, B. and Alberch, P. (1981). "The mechanical basis of morphogenesis I: Epithelial folding and invagination." *Dev. Biol.* **85**: 446-462.

93. Oliver, T., Lee, J. and Jacobson, K. (1994). "Forces exerted by locomoting cells." *Sem. Cell Biol.* **5**: 139-147.

94. Opas, M. (1989). "Expression of the differentiated phenotype by epithelial cells in vitro is regulated by both biochemistry and mechanics of the substratum." *Dev. Biol.* **131**: 281-293.

95. Oster, G.F., Murray, J.D. and Harris, A.K. (1983). "Mechanical aspects of mesenchymal morphogenesis." *J. Embryol. Exp. Morph.* **78**: 83-125.

96. Parsons-Wingerter, P.A. and Saltzman, W.M. (1993). "Growth versus function in the three-dimensional culture of single and aggregated hepatocytes within collagen gels." *Biotechnol. Prog.* **9**: 600-607.

97. Peshwa, M.V., Wu, F.J., Follstad, B.D., Cerra, F.B. and Hu, W. (1994). "Kinetics of hepatocyte spheroid formation." *Biotechnol. Prog.* **10**: 460-466.

98. Petroll, W.M., Cavanagh, H.D., Barry, P., Andrews, P. and Jester, J.V. (1993). "Quantitative analysis of stress fiber analysis during corneal wound contraction." *J. Cell Sci.* **104**: 353-363.

99. Ponder, K.P., Gupta, S., Leland, F., Darlington, G., Finegold, M., DeMayo, J., Ledley, F.D., Chowdhury, J.R. and Woo, S.L.C. (1991). "Mouse hepatocytes migrate to liver parenchyma and function indefinitely after intrasplenic transplantation." *Proc. Natl. Acad. Sci. USA* **88**: 1217-1221.

100. Powers, M.J. and Griffith-Cima, L.G. (1996). "Motility behavior of hepatocytes on extracellular matrix substrata during aggregation." *Biotechnol. Bioeng.* **50**: 392-403.

101. Pujades, C., Forsberg, E., Enrich, C. and Johansson, S. (1992). "Changes in cell surface expression of fibronectin and fibronectin receptor during liver regeneration." *J. Cell Sci.* **102**: 815-820.

102. Rana, B., Mischoulon, D., Xie, Y., Bucher, N.L.R. and Farmer, S.R. (1994). "Cell-extracellular matrix interactions can regulate the switch between growth and differentiation in rat hepatocytes: reciprocal expression of C/EBPalpha and immediate-early growth response transcription factors." *Mol. Cell. Biol.* **14**(9): 5858-5869.

103. Regen, C.M. and Horwitz, A.F. (1992). "Dynamics of β_1 integrin-mediated adhesive contacts in motile fibroblasts." *J. Cell. Biol.* **119**: 1347-1359.

104. Rescan, P., Clement, B., Yamada, Y., Glaise, D., Segui-Real, B., Gugen-Guillouzo, C. and Guillouzo, A. (1991). "Expression of laminin and its receptor LBP-32 in human and rat hepatoma cells." *Hepatol.* **13**(2): 289-296.

105. Rhim, J.A., Sandgren, E.P., Degen, J.L., Palmiter, R.D. and Brinster, R.L. (1994). "Replacement of diseased mouse liver by hepatic cell transplantation." *Science* **263**: 1149-1152.

106. Rodriguez-Boulan, E. and Nelson, W.J. (1989). "Morphogenesis of the polarized epithelial cell phenotype." *Science* **245**: 718-725.

107. Rozga, J., Podesta, L., LePage, E., Morsiani, E., Moscioni, A.D., Hoffman, A., Sher, L., Villamil, F., Woolf, G., McGrath, M., *et al.* (1994). "A bioartificial liver to treat severe acute liver failure." *Ann. Surg.* **219**(5): 538-546.

108. Ruoslahti, E. and Piersbacher, M.D. (1986). "Arg-Gly-Asp: A versatile cell recognition signal." *Cell* **44**: 517-518.

109. Ruoslahti, E. and Piersbacher, M.D. (1987). "New perspectives in cell adhesion: RGD and integrins." *Science* **23**: 491-497.

110. Salonen, J.I. and Persson, R.G. (1989). "Migration of epithelial cells on materials used in guided tissue regeneration." *J. Periodont. Res.* **25**: 215-221.

111. Saltzman, W.M., Parsons-Wingerter, P., Leong, K.W. and Lin, S. (1991). "Fibroblast and hepatocyte behavior on synthetic polymer surfaces." *J. Biomed. Mat. Res.* **25**: 741-759.

112. Schaller, M.D., Borgman, C.A., Cobb, B.S., Vines, R.R., Reynolds, A.B. and Parsons, J.T. (1992). "pp124 FAK, a structurally unique protein tyrosine kinase associated with focal adhesions." *Proc. Natl. Acad. Sci. USA* **89**(5192-5196).

113. Schmidt, C.E., Horwitz, A.F., Lauffenburger, D.A. and Sheetz, M.P. (1993). "Integrin-cytoskeletal interactions in migrating fibroblasts are dynamic, asymmetric, and regulated." *J. Cell Biol.* **123**(4): 977-991.

114. Schnittny, J.C. and Yurchenco, P.D. (1989). "Basement membranes: molecular organization and function in development and disease." *Curr. Opin. Cell Biol.* **1**: 983-988.

115. Schuetz, E.G., Li, D., Omiecinski, C.J., Mueller-Eberhard, U., Kleinman, H.K., Elswick, B. and Guzelian, P.S. (1988). "Regulation of gene expression in adult rat hepatocytes cultured on a basement membrane matrix." *J. Cell. Phys.* **134**: 309-323.

116. Schwartz, M.A. (1992). "Transmembrane signalling by integrins." *Trends in Cell Biol.* **2**: 304-308.

117. Sheetz, M.P. (1994). "Cell migration by graded attachment to substrates and contraction." *Sem. Cell Biol.* **5**: 149-155.

118. Shiraha, H., Koide, N., Hada, H., Ujike, K., Nakamara, M., Shinji, T., Gotoh, S. and Tsuji, T. (1996). "Improvement of serum amino acid profile in hepatic failure with the bioartificial liver using multicellular hepatocyte spheroids." *Biotechnol. Bioeng.* **50**: 416-421.

119. Sims, J.R., Karp, S. and Ingber, D.E. (1992). "Altering the cellular mechanical force balance results in integrated changes in cell, cytoskeletal and nuclear shape." *J. Cell Sci.* **103**: 1215-1222.

120. Stamatoglou, S.C., Bawumia, S., Johansson, S., Forsberg, E. and Hughes, R.C. (1991). "Affinity of integrin alpha1beta1 from liver sinusoidal membranes for type IV collagen." *FEBS Letters* **288**(1-2): 241-243.

121. Stamatoglou, S.C. and Hughes, R.C. (1992). "Dynamic interactions of hepatocytes with fibronectin substrata: temporal and spatial changes in the distribution of adhesive contacts, fibronectin receptors, and actin filaments." *Exp. Cell Res.* **198**: 179-182.

122. Stamatoglou, S.C. and Hughes, R.C. (1994). "Cell adhesion molecules in liver function and pattern formation." *FASEB J.* **8**: 420-427.

123. Stamatoglou, S.C., Hughes, R.C. and Lindahl, U. (1987). "Rat hepatocytes in serum-free primary culture elaborate an extensive extracellular matrix containing fibrin and fibronectin." *J. Cell Biol.* **105**: 2417-2425.

124. Stamatoglou, S.C., Rui-Chang, G., Mills, G., Butters, T.D., Zaidi, F. and Hughes, R.C. (1990). "Identification of a novel glycoprotein (AGp110) involved in interactions of rat liver parenchymal cells with fibronectin." *J. Cell Biol.* **111**: 2117-2127.

125. Stamatoglou, S.C., Sullivan, K.H., Johansson, S., Bayley, P.M., Burdett, I.D.J. and Hughes, R.C. (1990). "Localization of two fibronectin-binding glycoproteins in rat liver and primary hepatocytes." *J. Cell Sci.* **97**: 595-606.

126. Steinberg, M.S. (1963). "Reconstruction of tissues by dissociated cells." *Science* **141**: 401-408.

127. Steinberg, M.S. (1970). "Does differential adhesion govern self-assembly processes in histogenesis? Equilibrium configurations and the emergence of a hierarchy among populations of embryonic cells." *J. Exp. Zool.* **173**: 395-434.

128. Stolz, D.B. and Michalopoulos, G.K. (1994). "Comparative effects of hepatocyte growth factor and epidermal growth factor on motility, morphology, mitogenesis, and signal transduction of primary rat hepatocytes." *J. Cell. Biochem.* **55**: 445-464.

129. Stossel, T.P. (1993). "On the crawling of animal cells." *Science* **260**: 1086-1094.

130. Strom, S.C., Jirtle, R.L., Jones, R.S., Novicki, D.L., Rosenberg, M., Novotny, A., Irons, G., McLain, J.R. and Michalopoulos, G. (1982). "Isolation, culture, and transplantation of human hepatocytes." *J. Nat. Canc. Inst.* **68**: 771-778.

131. Sudhakaran, P.R., Stamatoglou, S.C. and Hughes, R.C. (1986). "Modulation of protein synthesis and secretion by substratum in primary cultures of rat hepatocytes." *Exp. Cell Res.* **167**: 505-516.

132. Takada, Y., Elices, M.J., Crouse, C. and Hemler, M.E. (1989). "Primary structure of the alpha4 subunit of VLA4; homology to other integrins and a possible cell-cell adhesion function." *EMBO J.* **8**: 1361-1368.

133. Takada, Y., Murphy, E., Pil, P., Chen, C., Ginsberg, M.H. and Hemler, M.E. (1991). "Molecular cloning and expression of the cDNA for alph3 subunit of human alpha3/beta1 (VLA3) an integrin receptor for fibronectin laminin and collagen." *J. Cell Biol.* **115**: 257-266.

134. Takeichi, M. (1988). "The cadherins: cell-cell adhesion molecules controlling animal morphogenesis." *Development* **102**: 639-655.

135. Tamkun, J.W. and Hynes, R.O. (1983). "Plasma fibronectin is synthesized and secreted by hepatocytes." *J. Biol. Chem.* **258**(7): 4641-4647.

136. Tamura, R.N., Cooper, H.M., Collo, G. and Quaranta, V. (1991). "Cell type specific integrin variants with alternative alpha chain cytoplasmic domains." *Proc. Natl. Acad. Sci. USA* **88**: 10183-10187.

137. Tilney, L.G., DeRosier, D.J. and Tilney, M.S. (1992). "How listeria exploits host cell actin to form its own cytoskeleton. I. Formation of a tail and how that tail might be involved in movement." *J. Cell Biol.* **118**(1): 71-81.

138. Tong, J.Z., Bernard, O. and Alvarez, F. (1990). "Long-term culture of rat liver cell spheroids in hormonally defined media." *Exp. Cell Res.* **189**: 87-92.

139. Townes, P. and Holtfreter, J. (1955). "Directed movements and selected adhesion of embryonic amphibian cells." *J. Exp. Zool.* **128**: 53-120.

140. Truskey, G.A. and Pirone, J.S. (1990). "The effect of fluid shear stress upon cell adhesion of fibronectin-treated surfaces." *J. Biomed. Mat. Res.* **24**: 1333-1353.

141. Truskey, G.A. and Proulx, T.L. (1993). "Relationship between 3T3 cell spreading and the strength of adhesion on glass and silane surfaces." *Biomaterials* **14**(4): 243-254.

142. Uludag, H., Horvath, V., Black, J.P. and Sefton, M.V. (1994). "Viability and protein secretion from human hepatoma (HepG2) cells encapsulated in 400 M Polyacrylate microcapsules by submerged nozzle-liquid jet extrusion." *Biotechnol. Bioeng.* **44**(10): 1199.

143. Usami, S., Chen, H., Zhao, Y., Chien, S. and Skalak, R. (1993). "Design and construction of a linear shear stress flow chamber." *Ann. Biomed. Eng.* **21**: 77-83.

144. Vacanti, J.P., Morse, M.A., Saltzman, W.M., Domb, A.J., Perez-Atayde, A. and Langer, R. (1988). "Selective cell transplantation using bioabsorbable artificial polymers as matrices." *J. Pediat. Surg.* **23**(1988): 3-9.

145. van Kooten, T.G. (1992). "Influence of substratum wettability on the strength of adhesion of human fibroblasts." *Biomaterials* **13**(13): 897-904.

146. Ward, M.D. and Hammer, D.A. (1993). "A theoretical analysis for the effect of focal contact formation on cell-substrate attachment strength." *Biophys. J.* **64**: 936-959.

147. Watanabe, M., Nagafuchi, A., Tsukita, S. and Takeichi, M. (1994). "Induction of polarized cell-cell association and retardation of growth by activation of the E-cadherin-catenin adhesion system in a dispersed carcinoma line." *J. Cell Biol.* **127**(1): 247-256.

148. Watt, F.M., Jordan, P.W. and O'Neill, C.H. (1988). "Cell shape controls terminal differentiation of human epidermal keratinocytes." *Proc. Natl. Acad. Sci. USA* **85**: 5576-5580.

149. Wilson, H.V. (1907). "On some phenomena of coalescence and regeneration in sponges." *J. Exp. Zool.* **5**: 245-258.

150. Wu, F.J., Friend, J.R., Hsiao, C.C., Zilliox, M.J., Ko, W., Cerra, F.B. and Hou, W. (1996). "Efficient assembly of rat hepatocyte spheroids for tissue engineering applications." *Biotechnol. Bioeng.* **50**: 404-415.

151. Yarmush, M.L., Dunn, J.C. and Tompkins, R.G. (1992). "Assessment of artificial liver support technology." *Cell Transplant.* **1**(5): 323-341.

152. Yuasa, C., Tomita, Y., Shono, M., Ishimura, K. and Ichihara, A. (1993). "Importance of cell aggregation for expression of liver functions and regeneration demonstrated with primary cultured hepatocytes." *J. Cell. Phys.* **156**: 522-530.

153. Zajicek, G., Oren, R. and M. Weinreb, J. (1985). "The streaming liver." *Liver* **5**: 293-300.

154. Zar, J.H. (1996). *Biostatistical Analysis*. Upper Saddle River, NJ, Prentice-Hall, Inc.

155. Palecek, S., personal communication.